Chapter 11
The State-of-Art of Global and Chinese Meso-Neoproterozoic Petroleum Resources

Tieguan Wang, Daofu Song, Chengyu Yang, and Ronghui Fang

Abstract Since 1960s, the significant research progress on the Proterozoic early lives and life diversity as well as on the Meso-Neoproterozoic shales and carbonate source rocks have established a material foundation for the studies of indigenous Meso-Neoproterozoic sedimentary organic matter and petroliferous nature, and providing the prerequisites for the prospectivity of indigenous petroleum resources. So far at least dozens oil and gas fields, some of considerables size, have been discovered in the Meso-Neoproterozoic strata, oil and/or gas of which were sourced from the Infracambrian source beds. Based on uncompleted global statistics, there are four countries, i.e., Lena-Tounguska Petroleum Province (LTPP) in Siberia Craton (Russia), Oman Basins in Arabian Craton (Oman), Baghewala Oilfield in Indian Craton (India), and Anyue Gasfield in western Yangtze Craton (China), in the world, containing proven geological reserves and/or commercial production of indigenous Infracambrian petroleum; nine regions/countries having been confirmed indigenous Meso-Neoproterozoic oil flow, oil-seep and/or asphalt, but so far no commercial production has been obtained yet; five regions/countries being revealed to possess hydrocarbon generation potential in the Infracambrian strata. China is one of the countries where the Meso-Neoproterozoic sequences are most completely developed and preserved, and Chinese Meso-Neoproterozoic geology was earlier studied in the word. However, both geological research and exploration of Meso-Neoproterozoic petroleum resources are faced with a challenging reality of more age-old strata, more complicated geological tectonics and more extensive scientific innovative possibility. Therefore, it is a considerable urgent question to study and evaluate the prospectivity of Meso-Neoproterozoic oil and gas resources in China. In this chapter, the distribution, exploration and development of Meso-Neoproterozoic oil and gas respectively in Russian LTPP, Sultanate of Oman, Pakistan and India basins, East European Craton, African Taoudenni Basin, Australian Centralian Basins, American Midcontinent Rift System as well as Chinese basins have been compiled, and their prospectivity approached.

T. Wang (✉) · D. Song · C. Yang · R. Fang
State Key Laboratory of Petroleum Resources and Prospecting, China University of Petroleum-Beijing, Beijing 102249, China

T. Wang, *Meso-Neoproterozoic Geology and Petroleum Resources in China*,
Springer Geology, https://doi.org/10.1007/978-981-19-5666-9_11

Keywords Meso-neoproterozoic · Lena-tounguska petroleum province (LTPP) · Anyue gasfield · Oman basins · Yanliao faulted-depression zone (YLFDZ)

11.1 Introduction

As for fossil fuels, oil and gas are generally preserved within various porous or fractured reservoir rocks with different geological age. However, it is common knowledge that petroleum is generated only within sedimentary strata rich-in organic matter, i.e., so called source beds/rocks. Global indigenous oil and gas fields are merely found in sedimentary basins as yet. In geological time, palaeo-organisms would be the sole material source for sedimentary organic matter. The Meso-Neoproterozoic sequences (1800–541 Ma in age) are the age-old sediments in the Earth. As recently as 1950s, it was generally accepted that sedimentary rock of Precambrian age located within basins, geosynclines, platforms and cratons could not contain hydrocarbon deposits. The absence of pre-Palaeozoic Era life characteristics in the Precambrian stratigraphic column was the most often presented reasons why Precambrian terrain should be ignored by the petroleum geologists (Dickes 1986a).

In recent 60 years, however, the researches of Proterozoic early life and life diversity in the Earth have made much headway (Diches 1986b; Chen et al. 1996; Hou et al. 1999; Chen 2004; Sun 2006; Du et al. 2009; Shu et al. 2016). In the meanwhile, petroleum geological and geochemical studies revealed that not only the age-old Meso-Neoproterozoic dark-colored shale and carbonate could contain abundant organic matter so as to become excellent source rocks, but also the source rock maturities would indicate various thermo-evolutional stages from marginal mature though mature, high-mature to over-mature phases, so that up to present some Precambrian sedimentary organic matter could be still within the category of "liquid window" for hydrocarbon generation. In some regions, therefore, numerous indigenous oil and gas seeps can be found, which could be very significant for the research of Meso-Neoproterozoic petroliferous nature and petroleum resources potential.

As a matter of fact, globally at least there are several dozen oil, gas-condensate and/or gas fields found within the Precambrian sequences in Russia, China, Oman and India since 1960s (Beijing Petroleum Exploration and Development Institute and North China Petroleum Bureau 1992; Fedorov 1997; IHS Energy Group. 2005. International Petroleum Exploration and Development Database. Colorado; Craig et al. 2009; Bhat et al. 2012). Based on the global statistics of petroleum resources published since 1990s, however, the geological reserve portion of indigenous Early Proterozoic petroleum only amount to 1–2% (Hunt 1991; Klemme and Ulmishek 1991). So far still no oil and gas reserve portions of Meso-Neoproterozoic sequences can be found in the published statistics in China (e.g., Fig. 11.1).

Menchikoff (1949) and Pruvost (1951) initially proposed an informally used geological term "Infracambrian". As currently used, the "Infracambrian" is loosely confined to formations including Precambrian-earliest Cambrian sedimentary

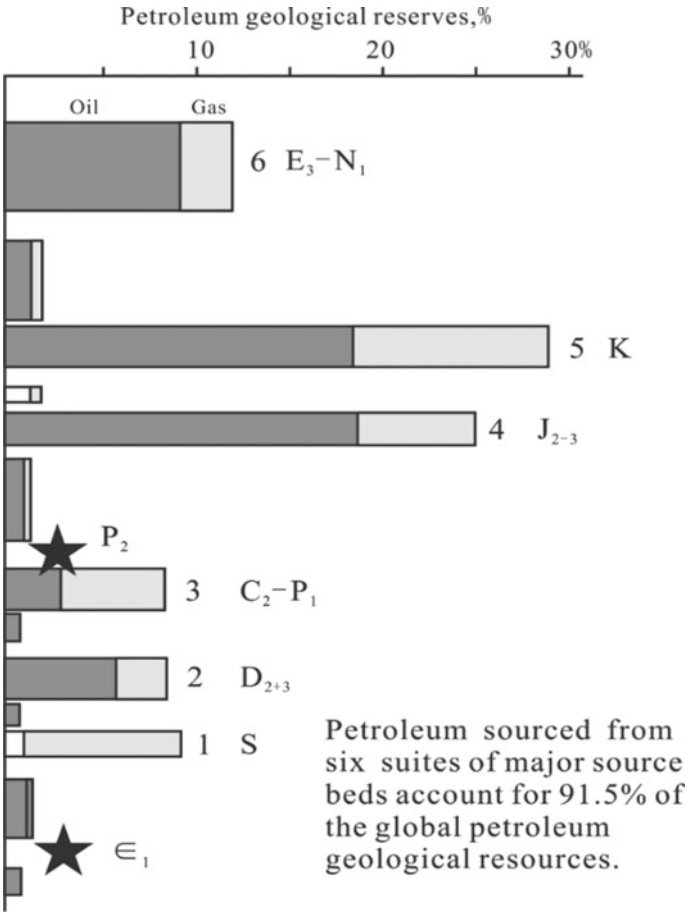

Fig. 11.1 Statistics of global petroleum geological reserves generated from the source beds of different geological time. [Liang (2008). Research progress of marine facies hydrocarbon generation and entrapment in south China (unpublished lecture notes)]

sequences that underlay known Cambrian strata and unconformably overlay crystalline basement (Smith 2009). In 2006, the Global Infracambrian Petroleum Systems Conference has been held at the Geological Society of London, the goal of which was to review current knowledge about Neoproterozoic–Early Cambrian petroleum systems worldwide (Craig et al. 2009). As a result of the conference, the Society Special Publication 326 entitled *Global Neoproterozoic Petroleum Systems: the Emerging Potential in North Africa* was published by the London Geological Society in 2009.

The Meso-Neoproterozoic sequences have well developed and more completely preserved in China, and the Meso-Neoproterozoic stratigraphy was earlier investigated by Chinese geologists in the world (Lee and Chao 1924; Kao et al. 1934).

However, quite a large area of the Meso-Neoproterozoic stratigraphic distribution is under the complicated tectonic and highly thermo-evolutional conditions in China, resulting in more difficulties for indigenous oil and gas preservation and exploration. Therefore, the researches of Meso-Neoproterozoic petroleum resources in China are facing the favorable advantages of completely developed strata and profoundly accumulation of scientific results as well as the challenging reality of more age-old strata and more complicated geological tectonics and more scientific innovative possibility. Therefore, it is a considerable urgent question that how to study and evaluate the prospectivity of Meso-Neoproterozoic petroleum resources in China.

In this chapter, the authors try to compile the distribution of currently known Meso-Neoproterozoic petroleum resources, investigate their petroleum geological conditions, and approach the prospectivity of indigenous Meso-Neoproterozoic oil/gas.

11.2 Global Distribution of Meso-Neoproterozoic Petroleum Resources

Based on incomplete global statistics, there are four regions/countries, i.e., ① Lena-Tounguska Petroleum Province (LTPP) in Siberia Craton (Russia), ② Anyue Gasfield in western Yangtze Craton (China), ③ Oman Basins in eastern Arabian Craton (Oman), and ④ Baghewala Oilfield in Indian Craton (India), in the world, containing proven geological reserves and/or commercial production of indigenous Meso-Neoproterozoic petroleum (Fig. 11.2).

Nine regions/countries, i.e., ① Moscow and Kama-Belsk Basins in East European Craton (Russia), ② Yanliao Faulted-Depression Zone (YFDZ, oil-seeps) in North China Craton (China), ③ Longmenshan Fronthill Belt (large asphalt veins) in Yangtze Craton (China), ④ Vindhyan uperbasin in Indian Craton (India), ⑤ Nonesuch (oil-seeps) in North American Craton (USA), ⑥ McArthur Basin and Centralian Superbasin in Australian Cratons (Australia), ⑦ Taoudenni Basin in West African Craton (Mauritania, Mali and Algeria), ⑧ Tindouf Basin (Morocco and Algeria), and ⑨ Sirte/Cyrenaica Basin in West African Craton (Libya), having confirmed indigenous Meso-Neoproterozoic oil flow, oil-seep, and/or asphalt, but no commercial production obtained yet.

Five regions/countries. i.e., ① Potwar and Mijalar Basins in Indian Craton (Pakistan), ② Saudi Arabia in Arabian Craton, ③ Sào Francisco Basin (Brazil) and ④ Argentina, Bolivia and Paraguay in Amazon Craton, ⑤ Al Kufra Basin in West African Craton (Libya), being revealed to possess the hydrocarbon generation potential of Meso-Neoproterozoic sequences (Craig et al. 2009; Ghori et al. 2009; Lottaroli et al. 2009; Wang and Han 2011).

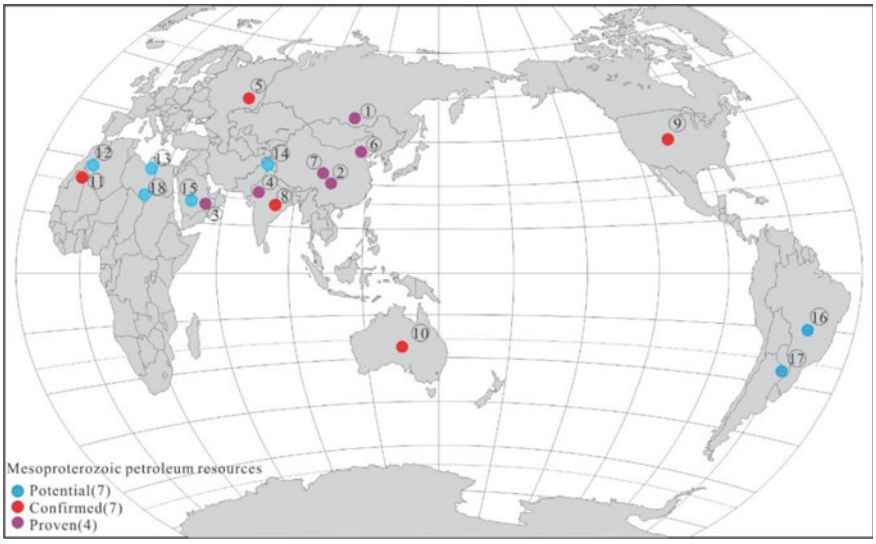

Fig. 11.2 Global distribution of proven, confirmed and potential Meso-Neoproterozoic petroleum resources (Craig et al. 2009; Smith 2009, modified). Proven resources (①–④): ① Lena-Tounguska Petroleum Province (LTPP, Russia); ② Anyue gasfield (China); ③ Oman Basins (Oman); ④ Baghewala Oilfield (India). Confirmed resources (⑤–(13)): ⑤ Moscow and Kama-Belsk Basins (Russia); ⑥ Yanliao oil-seeps (China); ⑦ Longmenshan asphalt veins (China); ⑧ Vindhyan Superbasin (India); ⑨ Nonesuch oil-seeps (USA); ⑩ McArthur Basin and Centralian Superbasin (Australia); (11) Taoudenni Basin (Mali, Mauritania and Algeria); (12)Tindouf Basin (Morocco and Algeria); (13) Sirte/Cyrenaica (Libya). Potential resources ((14)–(18)): (14) Potwar and Mijalar Basins (Pakistan); (15) Saudi Arabia; (16) Sào Francisco Basin (Brazil); (17) Argentina, Bolivia and Paraguay; (18) Al Kufra Basin (Libya)

11.2.1 Lena-Tunguska Petroleum Province in Siberian Craton

11.2.1.1 Regional Geological Setting

With areal extent of 4.5×10^6 km^2, the Siberia Craton is located in northeast Russia between the Yenisey and Lena Rivers. As a most important hydrocarbon-producing area in the craton, the Lena-Tunguska region is commonly called the Lena-Tunguska Petroleum Province (LTPP) in Russia, and covers an area of about 2.8×10^6 km^2, which is bounded on the east and northeast by the Archean-Early Proterozoic Aldan and Anabar Shields, and also encircled elsewhere by a series of Precambrian foldbelts, i.e., the west, southwest and south sides respectively by Yenisey, East Yenisey and Baikal-Patom Foldbelts (Fig. 11.3; Kuznetsov 1997).

In the LTPP, the principal source and reservoir beds are within Meso-Neoproterozoic to Early Cambrian sequences. Meso-Neoproterozoic sedimentary strata of great volume extend over a large territory of Siberia Craton, reaching 5 km

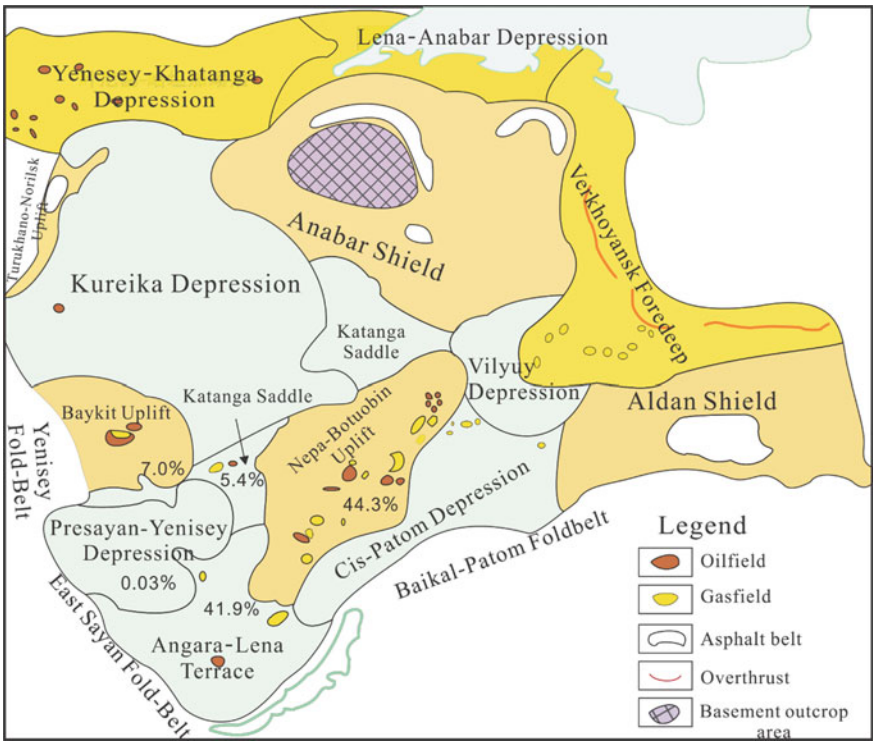

Fig. 11.3 Tectonic unit division and oil/gas field distribution of Siberia Craton in Russia (Tong and Xu 2004; Kuznetsov 1997 modified). The percentages indicate the portions of Meso-Neoproterozoic petroleum reserve in each tectonic unit (basic data based on IHS Energy Group 2005, International Petroleum Exploration and Development Database, Colorado)

or more in thickness. They have been formed lasting app. 1650–1600 to 540–530 Ma (Frolov et al. 2015). The oil- and gas-bearing sedimentary sequences are Riphean, Vendian and Early Cambrian in age. A thick Cambrian salt succession would provide regional super-seal that facilitated the preservation of hydrocarbons (Ghori et al. 2009).

11.2.1.2 Effective Source Beds

Hydrocarbon accumulations and their Riphean source rocks within the pericratonic Riphean palaeo-basins along the margin of Siberia Craton (i.e., the Cis-Patom Trough, Turukhansk and Udzha Basins in Fig. 11.4) were most likely destroyed by Baikal orogeny event with intensive erosion. For instance, even if the Riphean source rocks are characterized by up to 4% TOC content in Turukhansk Uplift, the generation potential (S_2) and hydrogen index (HI) are still very low (<0.1 mg HC/g Rock

and 50 mg HC/g TOC respectively), implying that organic matter of those rocks is completely exhausted (Forov et al. 2015).

By way of exception, the organic-rich shale of Upper Riphean Irmeken Formation in the intracratonic Riphean palaeo-basins (i.e., Irkineeva-Vanavara and Kureika-Anabar Basins in Fig. 11.4) are unlikely to be affected by the significant pre-Vendian erosion event. So far the Iremeken shale (sampled from the interval 2182–2186 m of Yurubchen-104 Well on Baykit Uplift, Fig. 11.4) are still chracterized by the

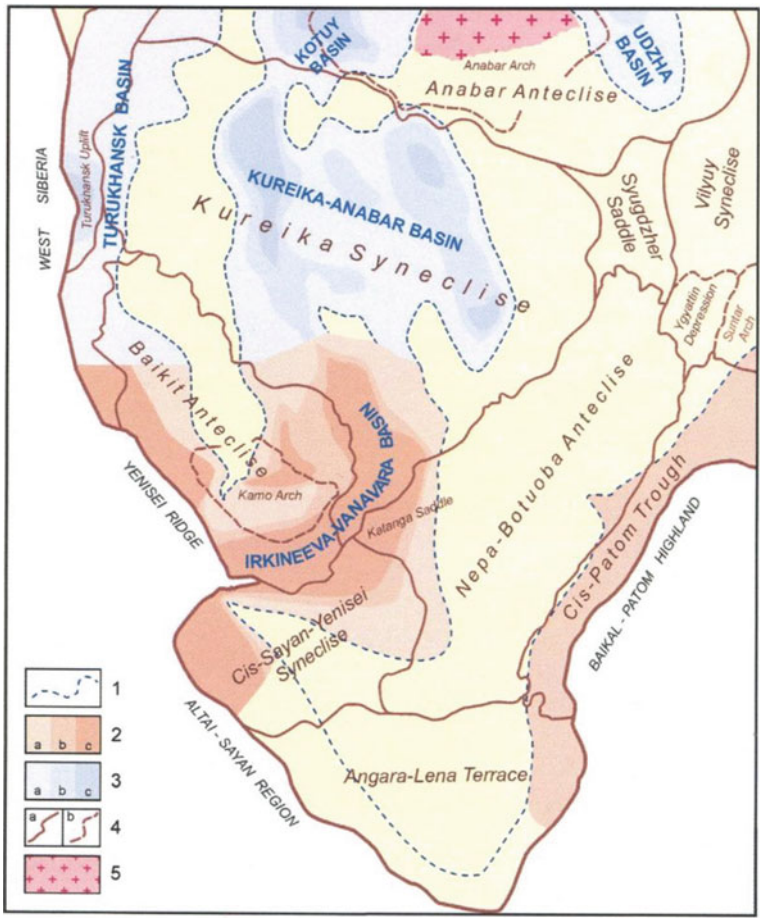

Fig. 11.4 Distribution of the Riphean palaeo-basins in the LTPP (Frolov et al. 2015). 1. Riphean palaeo-basin boundary; 2. Riphean palaeo-basin in the southern and central Siberia Craton and the inferred stratigraphic ages exposed under pre-Vrndian unconformaty surface: **a** Lower-Middle Riphean, **b** Middle-Upper Riphean, **c** Upper Riphean; 3. Riphean palaeo-basin in the northern part of the Craton and their assumed sedimentary infill thichness: **a** < 2 km, **b** 2–3 km, **c** > 3 km; 4. boundaries of recent major structural elements of the Siberian Craton: **a** 1st order structures, **b** 2nd order structures; 5. Modern outcrops of basement recks

following parameters: TOC 12.6%, chloroforn extractable bitumen content 0.56%, hydrocarbon index 463 mg HC/g TOC and T_{max} 445 °C (Larichev et al. 2004), which show a fair to high organic abundance and moderate maturity for hydrocarbon generation. Therefore, the Iremeken shale can act as a source bed for the oil and gas reservoirs/fields (e.g. the reservoirs of Riphean Kamov Group) in Baykit Uplift and Katanka Saddle, espetially for the Yurubchen-Tokhomo Zone (Fig. 11.3; Filipstsov et al. 1999; Ulmishek 2001; Melanie 2010; Frolov et al. 2015).

On the whole, Vendian and Lower Cambrian deposits would be the main source beds for present day oil fields in the central and northern parts of the Nepa-Botuobin Uplift and Turukhano-Norisk Uplift (cf. Fig. 11.3 and 11.4; Frolov et al. 2015).

11.2.1.3 Petroleum Resources

According to the basic data of IHS① (IHS Energy Group 2005. International Petroleum Exploration and Development Database. Colorado), totally there are 64 oil- and/or gas-fields composed of 168 individual reservoirs and found within the Meso-Neoproterozoic to Lower Cambrian strata in the LTPP. The proven plus probable petroleum reserves are 2.027×10^{12} m^3 for gas, 0.76×10^8 t for gas-condensate, 5.52×10^8 t for oil, and the total geological reserves would be up to 22.36×10^8 t in oil equivalent.

As assessed in twice by United States Geological Survey (USGS), however, the preserved volumes of both oil and gas in the Siberia Craton range from 2.8 bbbl (ca. 3.8×10^8 t) of oil and 48.9 Tcf (ca. 1.38×10^{12} m^3) of gas to 11.3 bbbl (ca. 15.5×10^8 t) of oil and 175 Tcf (ca. 5.0×10^{12} m^3) of gas (Ulmishek 2001). The main reason for the difference in the assessments is the assumption that much of undiscovered resources will be accounted for by reserve growth in two discovered giant fields, the Yurubchen-Takhoma Oilfield and the Kovyktin Gasfield (Ghori et al. 2009). Furthermore, Efimov et al. (2012) estimated that the proven recoverable reserves in Meso-Neoproterozoic silicaclastic and carbonate reaervoirs are about 6×10^8 t of oil and more than 2.7×10^{12} m^3 of gas in Siberia Craton (Ghori et al. 2009).

Based on statistics of the proven plus probable petroleum reserves in different tectonic units by IHS① (IHS Energy Group. 2005. International Petroleum Exploration and Development Database. Colorado), 86.3% of the total petroleum reserves are concentrated on two tectonic units, i.e., Nepa-Botuobin Uplift (individually accounting for 44.4%) and Angara-Lena Terrace (41.9%), while 7.0% of the total reserves are distributed at Baykit Uplift, 5.5% found at Khatenga Saddle and only 0.03% at Cis-Sayan Depression① (Fig. 11.3; IHS Energy Group. 2005. International Petroleum Exploration and Development Database. Colorado; Wang and Han 2011).

The stratigraphic horizon distribution of proven plus probable petroleum reserves are 5.31% in Cambrian, 1.26% in Cambrian plus Vendian, 86.77% in Vendian, 0.01% in Vendian plus Riphean, 6.58% in Riphean, and 0.07% still uncertain respectively① (IHS Energy Group. 2005. International Petroleum Exploration and Development

Table 11.1 Reserves of the largest oil and gas fields in the Siberia Craton①

Type	Field	Oil/10^6 t		Gas/10^9 m^3	
		Output from beginning of development	Reserve (A + B + C_1)[a]	Output from beginning of development	Reserve (A + B + C_1)[a]
Oil–Gas	Middle Botuobin	0.9	100	5.7	164
Gas	Chayandin	–	50	0.1	1200
Gas-Oil	Yurubcheno-Tokhm	0.7	168	–	140
Oil	Kuyumbin	0.3	110	–	20
Oil	Upper-Chona	16.1	150	0.5	16
Oil–Gas	Talakane	19.2	167	0.5	43
Gas	Kovyktin	–	115	0.5	1900

[a] A. proven develop and production reserve (PDP); B. proven undeveloped reserve (PUD); C_1. probable reserve

① Galimov (2014). Petroleum geology research of Precambrian in Russia (Eastern Siberia, Eastern European Platforms). An unpublished lecture notes in Beijing (in Russian)

Database. Colorado). Obviously the Vendian reservoirs contain the largest portion of proven plus probable oil and gas reserves. The major Vendian oil- and gasfields (incl. such large ones as Chayandin, Middle Botuobin and Upper Chona Fields) are located on the Nepa-Botuobin Uplift and some are situated on the Angara-Lena Terrace (incl. the giant Kovyktin Gasfield) and the Cis-Patom Depression. While the Riphean carbonate reservoirs only account for a minor reserve portion. To date, Riphean fields have been discovered only in one place on Baykit Uplif, i.e., the Yurrubchen-Tokhom Oil–Gas Field (Fig. 11.4), the oil and gas reserves in above mentioned major fields are listed in Table 11.1.

11.2.1.4 Oil and Gas Accumulation

Taking the large Middle Botuobin Oil–Gas Field as an example, it is located at the north of Nepa-Botuobin Uplift (Fig. 11.5), and tectonically referred to the structure type of complicated long-axis-anticline, containing a massive gas-condensate reservoir with oil-ring. The areas of gas reservoir and oil-ring account for 800 km^2 and 600 km^2 respectively, while the anticlinic area would be up to 1570 km^2 (Fig. 11.6). The field had been discovered at July 1970, somehow, it was developed after one decade. At least 108 wells have been drilled (Tong and Xu 2004) and its A + B + C_1 reserves are 164×10^9 m^3 of gas and 100×10^6 t of oil① (Table 11.1. Galimov (2014). Petroleum geology research of Precambrian in Russia (Eastern Siberia, Eastern European Platforms). An unpublished lecture notes in Beijing (in Russian).), both oil and gas were supplied by the source bed of Vendian shale. The reservoir driving types are attributed to water and gas drives as well as partly dissolved-gas drive. The gas

output of individual well could be up to 24 t/d of oil and 24 × 10^4–26 × 10^4 m^3/d of gas (Tong and Xu 2004).

As the second case, Yurubchen-Tokhm Oil–Gas Field situated on Baykit Uplift is also a large gas-condensate field with oil-ring and attributed to a karst-fissure type of reservoir confined by stratigraphic unconformable contact and faulting plane (Figs. 11.5 and 11.7). The first oil was tested in 1977. Since the high production of oil and gas flows was obtained from the Ю-2 exploratory well in 1982, it has been proven to be light oil (42°–45° API) with low sulphur content (0.2–0.3%; Ghori et al. 2009), at least 101 wells have been drilled, and it is ascertained that oil and gas are accumulated within the Vendian reservoir, while gas-condensate in the Upper Riphean reservoir (Tong and Xu 2004). Its proven oil- and gas-containing area is up to 3100 km^2 with A + B + C_1 reserves 1.68 × 10^8 t of oil and 140 × 10^9 m^3 of gas① (Table 11.1. Galimov (2014). Petroleum geology research of Precambrian in Russia (Eastern Siberia, Eastern European Platforms). An unpublished lecture notes

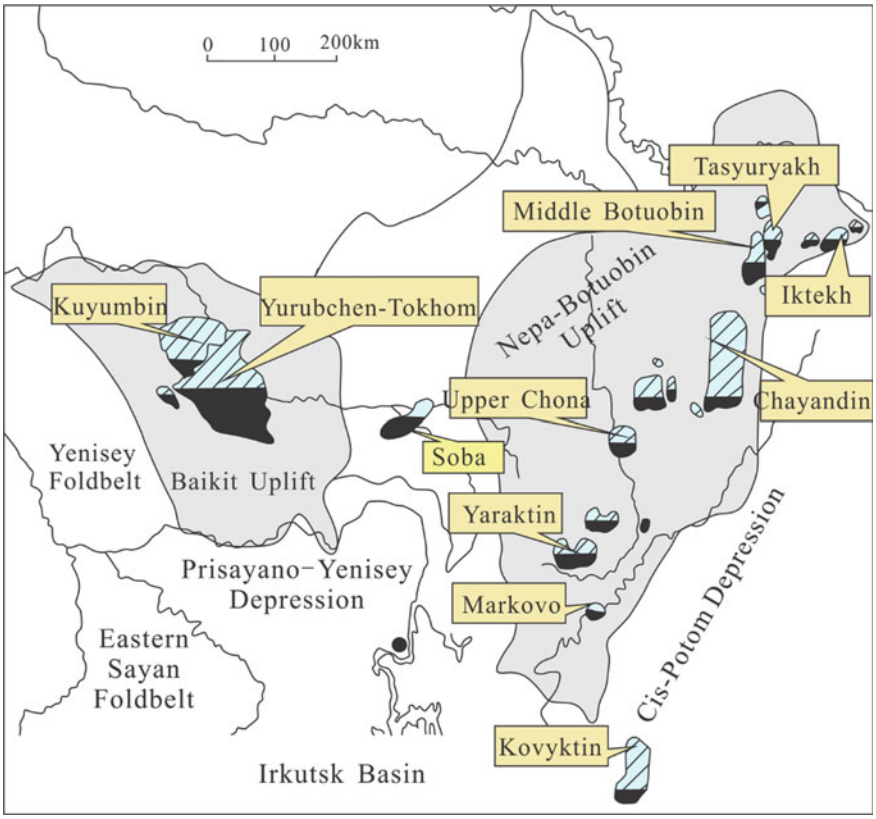

Fig. 11.5 Distribution of major oil- and gasfield at LTPP in Siberia Craton, Russia [Galimov (2014). Petroleum geology research of Precambrian in Russia (Eastern Siberia, Eastern European Platforms). An unpublished lecture notes in Beijing (in Russian)]. (Fedorov 1997, modified)

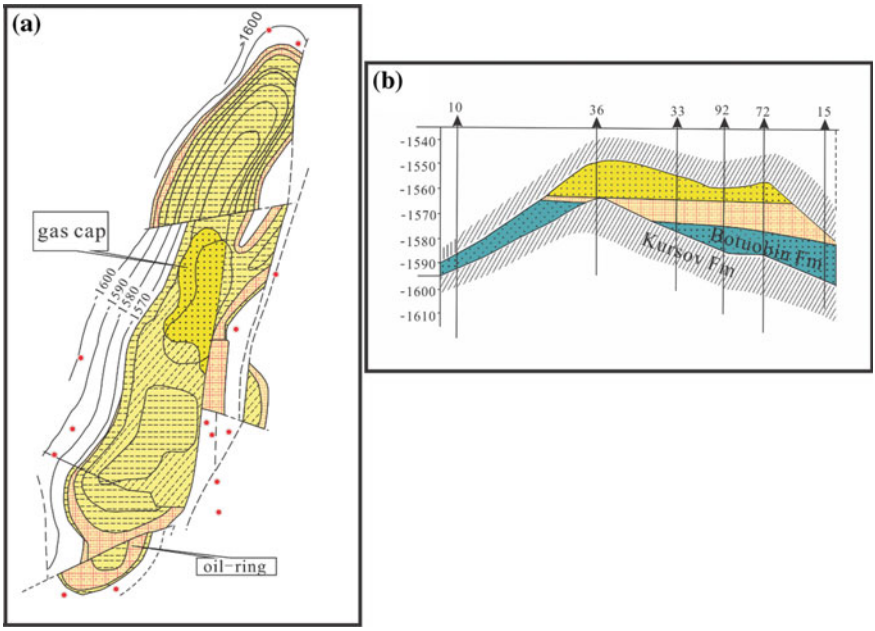

Fig. 11.6 Structural contour map (**a**) and oil and gas reservoir section (**b**) of Middle Botuobin Oil–Gas Field (Tong and Xu 2004)

in Beijing (in Russian).), the reservoir was sourced by Riphean muddy carbonate source bed② (Tong and Xu 2004; IHS Energy Group. 2005. International Petroleum Exploration and Development Database. Colorado; Frolov et al. 2015).

As for the oil and gas accumulation conditions, Kuznetsov (1997) proposed that Riphean source and reservoir beds are unconformably overlain by Vendian succession, which are distributed in the Baykit Uplift and Katanga Saddle. In this region, all the fields (such as Yurubchen-Tokhm Oil–Gas Field) produce oil and gas from topmost Riphean dolostone reservoirs and regional seals are provided by carbonate, mudstone and salt of Vendian and Early Cambrian age. Riphean thick shale beds may serve as intraformation seals. Frolov et al. (2015) proposed that the Riphean reached the maximum burial around mostly in Palaeozoic time in the intracratonic palaeobasins. While a modelling calculation shows that most of the hydrocarbons migrated prior to the Devonian and that subsequent migration was significant (Kuznetsov 1997).

11.2.1.5 Timing of Oil Entrapment

Based on oil geochemistry and basin modeling, Everett et al. indicate that the Eastern Siberian source beds as being Late Riphean to Early Vendian in age, the critical moment or timing of oil entrapment was controlled primarily by deposition of a

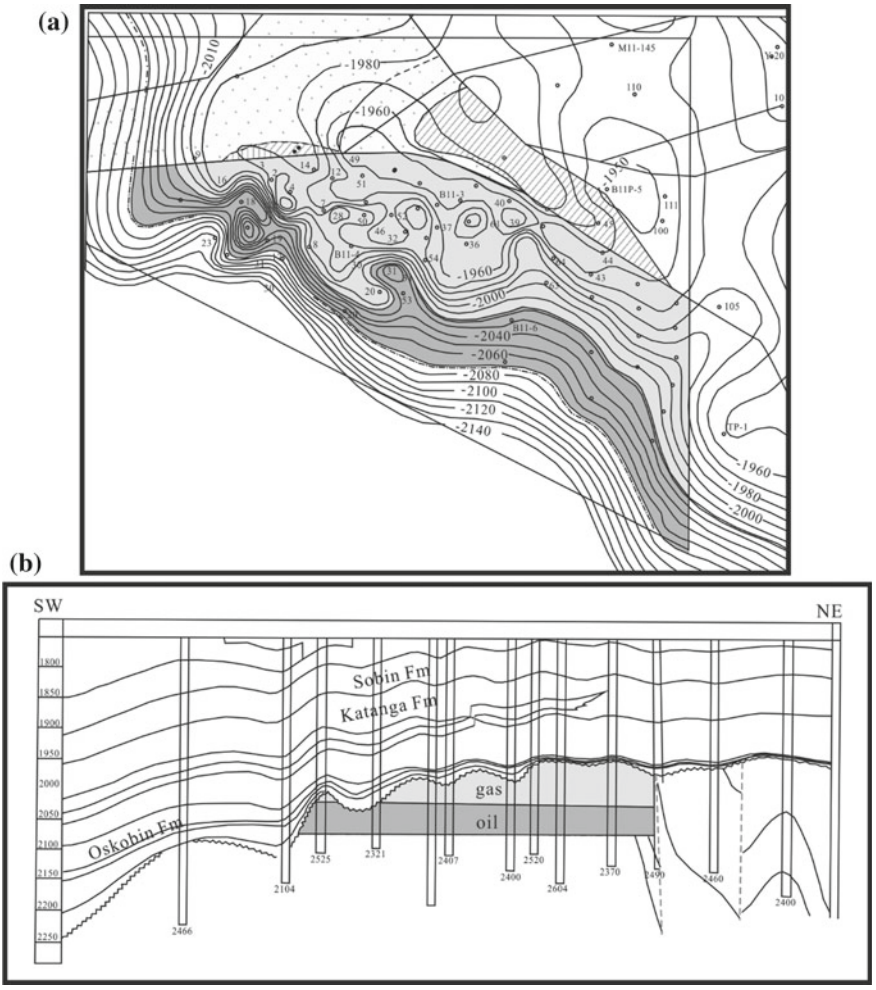

Fig. 11.7 Structural contour map (**a**) and oil and gas reservoir section (**b**) of Yurubchen-Tokhm Oil–Gas Field (Tong and Xu 2004)

salt seal in Early Cambrian, hydrocarbon accumulation was effectively ended in the Late Ordovician–Early Silurian, fifty percent of the Nepa-Botuobin gas samples may be classified as wet gases, implying source bed thermal maturity levels less than a vitrinite reflectance value of 2.0% with the remaining samples as thermogenic dry gases, most likely resulting from the relatively rapid over-maturation of the source rock during regional metamorphism and uplift.

11.2.2 Moscow and Kama-Belsk Basins in East European Craton (Russia)

East European Craton is also called Russia Craton, where oil and gas fields have been found in the Palaeozoic Devonian, Carboniferous and Permian strata. To present, however, no commercial hydrocarbon accumulations have been found within the Proterozoic sequences, while, in many cases, oil-seeps and low oil production in the Neoproterozoic Vendian sequence has been found in some exploratory wells. A number of large oil prospective regions could present in the East European Craton, e.g., Moscow and Kama-Belsk Basins① (Fig. 11.8; Fedorov 1997. Galimov (2014). Petroleum geology research of Precambrian in Russia (Eastern Siberia, Eastern European Platforms). An unpublished lecture notes in Beijing (in Russian).).

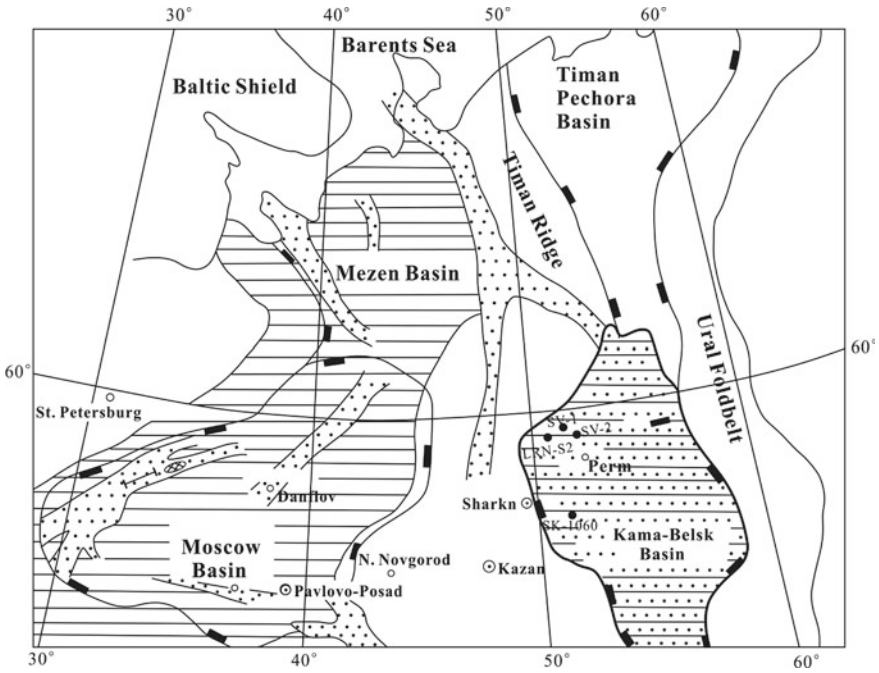

Fig. 11.8 Distribution of Proterozoic sedimentary basins on the East European Craton and related exploratory wells. LRN. Larionov; SK. Sharkan; SV. Sivinsk; ●.well site; ○.city. (Galimov (2014). Petroleum geology research of Precambrian in Russia (Eastern Siberia, Eastern European Platforms). An unpublished lecture notes in Beijing (in Russian)). (Fedorov 1997, compiled)

11.2.2.1 Moscow Basin

As a typical intracratonic depression, Moscow Basin is located at the central part of the East European Craton (Fig. 11.8). Stratigraphic column of the basin is up to 5 km thick, in which the Proterozoic and Palaeozoic intervals are of approximately equal thickness, while the overlying Mesozoic is relatively thin. Within the Proterozoic succession, the Riphean sequence is the thickest one, whereas the Vendian strata the most widespread① (Galimov (2014). Petroleum geology research of Precambrian in Russia (Eastern Siberia, Eastern European Platforms). An unpublished lecture notes in Beijing (in Russian).).

Deep Seismic Sounding (DSS) data indicate that a mantle diapir (i.e., an uplift of Moho discontinuity) may be present beneath the basin, resulting in a system of EN-SW striking grabens with Riphean sediments. The graben system is identified as a rift origin by DSS investigation (Fedorov 1997).

Light oil flows have been recorded from the sandstones of Upper Vendian Redkino Series in Wells 1, 4 and 9 in the Danilov area (Fig. 11.8). Oil flows of 50 L/d, with simultaneous 1000 m^3/d of gas containing 92% hydrocarbons, has been recorded in Well 9. The oil density is 0.79–0.83 g/cm^3 with gasoline fraction 26% to 35–42% and sulphur content 0.04–0.39%, while a dominance of paraffin (63–82%) over aromatics (3.7–3.9%) is distinctive. These light oils are referred to paraffinic-naphthenic hydrocarbons, its low-density fraction may not be removed, or to which a low-density fraction could be added by recent relatively young migration, possibly Meso-Cenozoic? (Fedorov 1997).

11.2.2.2 Kama-Belsk Basin

The Kama-Belsk Basin is a pericratonic depression located at the eastern margin of the East European Craton (Fig. 11.8). The basin contains the greatest thickness of Riphean sequence (up to 10 km), and is overlaid by Vendian sequence, according to drilling and geophysical data① (Galimov (2014). Petroleum geology research of Precambrian in Russia (Eastern Siberia, Eastern European Platforms). An unpublished lecture notes in Beijing (in Russian).).

In addition, heavy oil flows with output of 1 m^3/d–7 t/d have been recorded from the Vendian reservoirs respectively in Sivinsk-1, Sivinsk-2, Larionov-52 and Sharkan-1060 Wells (Fig. 11.8). Most of the oils belong to naphthenic-base crude. The oil in Sharkan Field is typical: its oil density is as high as 0.97 g/cm^3, resin plus asphaltene contents up to 30% and gasoline fraction 26% to 35–42%, which would be similar to biodegraded oil (Beijing Petroleum Exploration and Development Institute and North China Petroleum Bureau 1992; Fedorov 1997), whereas the oils are also "light" in carbon isotopic ratios showing a $\delta^{13}C$ value −31‰, which differs from that of Palaeozoic oils and sedimentary organic matter in the East European Craton, but is still similar to Riphean and Vendian oils and sedimentary organic matter on the Siberia Craton (Vysotsky et al. 1993).

11.2.3 Sultanate of Oman Basins in Eastern Arabian Craton

11.2.3.1 Regional Geological Setting

With a territory area of about 30×10^4 km^2, Sultanate of Oman is situated on the eastern margin of Arabian Peninsula or Arabian Craton (cf. the inset in Fig. 11.9). Oil exploration in Oman began in 1925, however the first discovery was not made until 1962. During early 1998, the average daily oil production in Oman was up to 900,000 bbl/d (ca. 12.3×10^4 t/d; Knott 1998).

A series of sedimentary basins are developed within the interior of Oman, and constitute a NNE-trending system of restricted basins, incl. South Oman Salt Basin (SOSB), Fuhud and Al Ghabah Salt Basins (Fig. 11.9; Peters et al. 2003; Amthor et al. 2005), which may have stretched from the Indian Craton across the eastern extremity of the Arabian Craton to the Hormuz Salt Basin of North Iran and possibly beyond (Amthor et al. 2005). Seismic data indicate that the western margin of the SOSB is delineated by structurally complex transpressional deformation fronts (Immerz et al. 2000). On the contrary, its eastern margin is characterized by onlap and thinning of basin strata onto a structural high close to modern-day coast of Oman (Fig. 11.9; Amthor et al. 2005).

11.2.3.2 Stratigraphic Division

Table 11.2a shows a generalized stratigraphic column of the Neoproterozoic–Cambrian in Oman (Amthor et al. 2005; Grosjean et al. 2009). The salt-bearing Late Neoproterozoic to Early Cambrian succession is represented by the Huqf Supergroup in Arabian Craton. The supergroup overlays unconformably on an old crystalline basement (Bowring et al. 2007) and is divided into three groups (from base to top): Abu Mahara, Nafun and Ara Groups. The Abu Mahara and Nafun Groups are subdivided into six lithostratigraphic units (not in stratigraphic order): siliciclastics (Ghadir Manqil, Masirah Bay and Shuram Formations) and carbonates (Khufai and Buah Formations).

The Ara Group consists of a thick cyclic sequence of carbonates, evaporites and associated siliciclastics, which can be subdivided into five formations., i.e., Birba, "U"-shale/Athel/Al Noor and Dhahaban Formations from base up (Table 11.2a). These formations are correlated to at least seven 3rd-order evaporite-carbonate sequences (A0 to A6 Cycles) established at the basin-center of the SOSB (Table 11.2a; Amthor et al. 2005), among which, Birba Formation comprises carbonate and evaporites of A0–A3 Cycles; the "U" Formation (in A4 Cycle) consists of organic-rich shales (ca. 80 m thick), carbonates, evaporat*e*s and ash interbeds, the ash beds could be used for providing U–Pb chronostratigraphic data; the Athel Formation (in A4 Cycle) comprises three members: ① Al Shomou Silicilyte Member, a thick (300–400 m) organic-rich chert; ② Thuleilat Shale Member; and ③ Athel Carbonate

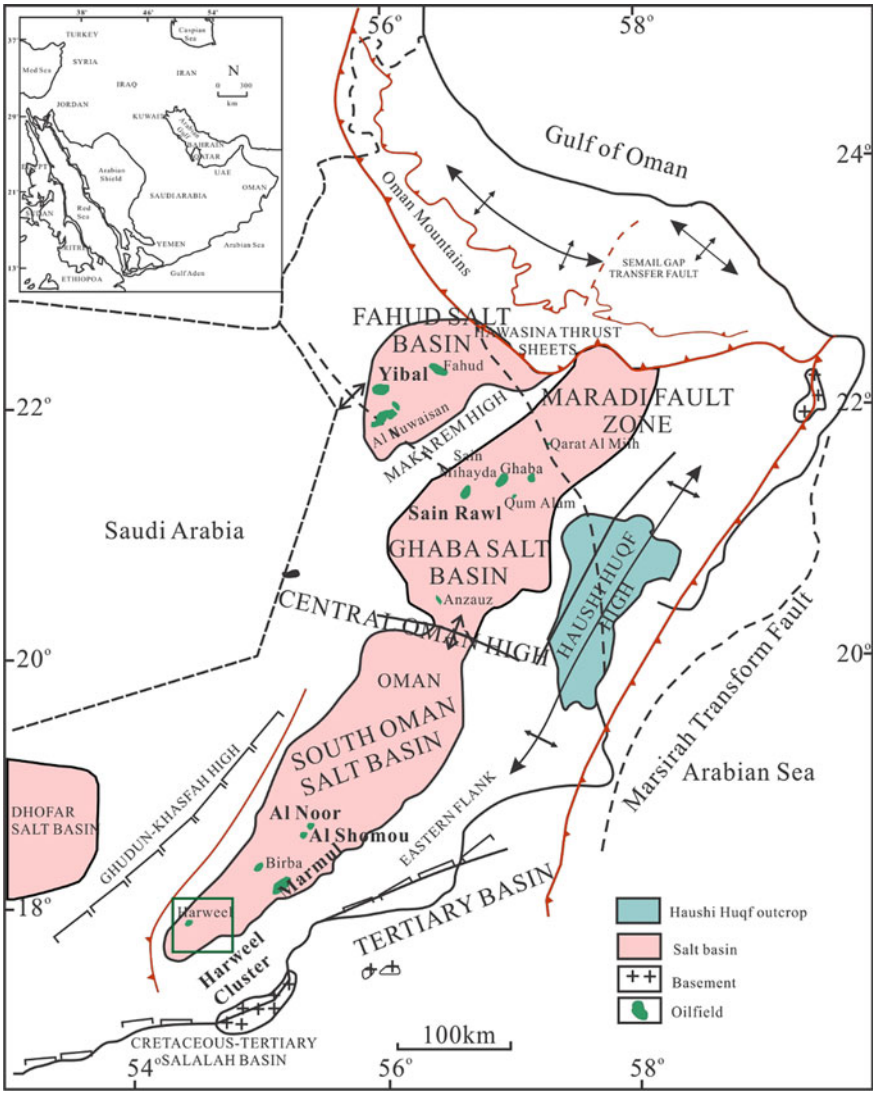

Fig. 11.9 Schematic tectonic map showing the distribution of the Neoproterozoic–early Cambrian salt basins and major oilfields in Oman (Peters et al. 2003; Amthor et al. 2005 compiled)

Member (Fig. 11.9b). The Al Shomou Silicilyte Member is stratigraphically "sandwiched" by two regional extensive organic-rich shale mems, the underlying "U"-Shale Formation and the overlying Thuleilat Shale Member (Table 11.2b; Amthor et al. 2005).

Table 11.2 Generalized stratigraphic column for neoproterozoic–Cambrian sequences in Oman

a

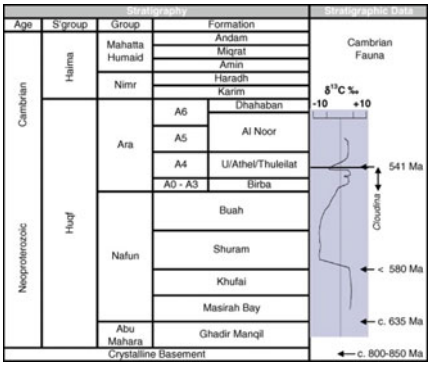

b

Group	Formation	Member	Sequence	Lithology
Huqf	Al Noor	Al Noor Salt	A6	Salt
			A5	Silicilyte
				Salt
	Athel	Thuleilat	A4	Thuleilat Shale / Athel Carbonate
		Al Shomou Silicilyte		Silicilyte
	"U"	"U"-Shale		Shale
		Salt		Salt

Note a. the composition of A4–A6 sequences in Ara Group (Grosjean et al. 2009); b. Amthor et al. 2005, simplified

11.2.3.3 Source Beds and Oil Types

Most of the South Oman oils have been proven to be associated with the source bed of the Huqf Supergroup by the correlation between the organic-rich rock units and reservoir fluids (Grosjean et al. 2009). Geochemically, two major oil types, the "Huqf" oil and "Q" oil, were recognized (Grantham et al. 1987), Both oil types show conspicuous mid-chain monomethyl-alkanes, trivially named "X compounds", similar to the organic matter within the Huqf source rocks, being considered a distinct character of Precambrian–Cambrian sedimentary organic matter. Accordingly, a straightforward correlation has been established between these oils and the Huqf Supergroup (Grantham 1986; Grantham et al. 1987; Terken et al. 2001).

11.2.3.4 Silicilyte and Carbonate "Stringer" Reservoirs

Huqf oils are found respectively in the Ara carbonate "stringer" and the intra-salt Athel silicilyte reservoirs (Figs. 11.10 and 11.11) as well as in the Cambrian Haima and Permo-Carboniferous Haushi reservoirs, particularly along the eastern flank of the SOSB. In contract, "Q" oils occur mostly in central Oman, but can also be found in the northernmost part of the SOSB, where encountered in the same well, "Q" oils occur in reservoir that overlie those of "Huqf" oils (Grosjean et al. 2009).

The most significant hydrocarbon reservoirs in Huqf Supergroup are the carbonate "stringer" and "silicilyte" reservoirs found at depth up to 4–5 km, both of which are stratigraphically intimately related and sealed by Ara salt in the SOSB (Figs. 11.10 and 11.11).

The "silicilyte" is a new petrological term specially for the microcrystalline silicon matrix, or called "microcrystalline chert", consisting of 80–90% microcrystalline

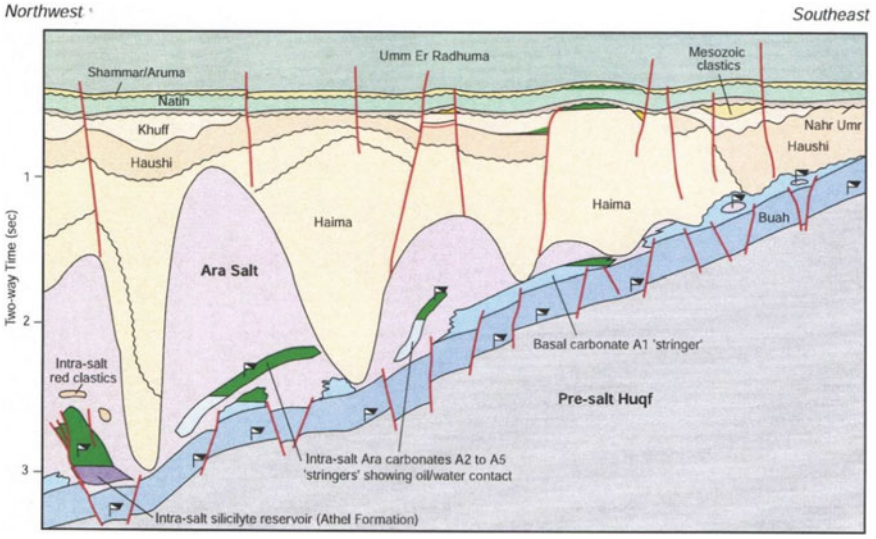

Fig. 11.10 Simplified geological cross-section through the SOSB to illustrate the geological occurrence of Ara "stringer" and "silicilyte" oil reservoirs enclosed by large, irregular salt. Bodies oil is indicated in green (Peters et al. 2003)

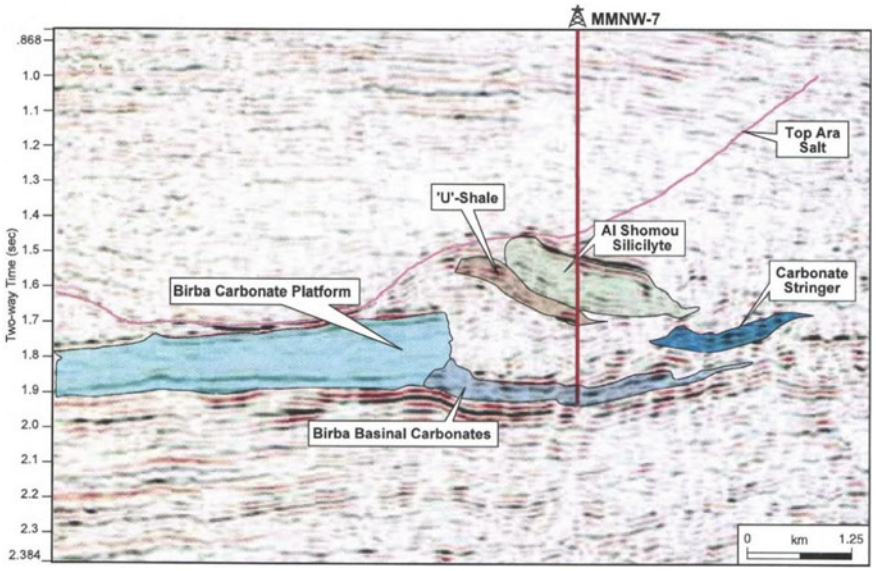

Fig. 11.11 Seismic section showing the geological occurrence of the carbonate stringer and silicilyte reservoir (Amthor et al. 2005)

quartz (crystal-size 2–3 μm), and commonly constitutes sheet-like aggregates, i.e., an up to 400 m thick and several kilometers wide slabs rich-in organic matter (TOC 7% in average). The Al Shomou silicilyte reservoir is typically characterized by light (48° API) sour oil, and finely laminated porous reservoir rocks with high-microporosity (up to 30%), low-permeability (only 0.02 mD), high overpressures (19.8 kPa/m in average gradient) and high present-day oil saturation (>80%; Amthor et al. 1998).

Whereas the Al Shomou Silicilyte is a unique source and reservoir rocks, and "sandwiched" by "U"-shale and Thuleilat shale (Fig. 11.11), all of which are rich-in organic matter, the 'silicilyte' reservoir should be self-charged, e.g., those in Al Noor and Al Shomou Fields (Fig. 11.9; Amthor et al. 2005), where unstimulated well initial flows of 250–600 bbl/d (ca. 34–82 t/d) could be increased to over 2500 bbl/d (ca. 342 t/d) by applying massive hydraulic fracturing technology (Wong et al. 1998). In August of 2000, the first oil was produced from the Al Noor Field (Fig. 11.9; Amthor et al. 2005).

Furthermore, the intra-salt Ara carbonate "stringer" reservoirs in the southern part of the SOSB (Figs. 11.10 and 11.11) are frequently dolomitized with an average porosity of 8–12% and 80–120 m-thick. Since they commonly contain intervals rich-in organic matter, "stringers" may form a self-charged oil reservoir encased in salt (Fig. 11.10), and such reservoirs can yield more than 6000 bbl/d (ca. 842 t/d) of oil in production tests, particularly if the reservoir is highly overpressured (Peters et al. 2003).

11.2.3.5 Petroleum Resources and Case Studies

Based on an earlier assessment of USGS, total petroleum resources of Ghaba and Fahud Salt Basins in north-central Oman were estimated as 11.3 bbbl of oil equivalent (ca. 15.5×10^8 t), The largest ones are Saih Rawl Field in the Ghaba Salt Basin and Yibal Field in Fahud Salt Basin (Fig. 11.9; Pollastro 1999).

During 1997–2002, there has been a string of exploration successes in discovering some 3.5×10^8 m^3 (ca. 2×10^{12} bbbl) of oil only at the Harweel Cluster region in SSOB (Fig. 11.9). This oil is deep and high pressure, comes with moderate gas-oil-ratio (GOR, 185 m^3/m^3), and the fluids contain 15% CO_2 and 5% H_2S. The Harweel Cluster consists of nine 'stringer' reservoirs found within intra-salt carbonate of Ara Group A2 and A3 Cycles in seven distinct oil fields. The fields are Dafag, Ghafeer, Harweel Deep, Rabab, Sakhiya, Sarmad and Zalzala. Only Ghafeer and Sakhiya have reservoirs in both of the Cycles. The reservoirs generally contain low permeability (1–10 mD), and a wide range of fluid properties from retrograde gas-condensate to black oil (O'Dell and Lamers 2003).

It is reported that the Marmul Oilfield, located in the south of SOSB (Fig. 11.9), contains an estimated 2 bbbl (ca. 2.74×10^8 t) of heavy oil (21.5° in average API gravity). Its glacial and periglacial reservoirs range from Cambrian to Permo-Carboniferous in age, with the oil being sourced by the source bed, which is ubiquitous in the middle potion of the Huqf Supergroup, and the oils display differing

degrees of biodegradation (Katz and Everett 2016). To add up the petroleum reserves in Marmul Oilfield, Ghaba and Fahud Salt Basins as well as Harweel Cluster region, it would be more than 21.2×10^8 t of oil equivalent in the aggregate.

11.2.3.6 Timing of Petroleum Generation and Reservoir Charging

As to oil generation, tacking the middle Huqf source bed at the Marmul Oilfield in South Oman Salt Basin (SOSB) as an example, Katz and Everett (2016) reviewed that based on its burial and petroleum generation histories, the oil generation was initialed at 520 Ma (i.e., Early Cambrian), occurring largely during the Ordovician and Silurian, and was complete by 350 Ma (i.e., Early Carboniferous; Terken et al. 2001). Apatite fission track data suggest a significant uplifting during the Devonian (Visser 1991), and so almost the entire Silurian, Devonian and Carboniferous are missing (Aley and Nash 1984). The equivalent vitrinite reflectance eqR_o values suggest that the maximum burial temperature was achieved during the Middle Cambrian–Early Silurian (Terken et al. 2001). Regionally, oil generation may have preceded trap development, thus requiring oil storage and remigration to develop the accumulation. Oil migration into the structure appears to have taken place during the Tertiary (Heward 1989).

Moreover, Pollastro (1999) considered that burial history reconstruction suggests an early minor stage of oil generation in Middle-Lower Huqf source bed during the Early Silurian and peak oil generation during Late Permian/Early Triassic (ca. 250 Ma) at the Yibal Field in Fahud Salt Basin, North Oman (Visser 1991). While Modelling suggests that cracking gas expelled from Huqf source bed charged structures across the Fahud Basin during a period ranging from 80 Ma to present day in the Fahud Basin (Amthor et al. 1998).

As a typical case for a successful Infracambrian-sourced play with Early Palaeozoic hydrocarbon generation, the structural stability of Oman, and the presence of a salt super-seal would facilitate the preservation of these early generated oils.

11.2.4 India and Pakistan Basins in Indian Craton

The Meso-Neoproterozoic sedimentary basins in India and Pakistan share similar tectonic settings and stratigraphic depositional environments, containing three major petroliferous regions, i.e., Central Indus, Vindhyan and Cuddapah Basins (Fig. 11.12).

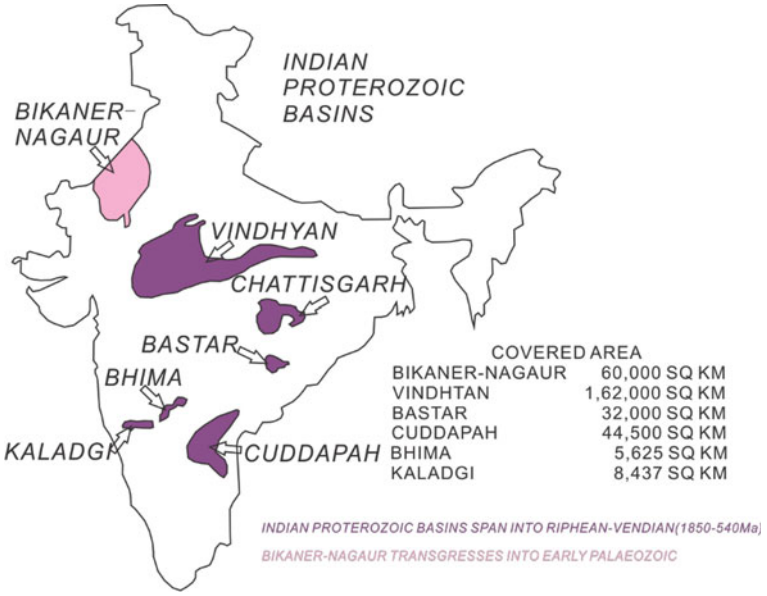

Fig. 11.12 Distribution of the major Meso-neoproterozoic sedimentary basins in the Indian Craton (Bhat et al. 2012)

11.2.4.1 Central Indus Basin: Punjab Platform and Bikaner-Nagaur Basin

(1) **Regional geological setting**: The Central Indus Basin (CIB) is situated geographically at the border area of Pakistan and India, and geologically on the northwestern segment of the Indian Craton. The limits of CIB are defined by the NE-SW trending Aravallis Range to the east and the Solaiman Range to the west (Fig. 11.13a). This large sedimentary basin covers approximately 29×10^4 km^2. There are different geological nomenclatures used in CIB, it is tectonically named the Punjab Platform on the Pakistan side within the centro-western CIB, and also the Bikaner-Nagaur Basin on the India side within eastern CIB, respectively (Fig. 11.13). On the Pakistan side, the CIB could be divided into three tectonic units from east to west: ① the Punjab Platform-Bikaner Basin, ② the Sulaiman Foredeep/Depression, and ③ the Sulaiman Range/Fold Belt (Qadri 1995; Fig. 11.13)

The Punjab Platform is a broad monocline dipping gently to the west towards the Sulaiman Depression (Fig. 11.13; Asim et al. 2015) covering an area of more than 10×10^4 km^2, and also extends eastward into India where it is called as Bikaner-Nagaur Basin (Fig. 11.13; Aadil and Sohail 2011; Bhat et al. 2012). Stratigraphically, evidence of drilled wells confirms the presence of the Neoproterozoic-Cambrian successions along and across the eastern border between Pakistan and India, and its thickness of ca. 1500 m is reported from Marvi-1 Well drilled at the southeastern part

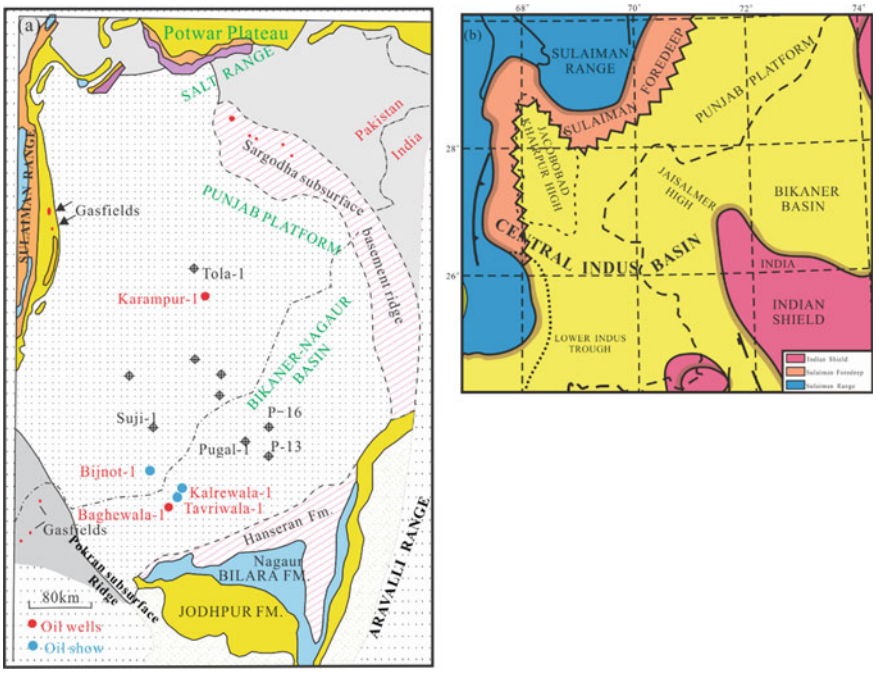

Fig. 11.13 The location and oil-exploratory well sites of the Bikaner-Nagaur Basin, India and the Punjab Platform, Pakistan (**a**) and the tectonic units of Central Indus Basin (**b**). **a** Ghori et al. 2009; **b** Aadil and Sohail 2011, modified

of Pakistan (Bhat et al. 2012). The location, oil-exploratory well sites and generalized stratigraphic correlation of the CIB are shown in Fig. 11.13 and Table 11.3 (Ghori et al. 2009; Aadil and Sohail 2011).

Table 11.3 Neoproterozoic-lower Cambrian stratigraphy of CIB (Ghori et al. 2009, modified)

Age	Punjab platform group/Formation	Bikaner-Nagau basin group/Formation
Cambrian	Kussak Khewra	Upper carbonate
Mesoprotereozoic	Salt range formation (Karampur-I Well)	Hanseran formation, evaporite
		Bilara Formation, laminated-dolostone (Baghewala-I Well)
		Jodhpur formation, sandstone (Baghewala-I Well)

Note Oil-producing wells are indicated within brackets

(2) **Petroleum geology and resources**: Oil exploration in the Punjab Platform started in 1950s. Neoproterozoic and Cambrian reservoirs have been unsuccessfully explored although only 12 wells have been drilled for Neoproterozoic and Cambrian (Hasany et al. 2012). Despite these failures, heavy asphaltic oil was first produced from fractured dolostone within the Neoproterozoic Salt Range Formation at the Karampur-1 Well of Punjab Platform in 1959, but no commercial hydrocarbon output obtained yet (Fig. 11.13a; Table 11.3; Ghori et al. 2009). However, the major heavy oil discovery was made at a shallower depth (1103–1117 m) in the Baghewala-1 Well, Bikaner-Nagaur Basin in 1991, only some 7 bbl (ca. 0.96 t) of sulfur-rich heavy oil (17.6°API, ca. 0.953 g/cm^3) was originally produced from Neoproterozoic Jodhpur sandstone and Bilara carbonate reservoirs (Fig. 11.13a; Peters et al. 1995; Ghori et al. 2009; Hasany et al. 2012; Asim et al. 2015). The oil is non-biodegraded as evident from the abundant presence of n-paraffin and acyclic isoprenoids (Peters et al. 1995; Asim et al. 2015), it should be the marginal mature oil. However, good oil shows were also reported from the Bijnot-1 Well on the Punjab Platform as well as the Kalrewala-1 and Tavriwala-1 Wells in the Bikaner-Nagaur Basin (Fig. 11.13a; Ghori et al. 2009). While the isopach maps show that the Cambrian and Precambrian depocenter were in southeast part of the Punjab Platform, and sediments would be buried at deeper level in west towards Sulaiman Depression in CIB (Aadil and Sohail 2011).

The Baghewala-1 oil is considered to be sourced from sulphur-rich organic matter in the laminated carbonates within the Neoproterozoic Bilara Formation which contain moderate to high TOC and HI typical of oil-prone organic matter, up to 400 mg HC/g TOC, and show T_{max} values of ≥436 °C, indicating marginally mature source bed within the early oil window based on the source biomarkers (Peters et al. 1995; Ram 2012; Asim et al. 2015). In addition, the geochemical characteristics of Baghewala-1, Karampur-1 and Kalrewala-1 oils are very similar to that of oils and source rocks from the Neoproterozoic-Lower Cambrian Huqf Supergroup in Oman (Peters et al. 1995; Sheikh et al. 2003; Ghori et al. 2009).

The reported geological reserves for the Baghewala Oilfield are 628 Mbbl (ca. 8540 × 10^4 t) of oil, and it contains four separate reservoirs. The oldest reservoir consists of sandstone within the Ediacaran Jodhpur Formation with a porosity of 16–24% and oil saturation ranging from 65 to 80%. The Early Cambrian upper Carbonate Formation dolostone forms the youngest reservoir with porosities ranging from 7 to 15% (Peters et al. 1995; Sheikh et al. 2003; Ghori et al. 2009).

11.2.4.2 Vindhyan Superbasin

(1) **Regional geological setting**: The arcuate-shaped Vindhyan Superbasin is located at the central segment of Indian Craton (Fig. 11.12). It contains a more than 5000 m-thick sequence of sandstones, shales and limestones with the Late Mesoproterozoic–Early Cambrian ages, and occupies an area of ca. 16.2 ×

10^4 km^2, among which ca. 8000 km^2 extends into the Ganga Valley Basin in the north and northeast beneath the Cenozoic sediments of the Himalayan Foredeep. To date, however, no commercial hydrocarbon has been discovered in the Vindhyan Superbasin yet (Ojha 2012).

The Ganga Valley Basin comprises the northern continuation of the Vindhyan Superbasin, as a Precambrian–Lower Cambrian interior sag basin overlain by the Cenozoic Himalayan Foredeep Basin (Fig. 11.14; Table 11.4). There totally are five subsags identified in the Ganga Valley Basin based upon gravity anomalies. As a larger one, the Sarda Subsag aligned east–west, with a sediment thickness of more than 7000 m. A schematic WE geological profile across the Sarda Subsag is shown in Fig. 11.15.

(2) **Petroleum geology and exploration:** Geochemical studies indicate that TOC contents in Ganga Valley Basin is fair to good for hydrocarbon generation. The Lower Vindhyan Supergroup Madhubani Formation represents alternating shale, sandstone and limestone of subtidal lagoon facies, within this, the interval 4670–5144 m of the Bilaspur Well in the Sarda Subsag gives TOC in the range 1.62–2.24% for oil source rock and also potential source rocks in the basin are essentially confined to the upper Vindhyan Subgroup Ujhani Formation.

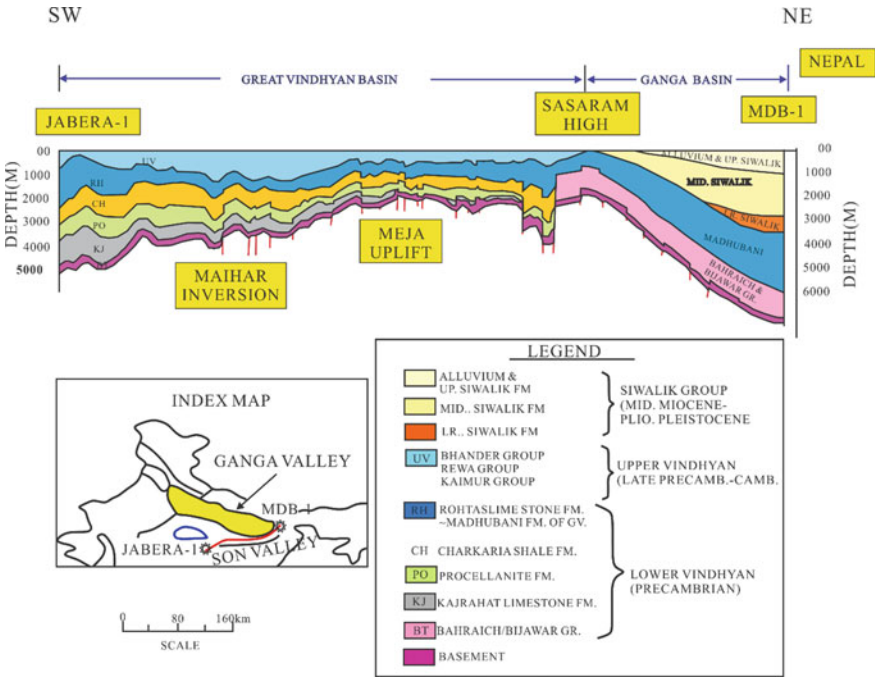

Fig. 11.14 A SW-NE trending schematic geological profile along the eastern Vindhyan Superbasin to the Ganga (Valley) basin (Ojha 2012)

Table 11.4 Generalized stratigraphic column of the Ganga Valley in Vindhyan Superbasin (Ojha 2012)

Period/Age	Group/Supergroup	Formation	Lithology in brief	Sedimentation cycle	Environment
Cenozoic Siwalik Sedimentation lower miocene onwards					
410–16 (394) Ma Hiatus					
Middle Silurian to lower devonian	Extension of upper vindhyan subgroup	Karnapur formation	Dominantly arenacious with fissile shale		Semi-arid, carbonate, shelf
Lower Ordovician to Lower Silurian		Tilhar formation	Limestones in association with calcarious shale	Puranpur-Gandak	
480–454 (26) Ma Hiatus					
Lower Ordovician to neoproterozoic	Upper vindhyan subgroup	Ujhani formation	Subgreywacke to arenite, fissile shales, occasionally intercalated with thin argillaceous-dolomitic limestones		Shallow, marine
1130–800 (330) Ma Hiatus					
Mesoproterozoic	Lower vindhyan subgroup (Semri Group)	Madhubani formation, Bahraich formation	Dolostone, limestone, Shale, siltstone and quartzite phyllites/schists	Bahraich-Sahaspur	Marginal, marine
Archaean	Basement		Granitic/gneiss rocks	Craton	

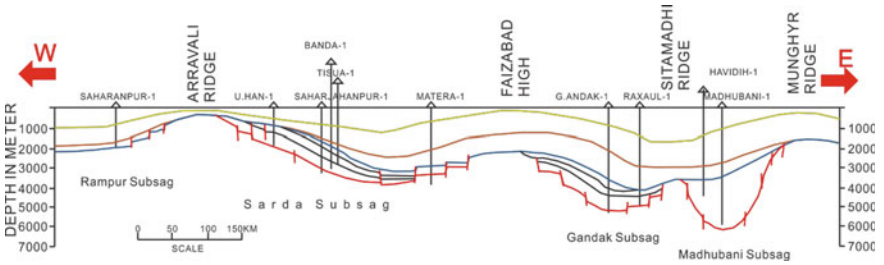

Fig. 11.15 A schematic WE geological profile across the Ganga (Valley) Basin showing the distribution of four subsags within the basin (Ojha 2012)

While the Madhubani Subsag also developed more than 7000 m thick sedimentary succession. As the deepest one, Madhubani-1 Well has been drilled up to a depth of 5957 m in this subsag (Fig. 11.15), and minor gas show was reported from the Madhubani Formation in this well with a C_1 count greater than 97% probably as deeply buried dry gas. Many zones have also displayed fluoresce, indicating the presence of hydrocarbons during drilling operations (Ojha 2012).

The Son Valley Basin constitutes the most-eastern segment of the Vindhyan Superbasin (see the index map in the Fig. 11.14). It shares the similar stratigraphic and petroleum geological conditions with the Vindhyan Superbasin. In addition, non-commercial hydrocarbon was discovered in the first exploratory well, Jabera-1 Well, within the Son Valley Basin. It was drilled to a depth of 3597.7 m, and showed the presence of gas at many levels during drilling (δC_1 value 39.0‰) and also flowed a non-commercial quantity of 2000–3000 m^3/d of gas from the upper part of the Jardepahar Formation in the Semri Group (or called Lower Vindhyan Subgroup; Ram 2012), but it is also reported that the flowed gas at 4000 m^3/d from the Lower Vindhyan Subgroup Charkaria Formation of Jabera-1 Well during DSTs (drill stem test). Its chemical composition is as follows: C_1 65.2–75.4%, C_2 5.3–13.6%, C_{3+} 0.8–17.8%, CO_2 0–0.3%, N_2 0–27.7%, He 0–0.21% as wet gas. However, these substantiated the hydrocarbon generation potential of the Vindhyan Superbasin (Ojha 2012).

11.2.5 Taoudenni Basin in West African Craton

11.2.5.1 Regional Geological Setting

As the largest broad intracratonic basin in the West and North Africa, with an area of ca. 2×10^6 km^2, the Taoudenni Basin developed over part of the West African Craton in southern and eastern Mauritania, and extends into northwestern Mali and southwestern Algeria (Fig. 11.16; Rahmani et al. 2009; Albert-Villanueva et al. 2016). The basin is bounded in the east by the Proterozoic Trans-Suharan Suture Zone and

in the west by the Hercynian Mauritanides Fold Belt. To the north is the Reguibat Shield and to the south the Ivory Coast Shield, both of which are composed of Archean metamorphic and granitic basement (Fig. 11.16; Bronner et al. 1980; Albert-Villanueva, et al. 2016).

The Taoudenni Bain preserves up to 1300 m of gently dipping (<1°) unmetamorphosed and virtually undeformed Proterozoic strata (Kah et al. 2009). The stratigraphic fill of the Taoudenn Basin can be divided into four supergroups which are bounded by four regional unconformities (Albert-Villanueva et al. 2016).

The Supergroup 1 of Meso-Neoproterozoic ages consists of continental to marine successions, which can be subdivided into five units, from bottom to top:

(1) The Mesoproterozoic Char Group onlaps the Archean basement, and comprises fluvial, aeolian and shallow-marine coarse- to fine-grained siliciclastics together with minor carbonate deposits, reaching a maximum thickness of 400 m at outcrop (Kah et al. 2009).

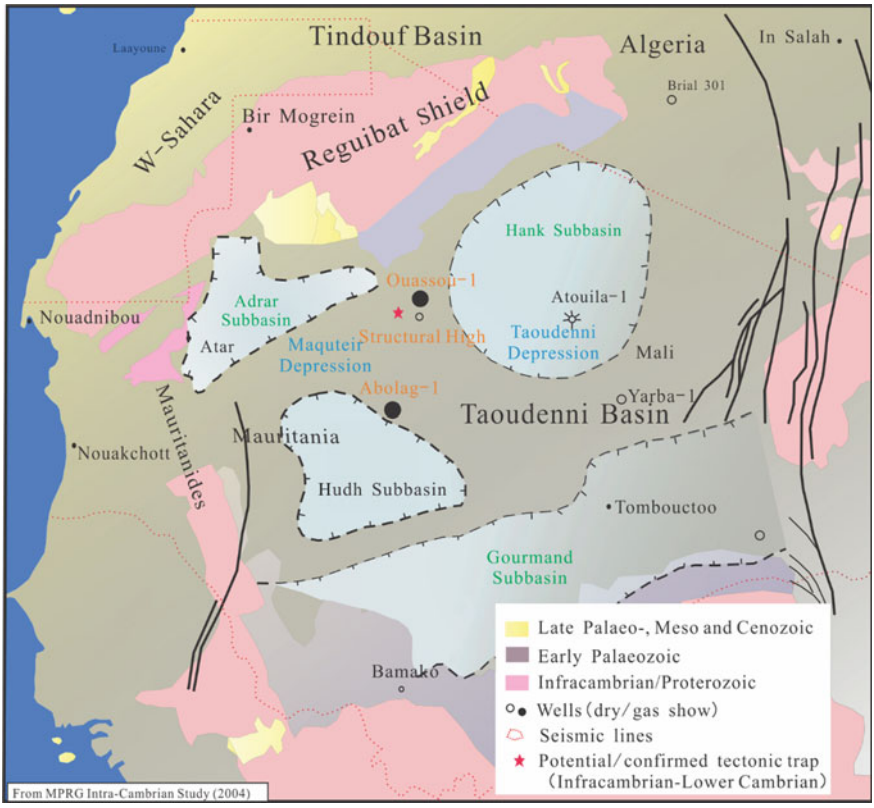

Fig. 11.16 Location of outcrops, wells and the extent of the Taoudenni Basin across Mauritania, Mali and Algeria (Lottaroli et al. 2009, compiled)

(2) The Late Mesoproterozoic-Early Neoproterozoic Atar Group consists of dolomitic carbonate, fine-grained siliciclastics and minor evaporitic strata, representing craton-wide flooding and shallow marine deposition (Kah et al. 2009), which has been reported in the Abolag-1 and Yarba-1 Wells with thicknesses of about 350 m and up to 600 m respectively (Gaters 2005). Rb–Sr analyses of glauconite and illite indicated that the Atar Group was deposited in Tonian-Cryogenian time (890 ± 35–775 ± 52 Ma, i.e. Early Neoproterozoic; Clauer 1981), but recent Re-Os geochemistry suggests that the group is some 200 Ma older, i.e., the Late Mesoproterozoic age (Rooney et al. 2010).
(3) Late Neoproterozoic Assabet el Haasiane Group is composed of prograding fluvio-deltaic sediments, including the Assabet Formation (thick fine-grained sandstones and siltstones), the Jebliat Formation (glacial deposits) and the Teniagouri Formation (thick Shales) in ascending order (Jean-Pierre et al. 2014). The fine-grained siliciclastic strata rich in Ediacara-type fauna (620–590 Ma, i.e., Late Ediacaran; Albert-Villanueva et al. 2016).

The Supergroup 2 of the Late Cambrian–Ordovician ages is composed of marine black sandy shales with epidote, sericite and siliceous shales, and siltstone interbedded with sandstones. The Supergroup 3 of Early Silurian age is constituted by quartzose sandstone and siltstone, while the Supergroup 4 of Devonian–Carboniferous age by marine and continental sandstone and shale successions (Albert-Villanueva et al. 2016). Furthermore, the Neoproterozoic–Carboniferous succession are covered by a thin sequence of Mesozoic–Cenozoic rocks in the center of this basin.

11.2.5.2 Petroleum Geology and Exploration

Organic-rich shales and limestones in the Taoudenni Basin have been reported from the Late Mesoproterozoic Atar Group in Mauritania nomenclature; equivalent to the Hank and Dar Cheikh Groups in Algrian nomenclature, and to the EI Mreiti Group in Khatt-Mauritanian Hank (Lahondére et al. 2005). These sediments are believed to have deposited between 890 and 620 Ma in northwest Africa. Infracambrian type I hydrocarbon source rocks, with TOC of 17–20% and hydrogen index (HI) of 800 mg HC/g TOC indicating a good oil generation potential, were penetrated in a water well drilled at the northwest part of the Taoudenni Basin (Gaters 2005).

Intense hydrocarbon exploration took place in this basin during 1972–1985. Only two deep exploratory wells have been drilled at the Taoudenni Basin, i.e., Abolag-1 (Texaco) and Quasa-1 (AGIP) Wells, in 1974 (Figs. 11.16 and 11.17). Gas show was recorded in the Abolag-1 Well at the interval of 2300–3000 m, and about 480 Mcf/d (ca. 13.6×10^6 m^3/d) of gas produced from the fractured limestones in the upmost Middle Infracambrian at ca. 3000 m depth during an "open hole" test, indicating the general viability of the Infracambrian play in the Taoudenni Basin. But the Quasa-1 Well was failed to reach the Infracambrian objective, and only recorded minor

uneconomic gas shows. It is likely that Quasa-1 Well did not test a valid closure (Figs. 11.16 and 11.17; Ghori et al. 2009).

In recent years, three wells were further drilled at the northwestern part of Taoudenni Basin, i.e., R Well (Albert-Villanueva et al. 2016), "A" (western well) and "B" Wells (eastern well), but no economical discovery was made so far (Fig. 11.17; Jean-Pierre et al. 2014). The R Well drilled by Repsol on the northwest margin of the

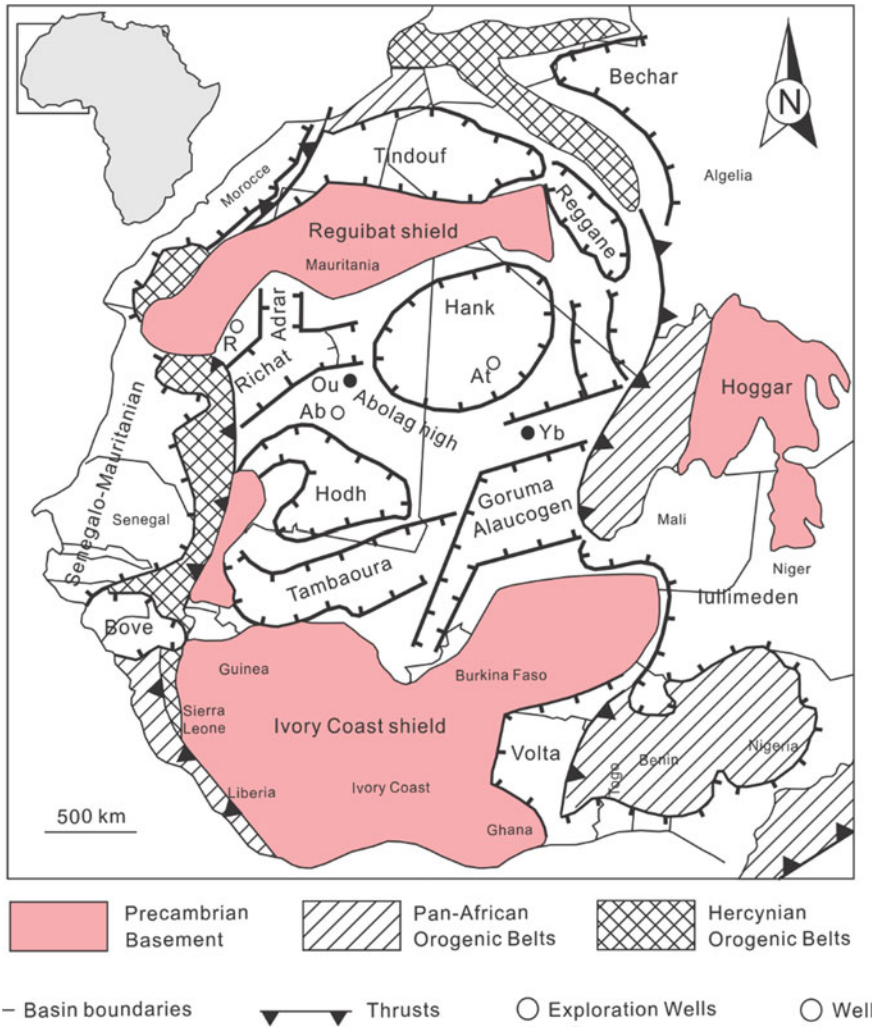

Fig. 11.17 Simplified structural map and oil exploratory well distribution of the Taoudenni Basin (Albert-Villanueva et al. 2016, modified). R. R Well; Ab. Abolag-1 Well; Qu. Quassou-1 Well; At. Atouila-1 Well; Yb. Yarba-1 Well

basin in 2000, which recorded solid bitumen and pyrobitumen within dolomitized stromatolitic carbonates in the Meso-Neoproterozoic Atar Group.

The presence of abundant pyrobitumen shards with a "jigsaw" disposition suggests that pyrobitumen may have been affected by hydraulic fracturing and hydrothermal process which affected the reservoir rocks possibly during Mesozoic times, causing hydraulic fracturing and the local thermal cracking of bitumen to pyrobitumen together with gas formation (Albert-Villanueva et al. 2016). Both "A" and "B" Wells yielded gas shows along the Assabet Formation sandstones and the Atar Group carbonates, but no significant hydrocarbon accumulation was found (Jean-Pierre et al. 2014).

Palynological and geochemical analyses indicate an age for the gas-bearing sequence ranging from Tonian to Early Cryogenian, with low organic abundance and high maturity (Kolonic et al. 2004. Infracambrian hydrocarbon potential of the Taoudenni Basin (Mauritania-Algeria-Mali). Maghreb Petroleum Research Group (MPRG). London-Bremen, 51 (unpublished)). As for the maturity of the Infracambrian source bed, the maximum values of equivalent vitrinite reflectance eqR_o are over 3.6% at the base, and over 2.6% on the top of the middle Infracambrian, while more than 2.0% on the top of the upper Infracambrian, indicating that an over-mature phase for the source bed (Gang 2009). Assuming present-day heatflow and a simple burial model, the Infracambrian should be within the gas-generating window in the deeper parts of the Taoudenni Basin (Gaters 2005).

11.2.6 McArthur Basin and Centralian Superbasin in Australian Craton

The Proterozoic strata are well developed within the boundaries of Australia, among which the Palaeo-Mesoproterozoic is distributed in the northern McArthur Basin and the southern Adelaide Fold Belt, while the Neoproterozoic principally in the Centralian Superbasin (or called "Centralian System"; Fig. 11.18).

11.2.6.1 McArthur Basin

(1) **Regional geological setting:** The McArthur Basin covers an area of ca. 20 × 10^4 km^2 and contains mainly Mesoproterozoic unmetamorphosed flat lying to folded sedimentary rocks that form a cratonic cover sequence near the eastern edge of the north Australian Craton (Fig. 11.18).

The Mesoproterozoic sequence has been subdivided into four lithostratigraphic sequences, i.e., Tawallsh, McArthur, Nathan and Roper Groups in ascending order, each is separated by regional unconformities (Jakson et al. 1988). The Tawallsh Group consist of over-mature arkose or quartz-rich sandstone about 4500 m thick. The McArthur and Nathan Groups have a total combined thickness of ca. 5500 m,

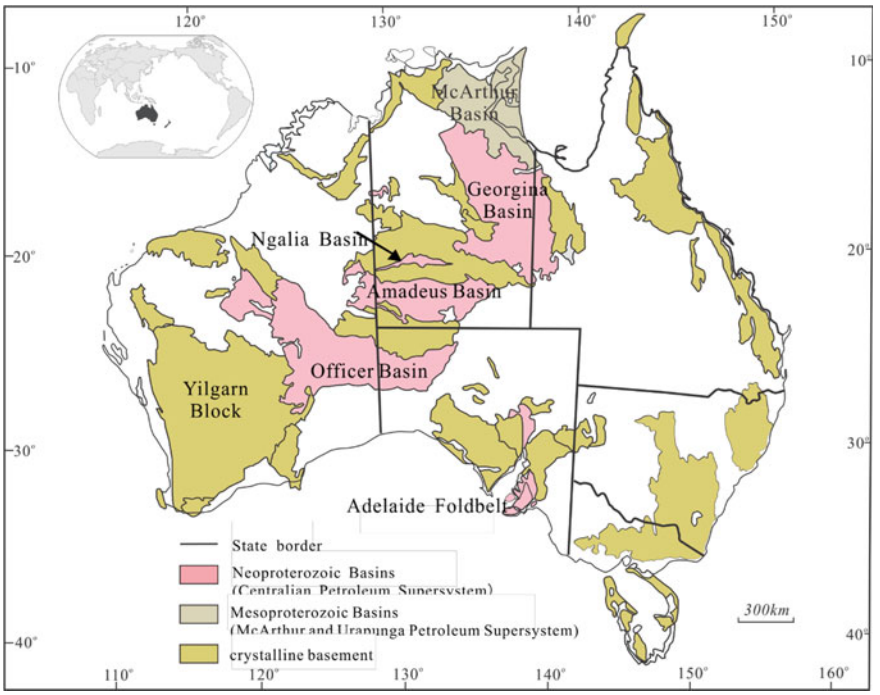

Fig. 11.18 Location of the proterozoic sedimentary basins in Australia (Ghori et al. 2009)

and consist mainly of evaporitic and stromatolitic cherty dolostones interbedded with dolomitic siltstone and shale that were deposited in a variety of marginal marine, lacustrine and fluvial environments, in which only the Barney Creek Formation in the middle of the McArthur Group has been dated. Three dates have been published: a U–Pb date of 1690 ± 30 Ma on Zircon crystals (i.e., Late Palaeoproterozoic age); two Rb–Sr dates of 1589 ± 28 Ma and 1537 ± 52 Ma on illite (i.e., Early Mesoproterozoic age). The uppermost Roper Group consist of 10–300 m thick quartz arenite, siltstone and commonly 100–400 m thick shale deposited in a stable marine setting, its oldest Rb–Sr age measured on glauconite sampled near the base of the group is 1390 ± 20 Ma; while a minimum age of 1280 Ma is indicated by K–Ar dating of dolostone sills that intrude the upper part of the group (ca. middle Mesoproterozoic age; Jackson et al. 1988).

(2) **Petroleum geology**: The most organic-rich source rocks in the Palaeo-Mesoproterozoic McArthur Basin are reported from the lacustrine Barney Creek Formation in the McArthur Group and from the marine Velkerri Formation in the Roper Group (Jackson et al. 1986; Womer 1986; Rawlings 1999a, b). Source rocks with comparable thickness and potential to Phanerozoic source rocks are

present in these sequences with TOC up to 7% containing types I and II kerogens, with thermal maturities ranging from marginal mature to over-mature (Crick et al. 1988).

Weeping oil and gas blowouts occurred in several shallow wells drilled in the McArthur Basin for lead–zinc exploration in the mid-1970s. Two different oil types have been observed: a heavily biodegraded oil containing associated galena, sphalerite and barite, which was probably generated during the phase of Pb–Zn mineralization; and a "golden honey color", very volatile oil generated during the later tectonic events (Wilkins 2007; Ghori et al. 2009). The Roper Group of McArthur Basin was one of the oldest sequence currently explored for HCs in Australia due to the presence of extensive oil and gas shows reported in stratigraphic and petroleum exploration wells drilled during the 1980s (Jackson et al. 1988; Ghori et al. 2009).

11.2.6.2 Centralian Superbasin

(1) **Regional geological setting**: The Centralian Superbasin includes the mid-Late Neoproterozoic fill (840–545 Ma) of the Amadeus, Geogina, Ngalia and Officer Basins, which developed as a single depositional system but separated into different structural units (Fig. 11.18; Walter and Gorter (1993). Centralian Superbasin, Australia. Petroconsultants Australia, Sydney (unpublished); Ghori et al. 2009). The superbasin contains four Neoproterozoic supersequences (Table 11.5):

① The Supersequence 1 (SS1; Early Cryogenian) commenced with a thick sand sheet, overlain by dolostones, limestones, evaporates and fine siliciclastics, which reaches a total thickness of more than 3000 m in the Officer Basin. This sequence is considered to be the most prospective for oil and gas exploration.

② The base of Supersequence 2 (SS2; mid-Late Cryogenian) is defined by the Sturtian glaciation deposits, which are overlain by widespread igneous sills and by shales with interbedded carbonates and sandstones. This supersequence is mainly developed within the Amadeus Basin.

③ The base of Supersequence 3 (SS3; Late Cryogenian) is defined by the Marinoan glaciation deposits which are continent-wide (Priss and Forbes 1981), and may be coeval with extensive tillites found over much of the globe as the products of global glaciation.

④ The basal part of Supersequence 4 (SS4: Edicaran) consists predominantly of sandstone, containing an "Ediacara fauna" and the upper part is Cambrian in age (Ghori et al. 2009).

Taking the Officer Basin as an example, this basin is elongated with a NW–SE trend, and contains over 8000 m of Neoproterozoic strata, overlain by Lower Palaeozoic rocks. Above three bounded sedimentary successions, i.e., the Supersequences 1, 3 and 4, exist unconformity throughout most of the Officer Basin, and these

Table 11.5 Generalized time and seismic stratigraphy, tectonic events, source, reservoir and seal rocks for the Officer Basin, western Australia (Ghori et al. 2009)

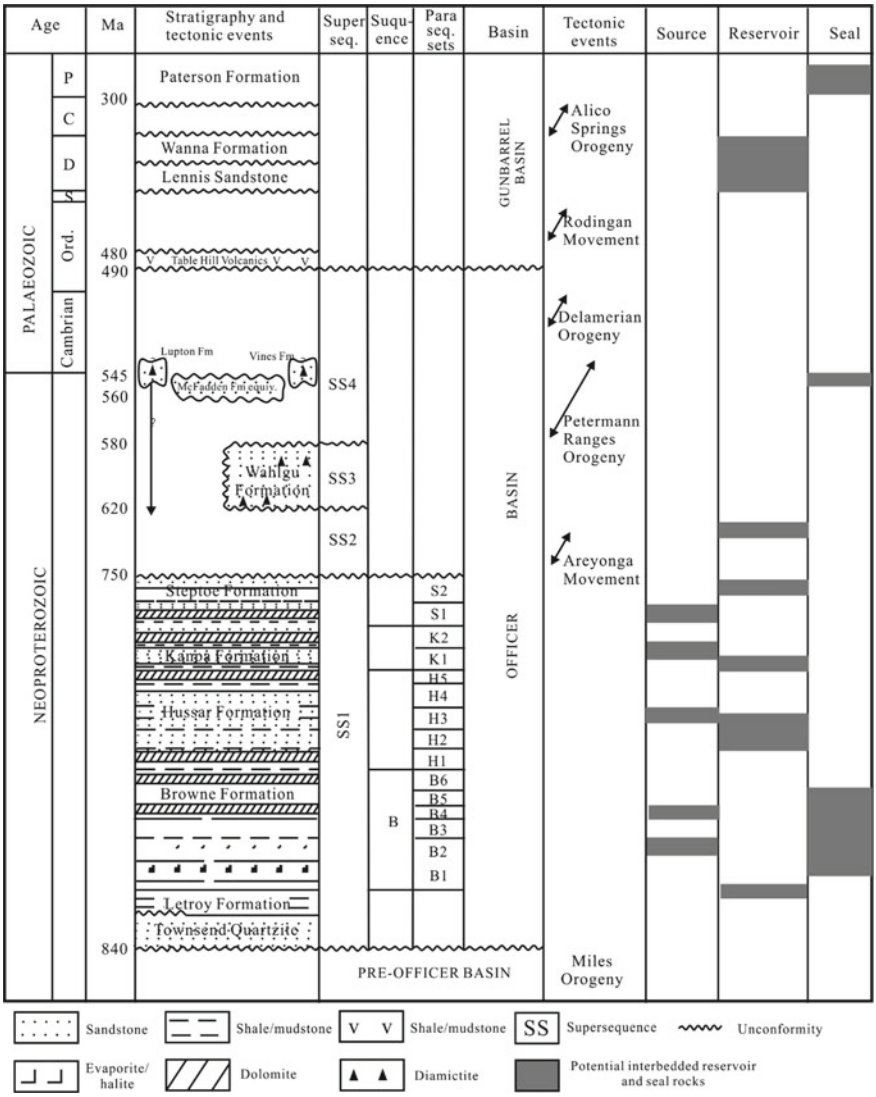

can be correlated with key tectonic episodes (Table 11.5). The Areyonga Movement appears to be responsible for the larger structures in the Officer Basin, and separates SS1 from SS3. Structural and stratigraphic variations within the overlying SS3 and SS4 are respectively attributed to later deformation related to the Petermann Ranges Orogeny and Delamerian Orogeny (Table 11.5; Wade et al. 2005). The overlying units within SS1 consist of conformable and laterally correlative genetic

parasequence units bounded by flooding surfaces. These units comprise the Browne (B1–6), Husssr (H1–5), Kanpa (K1–2) and Steptoe Formations (S1–2; Table 11.5). In most seismic lines, SS1 is characterized by continuous parallel reflectors that are traceable across most of the basin (Ghori et al. 2009).

(2) **Petroleum geology and exploration**: During three stages of petroleum exploration in the late 1960s, early 1980s and late 1990s, 16 wells and 19 seismic surveys have been undertaken (Fig. 11.19). The available geochemical data indicate the presence of thin source beds with fair-excellent HC generating potential in the Neoproterozoic successions in some exploratory wells and mineral drill holes. The organic-rich source beds occur in the B2 and B4 of the Browne Formation, the H3 of the Hussar Formation, the K1 of the Kanpa Formation and the S1 of the Steptoe Formation. Pyrolysis gas chromatography and extract analyses indicate that most of the organic matter in the source beds is oil- and gas-generating type II kerogen with TOC contents 0.93–2.05% (max. up to 21.5%), HI 131–498 mg HC/g TOC (min. 68–77 mg HC/g TOC) and T_{max} 413–471 °C. Basin modelling studies suggest that most of the HC generation potential of the Browne Formation was exhausted during the Neoproterozoic. However, the Hussar, Kanpa and Steptoe Formations were not so deeply buried, and the HC generation from these units extends into the Phanerozoic (Ghori et al. 2009).

Chronostratigraphy, tectonic events and location of source, reservoir and seal rocks are summarized in Table 11.5. Minor oil shows and numerous bitumen occurrences have been reported in many of the petroleum exploratory wells drilled in the basin (Table 11.6; Ghori et al. 2009). Despite early optimism for petroleum exploration, the Officer Basin has not been fulfilled yet (Jackson et al. 1988).

Since 1963, over 50 petroleum exploratory wells have been drilled in the Amadeus Basin, resulting in the significant discovery of the Dingo Gasfield in the Neoproterozoic-Lower Cambrian strata in 1981. Amadeus Basin is an EW-trending elongate downwarp about 17×10^4 km^2 in the central Australia (Figs. 11.18 and 11.20a). The basin margins are well defined to the north and south by igneous and metamorphic rocks of the Proterozoic Arunta and Musgrave Blocks. To the east and to the west, the basin margin is obscured by a cover of younger rocks.

The basin's major stratigraphic units are shown in Table 11.7. The stratigraphy reflects a basal Neoproterozoic succession of shelf, lagoonal, continental and shallow-marine sediments, including carbonate and evaporate, overlain by Palaeozoic sediments. The Neoproterozoic fine-grained clastic carbonate and evaporate rocks contain mainly gas-prone matter. A small amount of oil-prone kerogen derived from the Pertatataka and Areyonga Formations and Gillen Member of the Better Springs Formation suggests some oil-source potential for the Neoproterozoic succession.

Dingo Gasfield is located at approximately 75 km south of Alice Springs NT (Fig. 11.20b). Tectonically it appears as an anticline/dome structure with areal closure 68.9 km^2 and vertical closure 160 m (Fig. 11.20c). Stratigraphically, there are two gas-producing units discovered in the Dingo-1 Well, i.e., the Arumbera sandstone

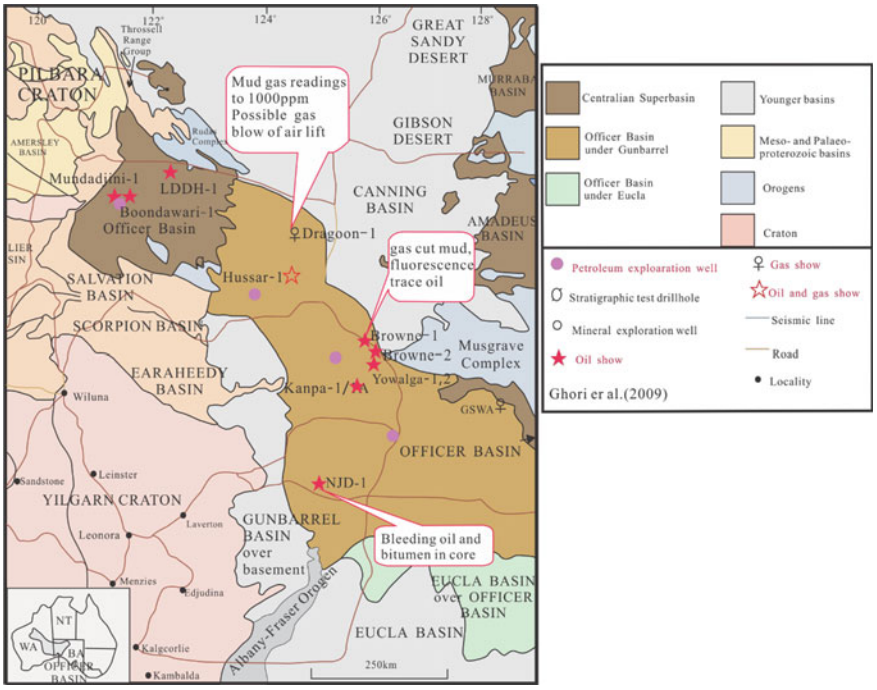

Fig. 11.19 Structural units, seismic survey and petroleum shows in the Officer Basin, western Australia (Ghori et al. 2009)

Table 11.6 Neoproterozoic hydrocarbon shows in Officer Basin, western Australia (Ghori et al. 2009)

Well	Quality of show	Formation
Boondawari-1	40% oil fluorescence, trace oil in core	Spearhole formation
Browne-1	Gas cut mud, cut fluorescence, trace oil in core	Browne formation
Dragoon-1	Mud gas to 10%, methane equivalent, including hydrocarbons up to pentane	Browne formation
Hussar-1	Mud gas readings to 1000 ppm; possible gas blow on air lift; trip gas to 4.6% total gas; 72% oil saturation from log analysis	Kanpa formation Hussar formation
Kanpa-1A	Dull yellow-orange sample fluorescence, light yellow-white cut fluorescence, brown oil stains in sandstone and dolostone cuttings	Kanpa formation
LDDH-1	Bitumen in core	Tarcunyah formation
Mundadjini-1	10% oil fluorescence in core	Spearhole formation
NJD-1	Bleeding oil and bitumen in core	Neoproterozoic
OD-23	Bleeding oil and bitumen in core	
Vines-1	Total gas peaks 25 times background	

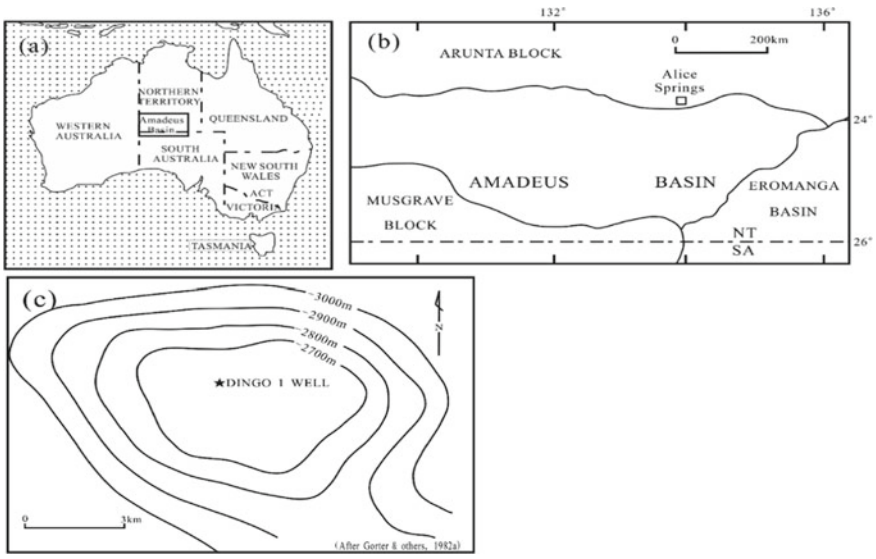

Fig. 11.20 Location of the Amadeus Basin (**a**) and Dingo Gasfield (**b**) as well as the structure contour map of Dingo Gasfield (**c**) (Ozimic et al. 1986)

Table 11.7 Stratigraphy of the Amadeus Basin (Wells et al. 1970)

Erathem/System/Series	Group/Formation/Member	Max. Thickness/m
Lower carboniferous–middle-upper devonian	Pertnjara group	3658
Lower-middle devonian–upper Silurian	Mereenie sandstone	975
Upper ordovician	Carmichael sandstone	91
Lower-middle ordovician	Larapinta group	2500
Cambrian	Pertaoorta group	>2102
Neoproterozoic	Julie formation Pertataka formation	610–1829
	Areyonga formation	396
	Bitter springs formation "Johnny Ck Beos"	914
	Heavitree Quartzite	457
Arunta complex		

at the base of the Lower Cambrian Pertaoorta Group, and the Julie Formation at the top of Neoproterozoic sequence. However, Dingo is an economic and undeveloped gasfield (Ozimic et al. 1986).

11.2.7 Midcontinent Rift System in the North American Craton (USA)

11.2.7.1 Regional Geological Setting

Although Precambrian rocks are distributed throughout the United States and commonly are present in the deeper parts of sedimentary basins, their hydrocarbon source rocks and resources are poorly known (Palacs 1997). However, the source rock potential and even some oil-seeps of the Meso-Neoproterozoic strata have been reported respectively in the Midcontinent Rift System in the North American Craton.

As a major structure unit in the North American Craton, the Midcontinent Rift System is delineated by strong gravimetric and magnetic anomalies, and infilled with up to 15 km of rift-related mafic volcanic rocks and up to 10 km of overlying sediments (Behrendt et al. 1988). Rocks of the rift system are exposed in the Lake Superior region of Michigan, northern Wisconsin and Minnesota, and extend in the subsurface through Iowa, Nebraska into northeastern Kansas (Dickas 1986c; Fig. 11.21). The 1500 km-long Midcontinent Rift System is a failed rift, characterized by a series of asymmetric basins filled with clastic rocks in places as thick as 9754 m (Anderson 1989; Palacs 1997). The rocks belong to the Meoproterozoic Keweenawan Supergroup, comprising a lower Oronto and an upper Bayfield Groups. The Oronto Group consists of the Copper Harbor Conglomerate, Nonesuch and Freda Formations in ascending order (Daniels 1982; Elmore et al. 1989). The Copper Harbor Conglomerate Formation is a red sandstone and conglomeratic unit up to 2 km thick, with an U–Pb age of 1087.2 ± 1.6 Ma (i.e., Late Mesoproterozoic age; Daniels 1982; Palacs 1997; Table 11.8), the 40–300 m thick green to gray siltstones and shales of the Nonesuch Formation have a whole-rock age of 1044 ± 45 Ma (Mauk and Hieshina 1992), while the Freda Formation is composed of up to 4 km thick red sandstones (Table 11.8; Mauk and Hieshina 1992).

11.2.7.2 Petroleum Geology

The potential for petroleum resources in the Midcontinent Rift System has long been recognized because of oil seeps and pyrobitumen within the Nonesuch Formation at the White Pine copper mine in the Lake Superior segment (Fig. 11.21; Dickas 1986c), where field and petrographic studies have established six types of petroleum occurrences:

① Liquid oil inclusions in veins filling or adjacent to thrust and tear faults;
② Droplet-shaped inclusions of solid pyrobitumen (altered petroleum) in veins, spatially associated with thrust and tear faults;
③ Subparallel trains of liquid oil inclusions in microfractures genetically related to microthrusts;
④ Solid pyrobitumen cement in sandstone;
⑤ Pore-filling petroleum in the “lower sandstone”;

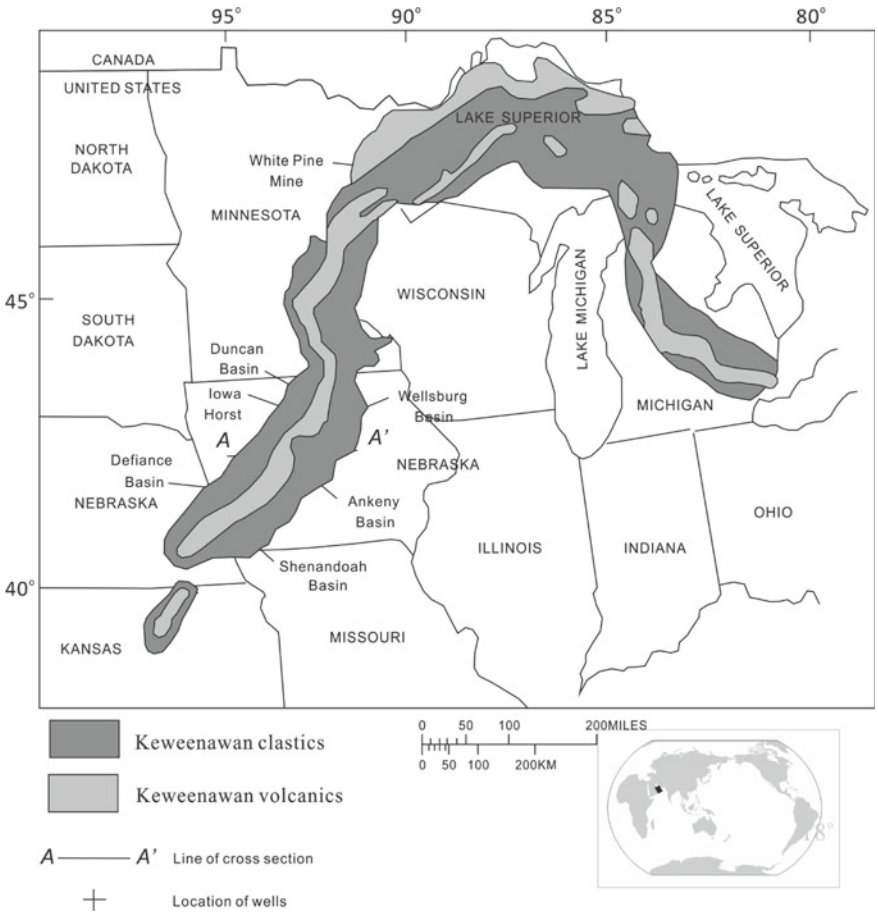

Fig. 11.21 Map showing the general location of major rock types of the midcontinent rift system. The four locations: ① Lake Superior segment outcrop belt; ② Minnesota segment, Lonsdale 65–1 Well, Rice County; ③ Iowa segment, Amoco Eischeid No. 1 Well, Carroll County; ④ Kansas segment, Texaco 1 Poersche Well, Washingron County and the Producers 1–4 Finn Well, Marshall County, which is 21 miles northeast of the 1 Poersche Well (Palacas 1997)

⑥ Active oil seeps occurred at shallow depth and in thin intervals of silty shales of the Nonesuch Formation throughout the mine, irrespective of local tectonic fabric. Oil seeps appear as 1–5 m-wide oozes of liquid oil emanating from faults, joints and roof bolt holes within the mine (Mauk and Hieshima 1992).

All seeps emerge from the back roof of the mine, suggesting that source or reservoir beds lie above the ore horizon. Oil also occurs locally in pores of sandstone, spatially associated with pyrobitumen cements, but no any bedding-plane parallel seep sources were observed (Palacs 1997). Types-①, ② and ③ inclusions, and Type-④ pyrobitumen cements in sandstone, are spatially associated with compressional

Table 11.8 Stratigraphic position of the Oronto Group Nonesuch Formation in Midcontinent Rift and the Chuar Group in Grand Canyon

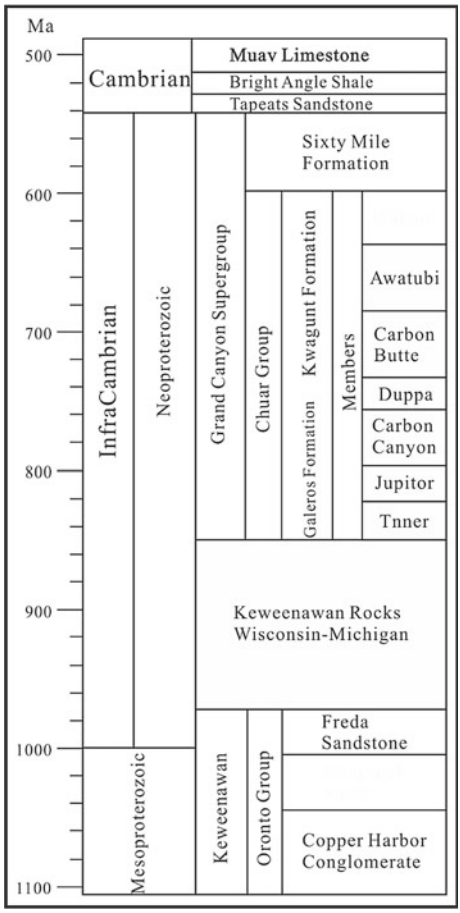

faults, suggesting that oil migrated into the White Pine mine along fault-related conduits synchronously with thrusting and mineralization (Mauk and Hieshima 1992).

In the Nonesuch Formation, the middle unit of the Oronto Group, ranging from ca. 76–213 m in thickness and averaging 183 m, consists of interbedded dark-gray to -green sandstone, siltstone and silty shale (Palacs 1997). The TOC for Nunesuch rocks is generally less than 0.3%. However, the TOC for finely laminated silty or calcareous shales in thin intervals ranges 0.25–2.8% and averages 0.6%, while the dichloromathane extractable bitumen contents averaged ca. 20 ppm with maximum of ca. 300 ppm (Pratt et al. 1991), while Rock–Eval T_{max} values of kerogen isolates were 435–440 °C, indicating maturity equivalent to the initial phase of oil generation for Type II kerogen (Pratt et al. 1991).

Palacs (1997) proposed that if thicker section of these finely laminated hydrocarbon- generating shales are downdip from the outcrop belt, and if those shales were subjected to high level of thermal maturation in the geologic past, the hydrocarbon source potential for the Lake Superior and the adjoining area in northern Wisconsin should be fair to good.

11.3 Distribution of Meso-Neoproterozoic Petroleum Resources in China

The Chinese Meso-Neoproterozoic sedimentary basins are distributed in three regions, i.e., the Yangtze Craton (YC) in South China, North China Craton (NCC) and Tarim Block (TB) in NW China (Fig. 11.22). So far two known Chinese Infracambrian gasfields, i.e., Weiyuan and Anyue Gasfields, are geographically situated within the centro-southern part of current Sichuan Basin, and tectonically referred to the Chuanzhong Uplift (used to be called Leshan-Longnvsi Uplift in geological literature) in western Yangtze Craton (cf. Chap. 14), while many asphaltic veins, with different size, sourced from the black shale of Neoproterozoic Sinian Doushantuo Formation, have been found in Longmenshan Nappe Zone on the northwest margin of western Yangtze Craton (Fig. 11.22; cf. Chap. 15). In addition, numerous Meso-Neoproterozoic indigenous liquid oil-seeps, asphalt, oil sandstone and bituminous sandstone have been discovered in the Jibei Depression within the Yanliao Faultd-Depression Zone (YFDZ), North China Craton (Fig. 11.22; cf. Chap. 12). However, so far there only are some potential Neoproterozoic-Lower Cambrian source beds found in Tarim Block (Fig. 11.22; cf. Chap. 6).

11.3.1 Chuanzhong Uplift and Anyue Gasfield in Western Yangtze Craton

11.3.1.1 Geological setting

In western Yangtze Craton, the Infracambrian sequences consist of Sinian Doushantuo and Dengying Formations as well as Lower Cambrian Maidiping, Qiongzhusi (or Jiulaodong), Canglangpu and Longwangmiao Formations in ascending order (Table 11.9), among which the black shales of Doushantuo and Qiongzhusi Formations are two major potential effective source beds. However, three stratigraphic/exploratory wells (i.e., Nvji, Wei-117 and Ziyang-1 Wells), have been drilled at the structural axial region of Chuanzhong Uplift, where there is an obvious trend of the Doushantuo stratigraphic thinning and/or lithofacies change from black shale of deeper water reducing sedimentary environment to purplish-red shale, dolostone and grey sandstone of shallow water oxidizing environments

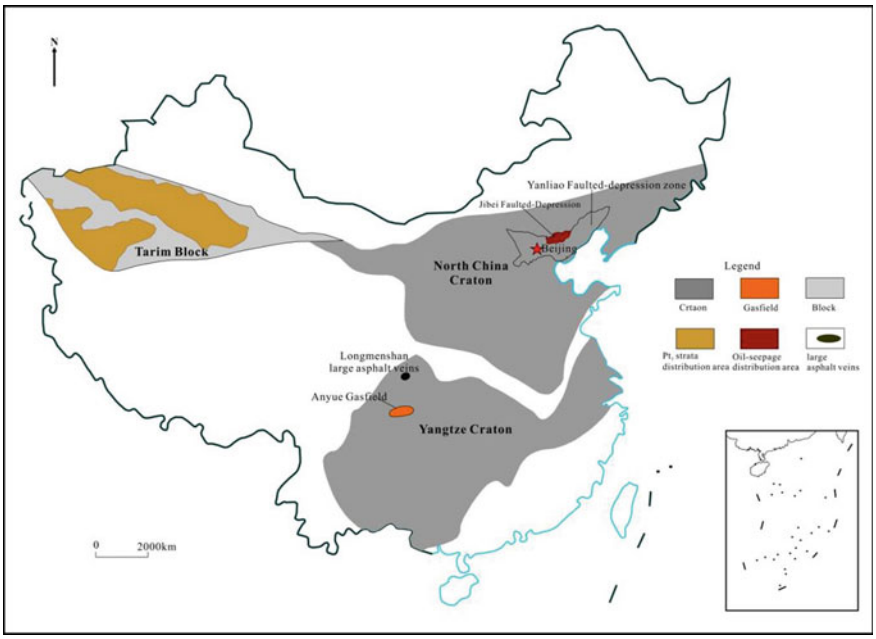

Fig. 11.22 Distribution of the Meso-neoproterozoic sedimentary basins in China

towards Chuanzhong Uplift by comparison with the surrounding depressions, which implies the emergence of Chuanzhong palaeo-uplift since early Sinian, and so Doushantuo shale source bed would be only distributed around the uplift. Moreover, the tops of Deng-2 and Deng-4 Members, Maidiping Formation as well as Longwangmiao Formation all appear as a disconformable contact with their overlying strata respectively (Table 11.9; cf. Chap. 14).

The seismic reflector structural contour map of Dengying top surface shows the current structural form of Chuanzhong Uplift, which occurs as a NEE-trending structural axis and shows the structural features of a large uplift with two secondary salients plus one faulted-sag. The western large domal salient occupies an area of ca. 1200 km^2 with the current structural highest point at Weiyuan Anticline, while the eastern dumbbell-like salient contains two high points respectively at Moxi and Gaoshiti Anticlines with a total trap area up to 3500 m^2, in between there is a structural saddle called Deyang-Ziyang Faulted-Sag (Fig. 11.23) which is constrained by a series of multi-order growth faults during the early sedimentary period of Qiongzhusi Formation. These growth faults can be clearly seen on cross seismic sections (Fig. 11.24), but no display on the seismic reflector contour map with contour interval of 100 m (Fig. 11.23), indicating their limited fault throws. However, these multi-order normal faults could obviously increase the stratigraphic thickness of Qiongzhusi Formation inside the faulted-sag so as to be the Qiongzhusi depocenter with a maximum stratigraphic thickness up to 540 m (at Gaoshi-17 Well; Fig. 11.24) as the main

Table 11.9 Sinian–lower Cambrian stratigraphy in Chuanzhong uplift

Stratigraphy					Lithology
System/Series	Formation/Member		Symbol	Thick/m	
Middle Cambrian	Gaotai		$\in_2$ g	0–200	Grayish-yellow shale and dolomitic sandstone
Lower Cambrian	Longwangmiao		$\in_1$ l	0–300	Gray grain dolostone, muddy dolostone and limestone
	Canglangpu		$\in_1$ch	0–300	Grayish-yellow, yellowish-green sandy shale, shale and sandstone
	Qiongzhusi		$\in_1$q	170–560	Gray and black muddy siltstone, carbonaceous shale
	Maidiping		$\in_1$ m	0–200	Dark-gray and black diamict interval
Sinian	Dengying	Deng-4	$Z_2dn_4^2$	110–200	Clotted dolostone with laminated dolostone, dolarenite and muddy dolostone interbeds argillaceous
			$Z_2dn_4^1$	100–170	Dolarenite, muddy dolostone and algal dolostone
		Deng-3	Z_2dn_3	50–100	Dark-colored shale, blueish-gray mudstone with dolostone and tuff interbeds
		Deng-2	Z_2dn_2	440–520	Upper section: micritic dolostone; Lower section: dolostone with grape-rim texture rim
		Deng-1	Z_2dn_1	20–70	Muddy micritic to very fine-grained dolostone, algal-laminated dolostone and partial gypseous salt

(continued)

Table 11.9 (continued)

Stratigraphy				Lithology
System/Series	Formation/Member	Symbol	Thick/m	
	Doushantuo	Z_1ds	10–50	Dark-gray and black shale, lime-shale with dolostone interbeds

hydrocarbon source kitchen within the Deyang-Ziyang Faulted-Sag, Chuanzhong Uplift.

The Chuanzhong Uplift is one of the palaeo-uplifts in western Yangtze Craton (cf. Chap. 13). As a Sinian-Early Palaeozoic palaeo-uplift, its stratigraphic denuded area of Silurian would exceed 6×10^4 km^2. It can also be seen from its pre-Permian palaeo-geological map that Chuanzhong Uplift appears as a palaeo-structural configuration of large south-steep and north-slow semi-anticline (or structural nose), with NEE-trending extension and eastwards pitching, keeping on Sinian–Cambrian as its core region, while Ordovician–Silurian as the pericline structure, showing the existence of a palaeo-uplift of early Sinian to Silurian time (Fig. 11.25).

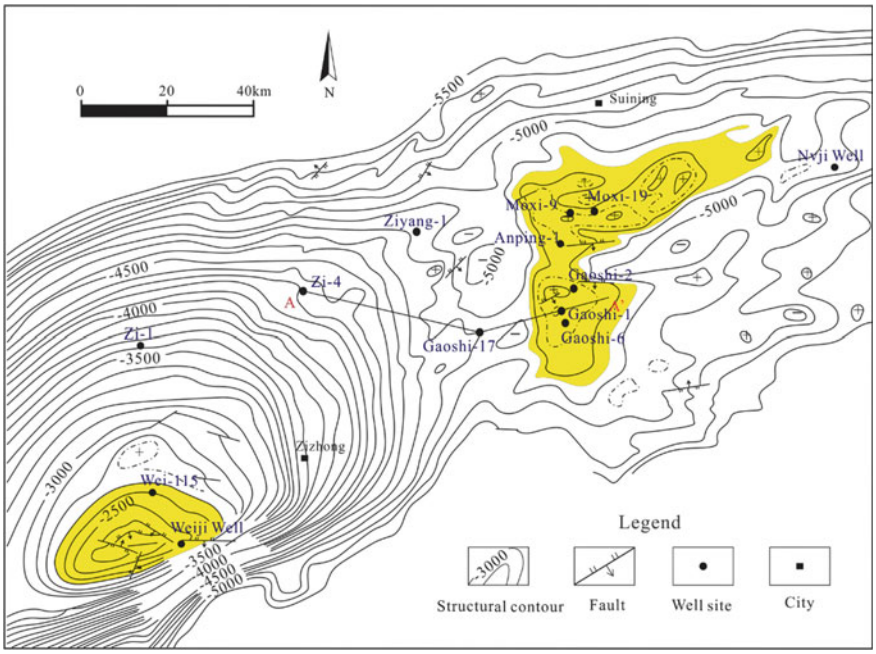

Fig. 11.23 Seismic reflector structural contour map of Sinian top surface on Chuanzhong Uplift in western Yangtze Craton with the contour interval 100 m

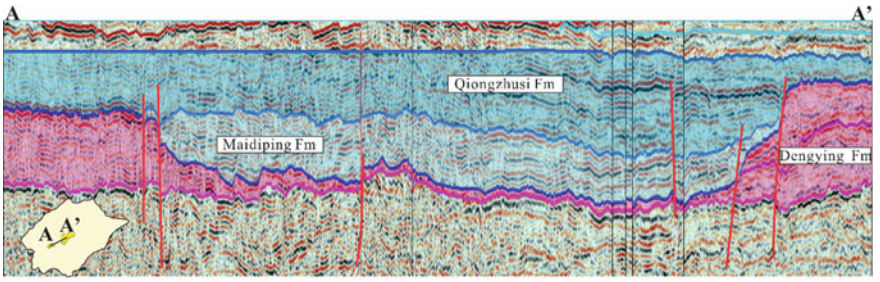

Fig. 11.24 Seismic cross section of Deyang-Ziyang Faulted-Sag. [Zou et al. (2014). Oil and gas characteristics of old carbonate and discovery of large Anyue Gasfield. China-Russia Academic Exchange Report Set on Old Carbonate Oil and Gas Geology. Hebei, Langfang: PetroChina Research Institute of Petroleum Exploration and Development (in Chinese and Russian)]

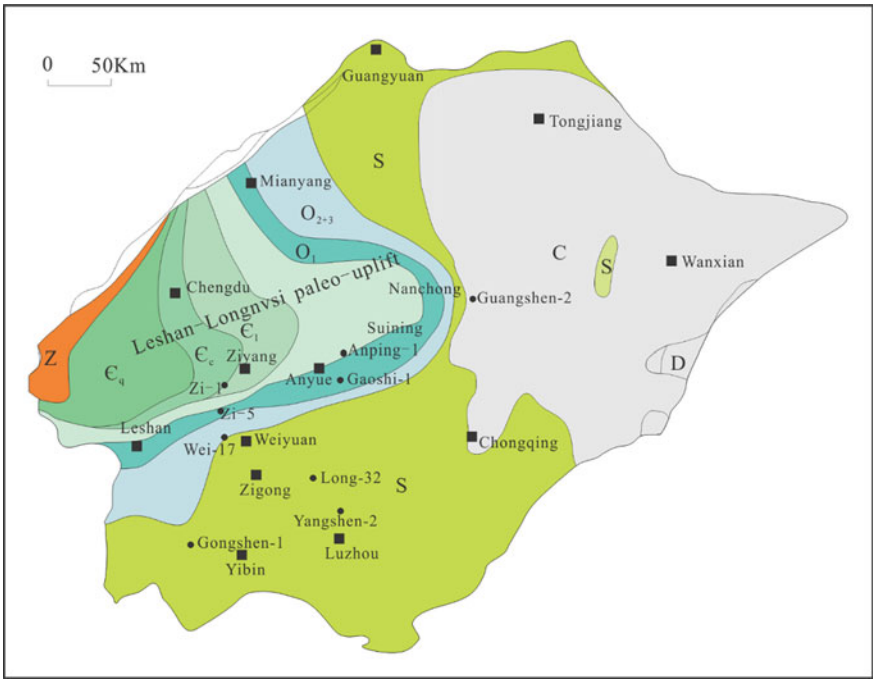

Fig. 11.25 Pre-Permian palaeo-geological map of Chuanzhong Uplift (Wei et al. 2013). The map range is only limited to the current Sichuan Basin

So far two known Chinese Infracambrian gasfields, Weiyuan and Anyue Gasfields, are situated on the Chuanzhong Uplift in the western Yangtze Craton. Weiyuan Gasfield is located at the western salient of the uplift (cf. Chap. 13), while the Anyue Gasfield at the eastern salient near the uplift axis, which is composed of two adjacent

Moxi and Gaoshiti Anticlines with Moxi at the north and Gaoshiti at the south, the latter is slightly higher than the former (Fig. 11.23; cf. Chap. 14).

11.3.1.2 Anyue Gasfield

(1) **Geological setting and petroleum geology:** The commercial gas flows have been produced from carbonate reservoirs at both the tops of Deng-2 and Deng-4 Members as well as the Longwangmiao Formation in Moxi and Gaoshiti Anticlines respectively (Table 11.9). The Deng-2 and -4 Members had developed dolostone building-up of algal mound and shoal facies, and then were reformed by late karstification, resulting in well-developed pore space of dolostone reservoir. As the first discovery well, a high production of gas flow of 102×10^4 m^3/d was obtained from the Deng-2 gas reservoir at Gaoshi-1 Well in 2011. While the Longwangmiao Formation contains the grain dolostone reservoir of shoal facies with multi-layers overlapped sheet-like occurrence, making these reservoir beds to be well-connected and highly productive, its gas-containing range would beyond the current structural trap area, resulting in the structural-lithological type of gas reservoirs at Moxi Anticline① (Wen et al. (2014). Studies on oil and Gas Entrapment and Play Evaluation in the Longnvsi Palaeo-uplift, Sichuan Basin (Internal Report). Chengdu: Institute of Petroleum Exploration and Development, PetroChina Southwest Oil and Gasfield Company (in Chinese)). A highly productive gas flows of 190.68 $\times 10^4$ m^3/d was gained from both upper and lower intervals of Longwangmiao Formation at Moxi-8 Well in 2012. Consequently, the Anyue Gasfield was further confirmed and named.

As major producing intervals, the Longwangmiao gas reservoir beds in Moxi Anticline are tectonically a south-steep and north-gentle brachyanticline with a reservoir high point at Moxi-9 Well (asl. −4226.3 m) and the reservoir bottom limit of −4458.3 m at Moxi-16 Well with a gas reservoir altitude 232 m (Fig. 11.26). While the gas-bearing altitude in individual wells averages 53.5 m. It has a proven gas reserve of 4403.8×10^8 m^3, and the natural gas is attributed to over-mature dry gas, with dry index 0.99–1.00, resulted from liquid oil cracking① (Wen et al. (2014). Studies on oil and Gas Entrapment and Play Evaluation in the Longnvsi Palaeo-uplift, Sichuan Basin (Internal Report). Chengdu: Institute of Petroleum Exploration and Development, PetroChina Southwest Oil and Gasfield Company (in Chinese)).

(2) **Reservoir pyrobitumen and fossil-oil-reservoir**: Reservoir pyrobitumen is wide-spread in the Chuanzhong Uplift (Liu et al. 2009; Du et al. 2016; Yang 2018). Du et al. (2016) reported that the pyrobitumen-containing cores of gas reservoir beds, with equivalent vitrinite reflectance eqR_o values 2.5–3.5%, had been recorded in 22 gas wells in Anyue Gasfield including Moxi and Gaoshiti Anticlines, among which 8 wells for the Dengying gas reservoirs (Fig. 11.27a) and 14 wells for the Longwangmiao gas reservoir (Fig. 11.27b). While the total numbers of pyrobitumen-sampling wells are increasing up to 73 wells in Moxi

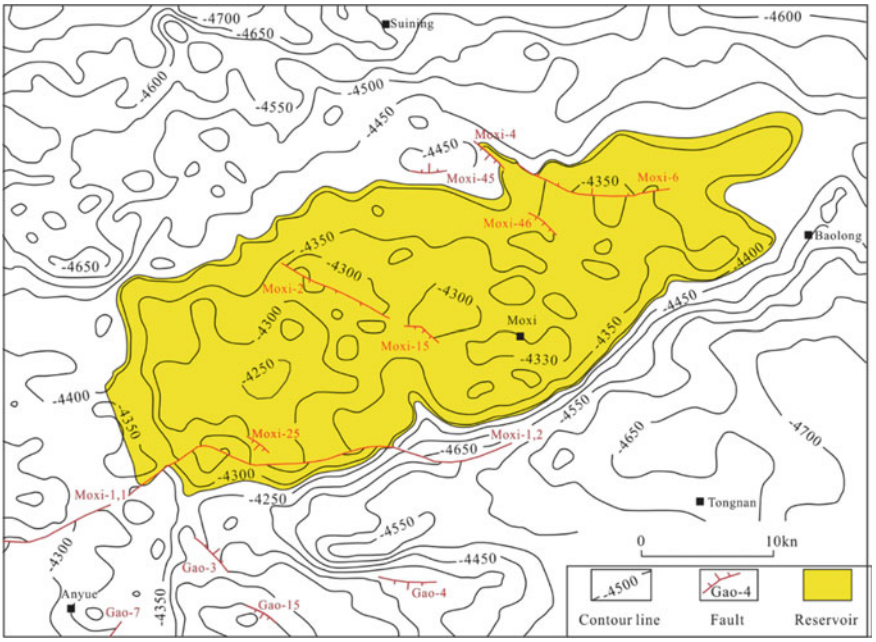

Fig. 11.26 Seismic reflector contour map of lower Cambrian Longwangmiao top surface indicating the distributional range of gas reservoir (shown in yellow color) in Moxi Anticline. MX. Moxi. [Wen et al. (2014). Studies on oil and Gas Entrapment and Play Evaluation in the Longnvsi Palaeo-uplift, Sichuan Basin (Internal Report). Chengdu: Institute of Petroleum Exploration and Development, PetroChina Southwest Oil and Gasfield Company (in Chinese)]

and Gaoshiti Anticlines (Fig. 11.27c; Yang 2018). The pyrobitumen is associated with over-mature cracking gas as a pair of paragenetic products, resulted from the disproportionation of liquid oil during the thermo-evolutional process in the palaeo-oil-reservoir. In other words, the original liquid oil was cracked into dry gas and meanwhile polymerized into solid reservoir pyrobitumen respectively. As a whole, the in-situ reservoir pyrobitumen could be attributed to the occurrence of fossil-oil-reservoir.

(2) **Palaeo-oil filling pathway and source kitchen**: Based on the analysis of chloroform extract in reservoir pyrobitumen, DMDBTs (i.e., dimethyldibenzothiophenes) can be used as molecular tracing indicators of oil-filling in oil reservoir (Wang et al. 2004). The palaeo-oil-filling pathway has been traced for the fossil-oil-reservoirs of both Deng-4 Member and Longwangmiao Formation in Anyue Gasfield (Fig. 11.28a, b). As the effective molecular tracing parameters, the isopleth map of 4,6-/(1,4 + 1,6-)DMDBT ratio shows the main oil-filling pathways from west to east in the fossil-oil-reservoirs of Deng-4 Member and Longwangmiao Formation, taking Moxi-12 Well as well as Gaoshi-7 and Gaoshi-10 Wells as oil-filling points respectively at the centro-western

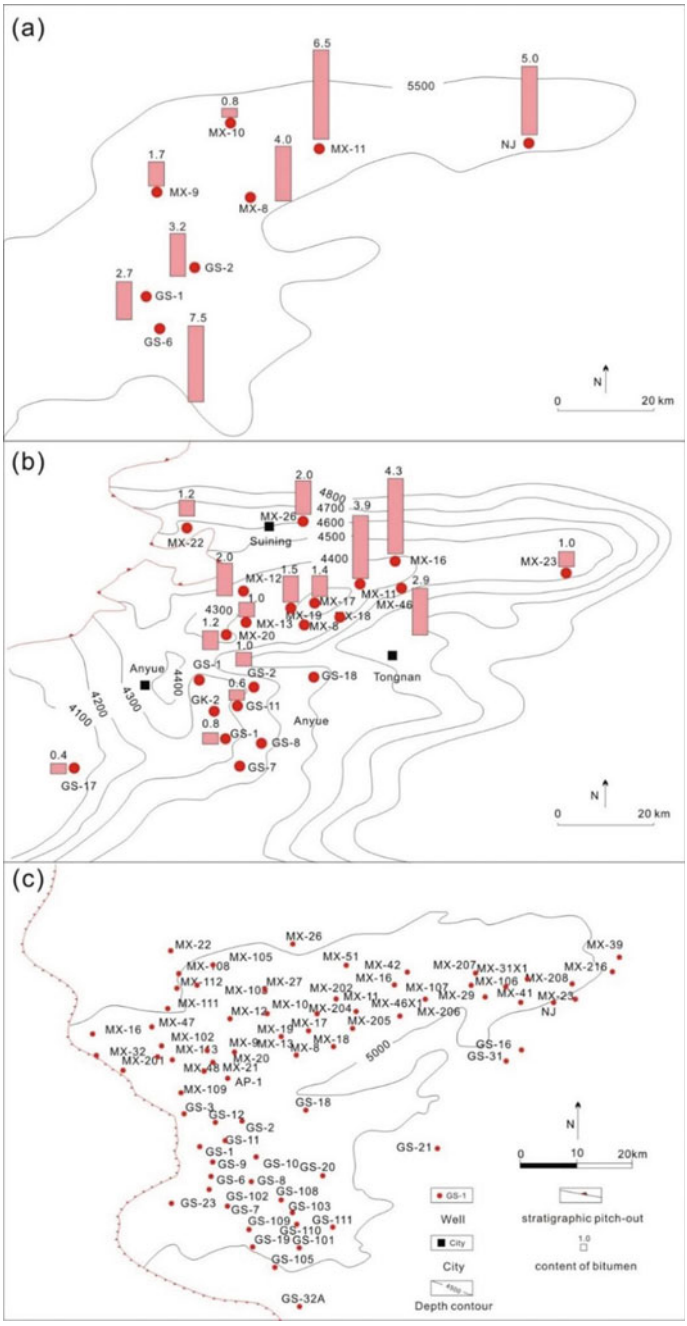

Fig. 11.27 Distribution of reservoir pyrobitumen (**a**, **b**) and pyrobitumen-sampling well sites (**c**) within Dengying and Longwangmiao reservoir beds in Moxi and Gaoshiti Anticlines. **a** Dengying gas reservoir, 8 wells; **b** Longwangmiao gas reservoir, 14 wells (Du et al. 2016, modified); **c** Pyrobitumen-sampling will sites in Longwangmiao plus Dengying Formations, totally 73 wells. MX. Moxi; GS. Gaoshiti; NJ. Nvji Well

segment of Moxi and Gaoshiti Anticlines, and tracing the major Qiongzhusi source kitchen back to the Deyang-Ziyang Faulted-Sag (Fig. 11.28a, b). In addition, two secondary oil-filling pathways are also traced from north to south within both the fossil-oil-reservoirs at the eastern segment of Moxi and Gaoshiti Anticlines, respectively with Moxi-11 and Moxi-39 Wells as well as Moxi-26 and Moxi-39 Wells as the oil-filling points for the fossil-oil-reservoirs of Deng-4 Member (Fig. 11.28a) and of Longwangmiao Formation respectively (Fig. 11.28b), The secondary oil-filling pathways would make a significant contribution to the oil entrapment for palaeo-oil-reservoir, especially in the east of Moxi Anticline. Moreover, the secondary filling pathways have also revealed a potential oil source kitchen and predicted a favorable exploration direction on the north of Moxi Anticline (Fig. 11.28).

Based on geological interpretation of seismic data, Guo[①] (Guo (2016). Carbonate reservoir bed, formational rules and explorational evaluation of large gasfield in south China. National Science and Technology Major Project (internal report). Sinopec Exploration Branch (in Chinese)) had reported some potential depression(s) on the north and/or northwest of Chuanzhong Uplift, where the Sinian Doushantuo and/or Lower Cambrian Qiongzhusi shale source beds could be available (Fig. 11.29a). Moreover, one exploratory well, Mashen-1 Well, at the northernmost margin of a potential northern depression revealed the Qiongzhusi black shale at well interval of 7090–8058 m contains TOC 1.89–8.95% (avg. 4.99%), and the black shale with TOC > 2.0% is up to 128 m-thick (Fig. 11.29b), thus a potential source kitchen could be preliminarily revealed, but it still needs further study due to the lack of enough drilling data.

However, a high producing gas flow of 51.62×10^4 m^3/d was obtained from the sandstone gas reservoir of Lower Cambrian Canglangpu Formation (cf. Table 11.9) in another new exploratory well, Jiaotan-1 Well, at 3 well intervals between 6972 m and 7026 m in 2020, which just lies to ca. 126 km north of Gaoshi-1 Well at Moxi-Gaoshiti Anticlines and on the way from the potential source kitchen to the Anyue Gasfield for hydrocarbon migrating and filling.

(4) **Palaeo-oil entrapment age:** Using fission track dating, combined with equivalent vitrinite reflectance eqR_o data, a terrestrial heatflow curve has been measured by Qiu et al.[①] (Qiu et al. (2015). Temperature and pressure fields for the formation of typical large gas fields. Technical summary report on major national science and technology projects. Beijing: China University of Petroleum-Beijing (in Chinese)) at Nvji Well in the eastern ends of the Chuanzhong Uplift (Fig. 11.30) where the regional thermo-evolutional history could be reconstructed (Liu et al. 2018), which can be divided into three thermo-evolutional periods, including the slow and steady rising, peak and decay periods (Fig. 11.30; Table 11.10).

Based on the previous long-term sstudies, a correlativity of terrestrial heatflow and hydrocarbon-generating threshold depth for the Mesoproterozoic strata in the Jibei Depression, North China Craton has been established, i.e., the heatflow values of

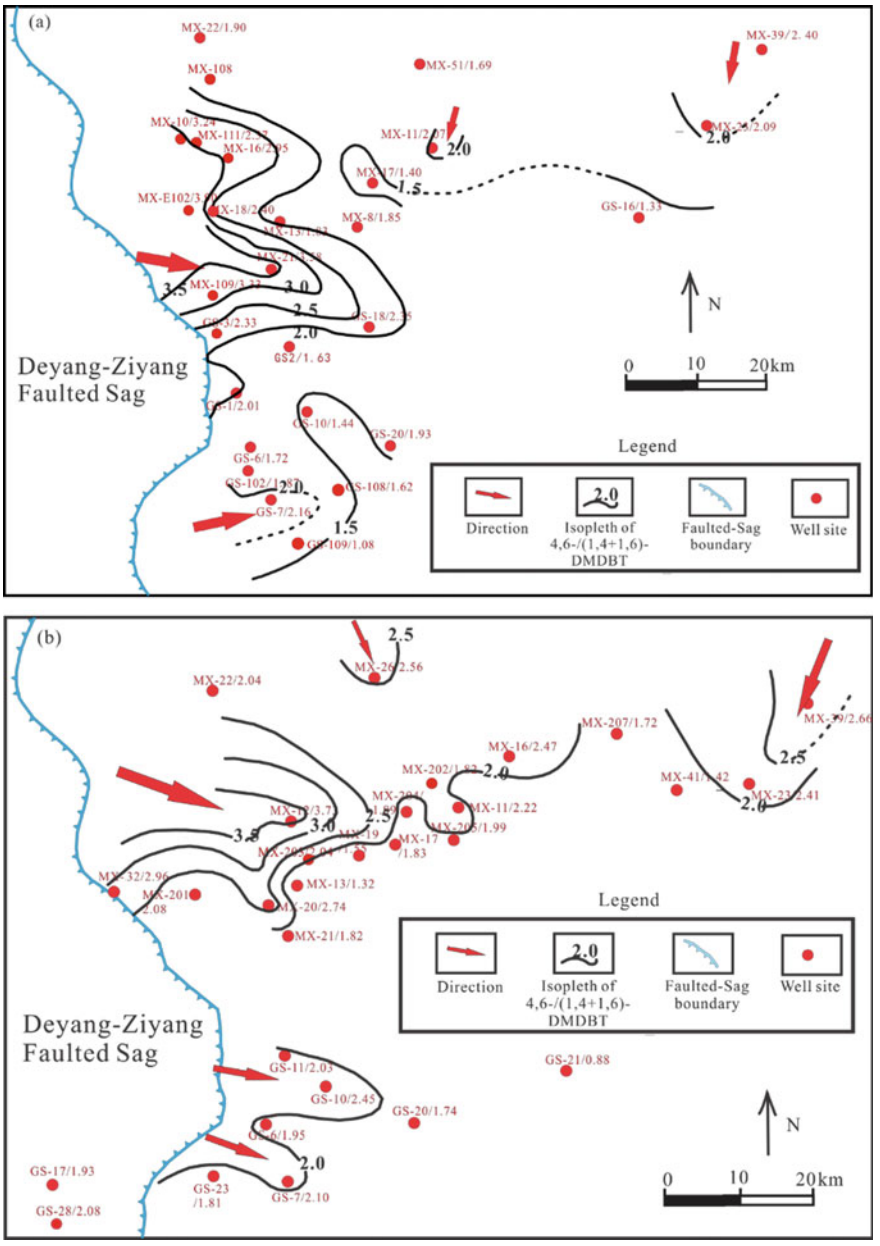

Fig. 11.28 Isograms of 4,6-/(1,4 + 1,6)DMDBT molecular parameter tracing the oil-filling pathways in fossil-oil-reservoirs. a. The fossil-oil-reservoir of Sinian Deng-4 Member, totally 28 wells; b. the fossil-oil-reservoir of Longwangmiao Formation, totally 29 wells. MX. Moxi; GS. Gaoshiti; DMDBT. Dimethyldibenzothiophene

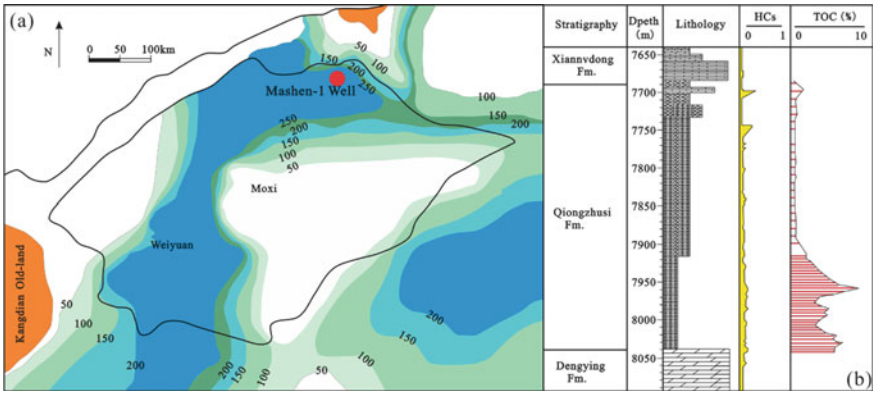

Fig. 11.29 The distribution of potential source kitchen on the north of the Chuanzhong Uplift (**a**) and a geochemical profile of Mashen-1 Well (**b**) HCs. total hydrocarbons. [Guo (2016). Carbonate reservoir bed, formational rules and explorational evaluation of large gasfield in south China. National Science and Technology Major Project (internal report). Sinopec Exploration Branch (in Chinese)]

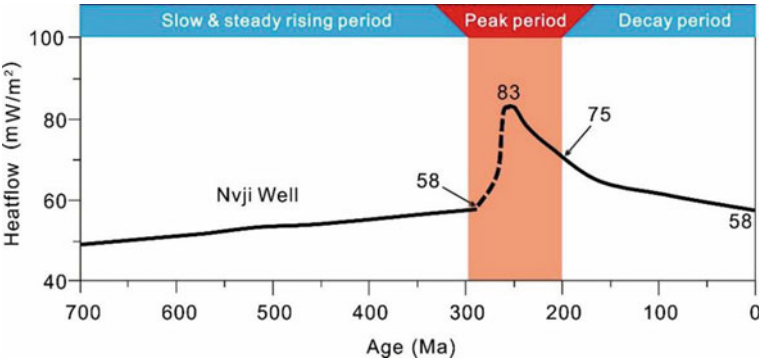

Fig. 11.30 The measured terrestrial heatflow curves at Nvji Well by means of fission track dating (Qiu et al. (2015). Temperature and pressure fields for the formation of typical large gas fields. Technical summary report on major national science and technology projects. Beijing: China University of Petroleum-Beijing (in Chinese), modified)

30–54 mW/m^2 possess corresponding threshold depth ≥3500 m (Table 11.11; Wang et al. 2016). While a distributional range of 60.7–79.5 mW/m^2 for the measured Eogene terrestrial heatflow values has corresponding threshold depth range from 2300 to 3000 m respectively in many oilfields such as Dagang, Shengli, Huabei and Jidong Oilfields in the north of NCC (Table 11.11; Zhu and Chen 2002; Hao et al. 2006; Gang et al. 2012; Cai 2012).

In the basis of geological analogy on the correlativity of terrestrial heatflow and threshold depth, according to the terrestrial heatflow curve of Nvji Well, the threshold depths of different geological times can be determined in the Qiongzhusi source

Table 11.10 The thermo-evolutional periods of terrestrial heatflow at Nvji Well (data cited from Qiu et al. 2015[a]

Thermo-evolutional periods	Slow and steady rising period	Peak period	Decay period
Terrestrial heatflow/mW/m^2	40–58	58–83–75	75–58
Geological age/Ma	700–300	300–200	200–0
Geological time	Nanhuan–Early Permian	Early Permian–Triassic	Jurassic–present

[a] Qiu et al. (2015). Temperature and pressure fields for the formation of typical large gas fields. Technical summary report on major national science and technology projects. Beijing: China University of Petroleum-Beijing (in Chinese)

Table 11.11 The geological analogy of terrestrial heatflow value and threshold depth

Region		Terrestrial heatflow value/(mW/m^2)	Threshold depth/m	References
Jibei depression (Mesoproterozoic)		30–54	$\geq$ 3500	Wang et al. (2016)
Chuanzhong Uplift	Nanhuan–early permian	40–58	ca. 3500	Geological analogy
	Early permian–triassic	58–83–75	in Btwn. 2500 and 2800	
Adjacent oilfields in the great North China plains (Eogene)		60.7–79.5	2300–3000	Zhu and Chen (2002) etc

kitchen, Chuanzhong Uplift (Table 11.11). The terrestrial heatflow values of Nvji Well are 40–58 mW/m^2 for the slow and steady rising period during Nanhuan-Early Permian (700–300 Ma; Fig. 11.30; Table 11.10), which are equivalent to these of the Mesoproterozoic in Jibei Depression, and accordingly, the threshold depth of Chuanzhong Uplift could be assign to ca. 3500 m (Table 11.11). While the terrestrial heatflow values of 58–83–75 mW/m^2 for the heatflow peak period during Early Permian–Triassic in Chuanzhong Uplift (Fig. 11.30; Table 11.11) are comparable with those of 60.7–79.2 mW/m^2 at the Eogene oilfields in NCC, which contain the threshold depth between 2300 m and 3000 m, thus the threshold depth could be approximately assigned in between 2500 m and 2800 m in Nvji Well for the peak period of Chuanzhong Uplift (Table 11.11).

Using BasinMod I software, the timing of palaeo-oil generation, migration and entrapment events can be estimated by means of single-well numerical modelling on the stratigraphic burial history and associated hydrocarbon threshold depth of source bed. Thus, the Gaoshi-17 Well within the Qiongzhusi source kitchen has been preferentially selected for reconstruction of the burial history of Qiongzhusi source bed in Deyang-Ziyang Faulted-Sag, and for presumption of oil entrapment age of fossil-oil-reservoirs in Moxi-Gaoshiti Anticlines. The modelling result shows

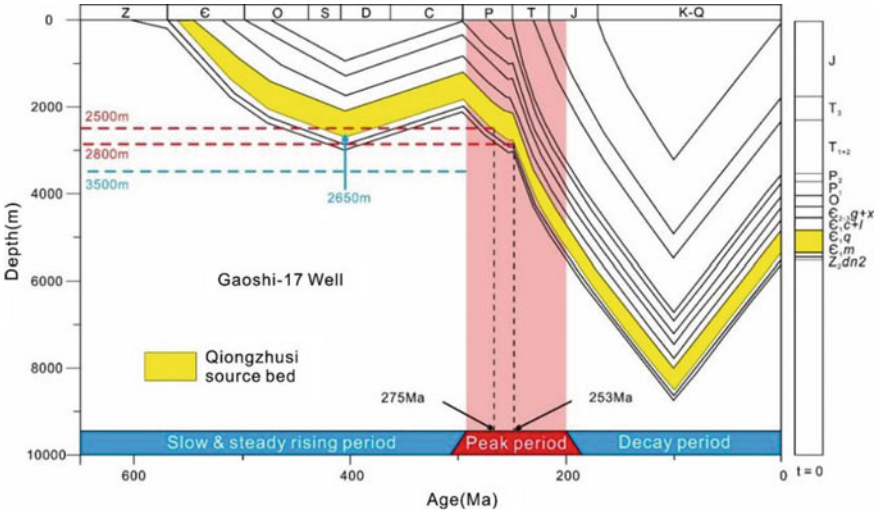

Fig. 11.31 Reconstructed burial history of Gaoshi-17 Well in Deyang-Ziyang Faulted-Sag and presumed oil entrapment age of Qiongzhusi fossil-oil-reservoir in Moxi-Gaoshiti Anticlines (Yang 2018; Yang et al. 2020 modified)

that the Qiongzhusi source bed had reached a maximum burial depth only 2650 m at the end of Silurian (Fig. 11.31; Yang 2018; Yang et al. 2020), which is less than the threshold depth ca. 3500 m, during the slow and steady rising period of terrestrial heatflow (Table 11.11), when the Qiongzhusi source bed should still be immature one, no oil/gas could be generated and sourced to the fossil-oil-reservoir at that period (i.e., Nanhuan to Early Permian; Table 11.11).

Due to the thermal effect of Emeishan mantle plume or large Igneous Province (Zhu et al. 2016) during the heatflow peak period, however, the heatflow values of Qiongzhusi source bed quickly raised to 58–83–75 mW/m^2 in Early Permian to Triassic with corresponding threshold depth in between 2500 m and 2800 m (Table 11.11), consequently the initial oil entrapment age could be assigned in between 275 and 253 Ma (in btwn. late Early and Late Permian) based on the threshold depth and reconstructed burial history of Qiongzhusi source bed in Gaoshi-17 Well (Fig. 11.31).

(5) **Emplacement age of cracking gas reservoir:** Based on microscopic observation, the Dengying and Longwangmiao gas reservoirs contain numerous fluid inclusions, including gas (methane) and its paragenetic gas–water two-phase inclusions, in authigenic minerals of quartz and late saddle dolomite (Fig. 11.32b, c). Moreover, pure methane inclusion can be distinguished from other gas inclusions by Raman spectrum (Fig. 11.32a).

A prerequisite for fluid entrapment/emplacement timing is that the fluid was trapped as a single-phase, accordingly, the dominant homogenization temperature of gas–water two-phase inclusion could be considered as a minimum trapping temperature (Emerry and Robinson 1993), and viewed approximately as the lower

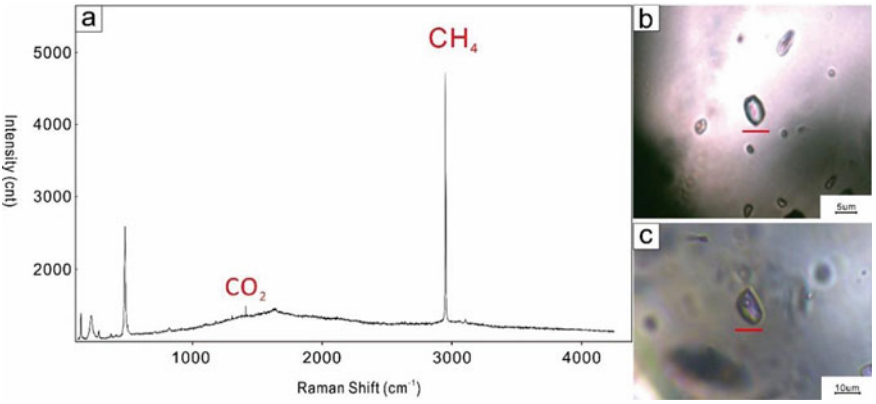

Fig. 11.32 Microphotograph and Raman spectrum of fluid inclusions in the dolostone of Deng-4 gas reservoir at Gaoshi-6 Well (Yang et al. 2018). **a** Raman spectroscopes of methane inclusions, well depth 5049 m; **b** Methane inclusion under plane-polarized transmitted light microscope, well depth 5049 m; **c** Gas–water two-phase inclusions under plane-polarized transmitted light microscope, well depth 5048.97 m

limit of entrapment/emplacement temperature for the oil/gas. Taking the dolostone gas reservoir of Deng-4 Member at Gaoshi-6 well, Gaoshiti Anticline as a case study to determine the emplacement age of cracking gas reservoir by means of microthermometry.

The microthermometric result shows that the homogenization temperature histogram of paragenetic gas–water two-phase inclusions appears as a unimodal distribution, with a dominant frequency at 170–180 °C (avg. 180 °C), for the Deng-4 gas reservoir at Gaoshi-6 Well (Fig. 11.33). As for the phase analysis of cracking gas reservoir, however, the dominant homogenization temperature of two-phase inclusions should be just a critical temperature of phase transformation from the two-phase towards the single phase, and also the minimum trapping temperature of fluid inclusions, which need to be carefully corrected into a real in-situ fluid trapping temperature by pressure correction of inclusion (Emeryy and Robinson 1993).

On a heating–cooling microscope stage, Hanor (1980), Emerry and Robinson (1993), Aplin et al. (2000), Liu et al. (2003) and Ni et al. have respectively approached the pressure correction methodology of homogenization temperature to acquire the real in-situ trapping temperature of fluid inclusions, especially for gas reservoir. In this way, Yang (2018) obtained the corrected homogenization temperature of fluid inclusion in the Deng-4 cracking gas-reservoir at Gaoshi-6 Well (well depth 5049 m; Yang et al. 2018). The research procedure is as follows:

First, the measured homogenization temperature and salinity (or freezing point) of paragenetic methane and two-phase inclusions are respectively measured.

Second, two sets of isochores respectively for methane and two-phase inclusions are established on the pressure–temperature plot (Fig. 11.34), and the intersection for both sets of isochores would indicate the really trapping temperature and pressure

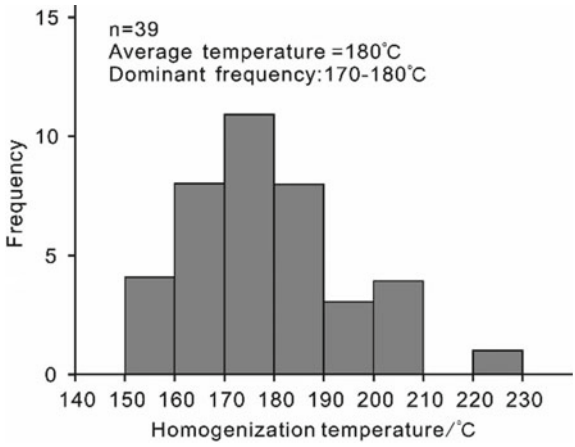

Fig. 11.33 Homogenization temperature histogram of gas–water two-phase inclusion in the Deng-4 dolostone gas reservoir, Gaoshi-6 Well (Yang 2018; Yang et al. 2018)

of paragenetic fluid inclusions. In this case, however, there are two intersections for both sets of isochores on the plot, i.e., the lower one at 185–227 °C/484–700 Bar and the higher one at 249–319 °C/1619–2300 Bar (Fig. 11.34).

Third, by comparison to the measured homogenization temperatures with dominant frequency at 170–180 °C (avg. at 180 °C; Fig. 11.33), the lower intersection is comparable and reasonable to indicates the corrected fluid trapping temperature/pressure for the Deng-4 gas-reservoir in Anyue Gasfield (Yang 2018; Yang et al. 2018). While the higher intersection is far beyond the measured range of homogenization temperature in fluid inclusions (Fig. 11.33), which should be noting to the

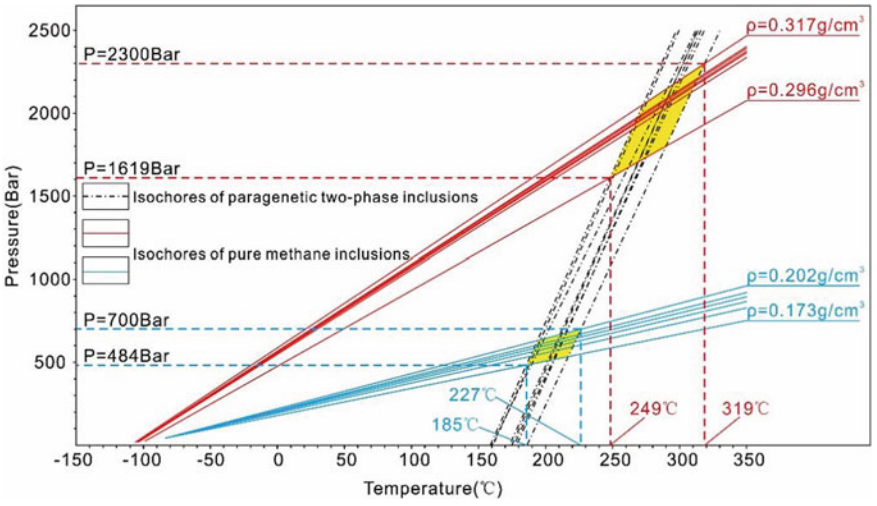

Fig. 11.34 Temperature–pressure plot of Anyue Gasfield data. The intersections of two sets isochores for pure methane and gas–water two-phase inclusions are indicated

origin of cracking gas as well as to the fossil-oil-reservoir. Since the host minerals (quartz and late saddle dolomite) of fluid inclusions belong to hydrothermal authigenic minerals and the presence of Emeishan mantle plume/large Igneous Province, nevertheless, it would be most probably that the higher temperature/pressure methane inclusions are associated with a mesothermal origin.

In order to transfer the corrected gas trapping temperature into the gas trapping age or cracking gas emplacement age for the Deng-4 gas reservoir, the Gaoshi-6 well in Gaoshiti Anticline is selected to reconstruct its stratigraphic burial-thermal histories of Dengying and Longwangmiao Formations by means of single-well numerical modelling (Fig. 11.35). The burial-thermal histories are similar either at Gaoshi-6 or at Gaoshi-17 Wells (Fig. 11.31), both wells are 20 km apart on the axis of Chuanzhong Uplift. The Deng-4 gas reservoir has experienced two subsidence-uplift tectonic cycles, the palaeo-geotherm of Deng-4 palaeo-oil reservoir had been lower than 140°C, which was not going to cause palaeo-oil cracking and thermos-alteration during the first tectonic cycle, while the burial depth was beyond 8500 m with the palaeo-geotherm higher than 220 °C and overstepping the temperature scope of oil cracking during the subsidence of the second tectonic cycle (Fig. 11.35). Consequently, the corrected trapping temperature 185–227°C for the fluid inclusions in Deng-4 gas reservoir can be intuitively transferred into the trapping age of gas inclusions, i.e., 175–144 Ma (late Middle Jurassic to early Early Cretaceous), which can be considered to be the emplacement age of cracking gas reservoir.

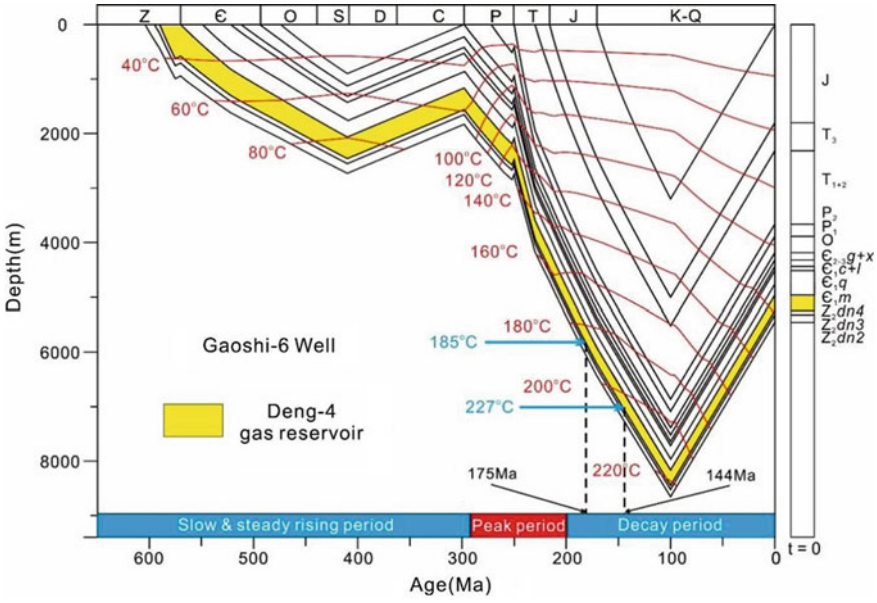

Fig. 11.35 Reconstructed stratigraphically burial and thermal histories of Gaoshi-6 Well based on single-well numerical modelling using Basin Mod I software (Yang et al. 2018)

11.3.2 Yanliao Faulted-Depression Zone (YFDZ) in North China Craton

11.3.2.1 Regional Geological Setting

The YFDZ is situated on the north margin of the North China Craton (NCC). It shows EW-trending and stretches across Hebei, Beijing, Tianjin and Liaoning Provinces/Cities, occupying totally an area of ca. 10.6×10^4 km^2. Tectonically, its central parts are mainly Shanhaiguan and Mihuai Uplifts, composed of the crystalline basement of Archean metamorphic rocks and multiphase granites, while two Meso-Neoproterozoic depressional belts are respectively developed on its north and south sides, which could be divided into Liaoxi-Jibei-Xuanlong Depressions on the north side as well as Jidong-Jingxi Depressions on the south side from east to west (Fig. 11.36), where Mesoproterozoic Changchengian (Pt_2^1), Jixianian (Pt_2^2), Xiamaling Formation (Pt_2^3x) and Neoproterozoic Qingbaikouan (Pt_3^1) sequences are deposited, and overlaid by Palaeozoic and Mesozoic strata (Table 11.12).

On the whole, the total Meso-Neoproterozoic sequences are relatively thick at the eastern segment and thin at the western one of the YFDZ, i.e., the maximum thicknesses up to 9260 m in Jidong Depression, 8043 m in Jibei Depression and 7567 m in Liaoxi Depression, as well as the minimum only 4877 m in Jingxi Depression and 4095 m in Xuanlong Depression (Fig. 11.36 and Table 11.12), among which the main sediments are attributed to Mesoproterozoic stromatolitic carbonates and partial clastic rocks. Obviously, the depocenter of Mesoproterozoic sequences would

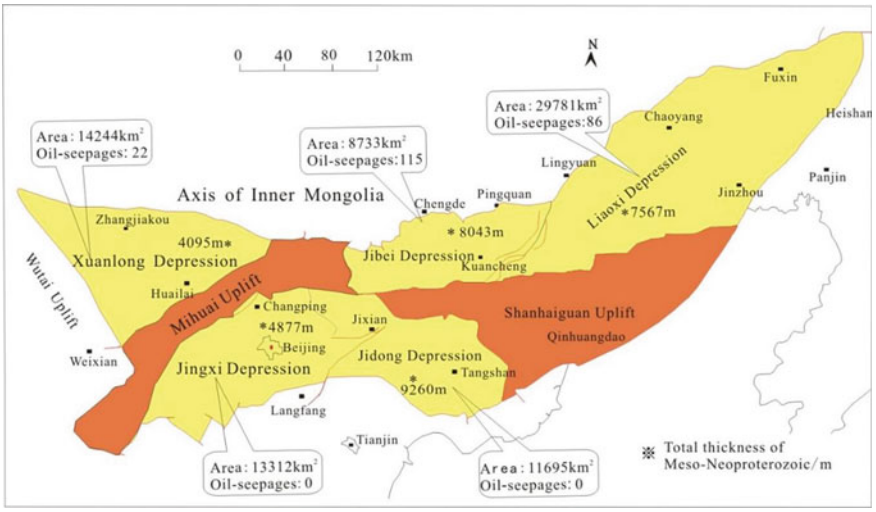

Fig. 11.36 Meso-Neoproterozoic tectonic division and stratigraphic thickness-oil seep distribution in YFDZ (Wang 1980, modified). Symbol * indicates the Meso-Neoproterozoic stratigraphic thickness in each depression

Table 11.12 Meso-neoproterozoic stratigraphic sequences and stratum thicknesses in YFDZ

Depression		Southern belt		Northern belt		
		Jiangxi	Xuanlong	Jibei	Liaoxi	Jidong
Stratigraphiy	Qingbaikouan (760–1000 Ma)	193.2	71.9	111.8	168.2	230[a]
	Xiamaling formation (1320–1400 Ma)	249.0	540.6[a]	369.5	303.4	168
	Jianxianian (1400–1600 Ma)	3448.1	2967.3	4519.0	4563.8	6175[a]
	Tieling formation	209.7	213.9	211.1	328.8	325
	Hongshuizhuang formation	100.9	41.6	101.7	92.1	131
	Wumishan formation	2168.4	1874.6	2947.2	2936.4	3416
	Yangzhuang formation	78.3	36.0	322.4	255.8	707
	Gaoyuzhuang formation	890.8	801.2	936.6	950.7	1596
	Changchengian (1600–1670 Ma)	387.6	515.0	3042.6[a]	2586.5	2687
Total stratigraphic Thickness/m		4280	4095	8403	7621.9	9260

Note [a] indicates depocenter of different strata

be around Jidong-Jibei Depressions especially at Jibei for Changchengian, Jidong for Jixianian and Qingbaikouan, while the depocenter of Xiamaling Formation is at Xuanlong (Table 11.12). Their stromatolite and macrofossil assemblages, lithology-lithofacies and stratigraphic division show as a highly correlativity in whole the YFDZ, which implies that the palaeo-oceanic waters are well connected and so the palaeo-oceanic sedimentary environments unified in all the depressions during the Mesoproterozoic time. The current Shanhaiguan and Mihuai Uplifts, which have separated both northern and southern depression belts (Fig. 11.36), are predominantly referred to the late uplifting tectonic units in the YFDZ, and never completely separated the Meso-Neoproterozoic palaeo-oceanic waters.

11.3.2.2 Petroleum Geology

Numerous oil-seeps, asphalt and bituminous sandstone are widely distributed within the three depressions of northern depression belt. Taking Jibei Depression as an example, so far totally 115 sites of oil-seeps, asphalt and bituminous sandstone have been found, among which 98 sites are attributed to Mesoproterozoic strata, accounting for 85.2% of the total sites, and mainly appearing as liquid oil phase (Plate 11.1b; Table 11.13).

Table 11.13 Oil-seep phases and their productive layers in Jibei Depression, YFDZ

No	Oil-seep occurrence			Oil-seep phase	Oil-seep number ∑115 sites		Percentage /%	
	Era	System	Formation					
1	Mesozoic	Cretaceous	Xiguayuan, K_1x	Oil, asphalt	2		1.7	
2	Lower Palaeozoic	Ordovician	Majiagou, O_2m	Asphalt	1	3	0.9	2.6
3			Yel, O_1y	Oil, asphalt	2		1.7	
4		Cambrian	Changshan, $\in_3 c$	Asphalt	1	13	0.9	10.5
5			Mantou, $\in_1 m$	Oil, asphalt	8		7.0	
6			Fujunshan, $\in_1 f$	Asphalt, oil	3		2.6	
7	Mesoproterzoic	Xiamaling, Pt_2^3x		Asphalt, oil	20		17.4	85.2
8		Jixianian	Tieling, Pt_2^2t	Oil, asphalt	60	77	52.2	66.9
9			Hongshuizhuang, Pt_2^2h	Oil	2		1.7	
10			Wumishan, Pt_2^2w	Oil, asphalt	15		13.0	
11			Gaoyuzhuang, Pt_2^2g	Asphalt	1		0.9	0.9

However, Mesoproterozoic oil-seeps are never found in the Jingxi and Jidong Depressions of southern depression belt during (Wang 1980; Wang and Han 2011; Fig. 11.36).[1,2,3]

Occurrence of oil-seep and bituminous sandstone in Jibei Depression, YFDZ. **a** Bituminous sandstone in the basal sandstone of Xiamaling Formation (photograph on outcrop); **b** liquid oil-seep in the dolostone of Wumishan Formation (photograph at mine drift); **c**, **d** bituminous sandstone in the basal sandstone of Xiamaling Formation (microphtograph)

As major source beds in Jibei Depression, both Gaoyuzhuang black micritic dolostone and Hongshuizhuang black shale contain high organic abundance with

[1] Wang et al. (1978). The bright prospects of Sinian primary oil and gas reservoirs. Oral Presentation on the Scientific Conference of Petroleum Geology and Seismic Exploration in East China. Beijing: China Petroleum Chemistry Industry Ministry (in Chinese).

[2] Wang et al. (1979). Principal characteristics of petroleum geology in the eastern segment of Yansan region (Internal Report). The 3rd Regional Geological Survey Team, Jingzhou: Jianghan Institute of Petroleum (in Chinese).

[3] Wang et al. (2009). Petroleum prospectivity and regional play predication of the lower stratigraphic assemblage in North China Platform (Internal Report). Beijing: China University of Petroleum-Beijing.

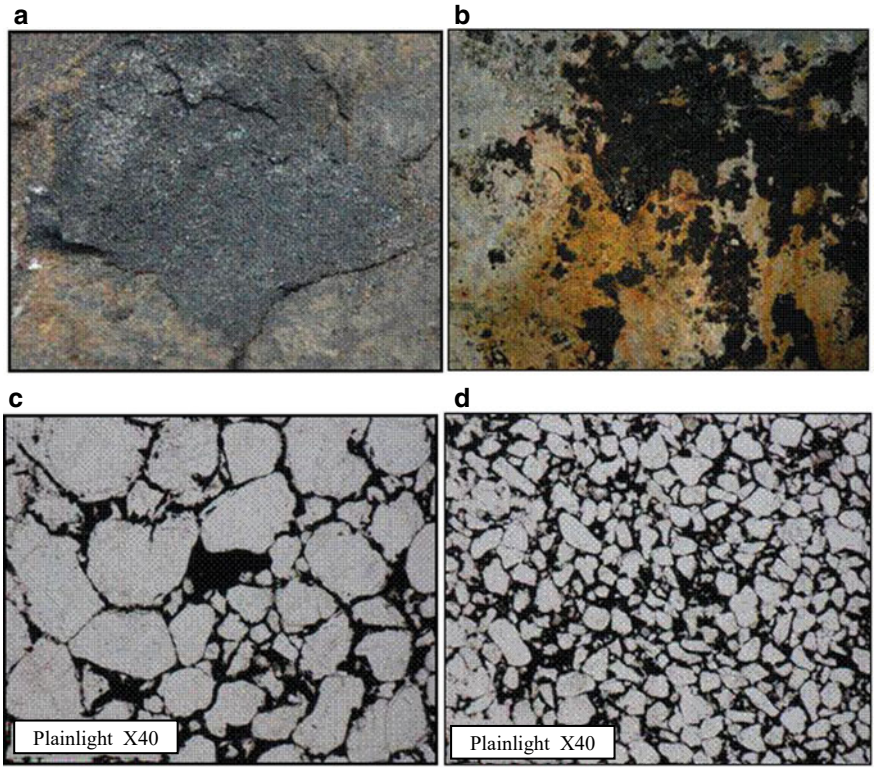

Plate 11.1 The *m*/*z* 123 mass chromatographs for oil-source correlation of the Mesoproterozoic bituminous sandstone and asphalts in Jibei Depression. **a**–**c**. Degradation products of catalytical hydrocracking for source rock kerogens; **d**–**f**. Aliphatic fractions of oil-seeps and bituminous sandstone; C_{18}–C_{23}. 13α(*n*-alkyl)-tricyclic terpanes

TOC 1.16% and 4.65% in average (max. 4.29% and 7.21%) as well as chloroform extractable bitumen 63 ppm and 265 ppm (max. 152 ppm and 4510 ppm) respectively. The measured equivalent vitrinite reflectance eqR_o values 1.38–1.75% (avg. 1.59%) and 0.9–1.42% (avg. 1.19%) respectively, which are referred to high-mature to over-mature phase for Gaoyuzhuang and mature to high-mature phase for Hongshuizhuang source beds. If taking TOC 0.5% as the lower limit of effective source rock, the cumulative thicknesses of source beds would be 164 and 60 m for Gaoyuzhuang and Hongshuizhuang Formations respectively (Table 11.14).

In Xiamaling Formation, the basal medium- to thin-bedded sandstone layers or lens are composed of quartz and chert, and well-cemented by silica and/or asphalt, appearing as white tight and hard quartzose sandstone or black bituminous sandstone, respectively (Plate 11.1a, c, d), even uncemented loose bituminous sands could be found at both south and north flanks of the central syncline belt (called Dangba Syncline Belt) in Jibei Depression. The 3.8 m-thick bituminous sandstone is outcropped at Longtangou (in Lingyuan, western Liaoning), while the outcrop

Table 11.14 Geochemical parameters of effective source beds in Jibei Depression, YFDZ

Parameters	Gaoyuzhuang formation	Hongshuizhuang formation
TOC/%	0.50–4.29/1.16 (69)[a]	0.50–7.21/4.65 (36)
Chloroform bitumen content/ppm	26–152/63 (11)	34–4510/2650 (10)
Hydrogen index/(mg HC/g rock)	11–45/21 (61)	97–311/233 (36)
Oil-generating potential $S_1 + S_2$/(mg HC/g rock)	0.09–2.39/0.32 (61)	0.52–18.2/12.2 (36)
Equivalent vitrinite reflectance eqR_o/%	1.38–1.75/1.59	0.90–1.42/1.19
Cumulative source rock thickness/m	164	60

[a] Minimum–maximum/average (sample number)

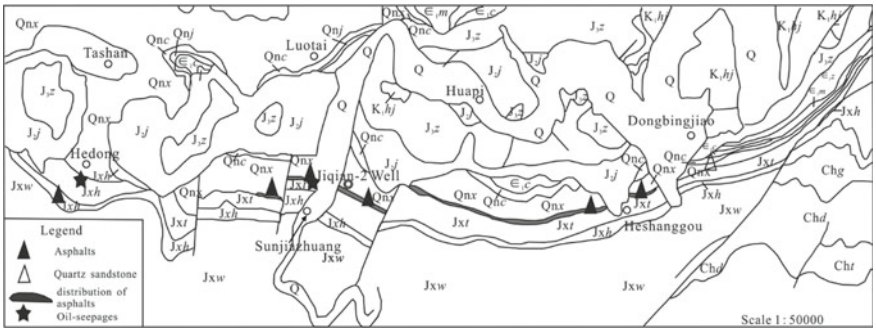

Fig. 11.37 Geological map showing the distribution of outcrop sites for Xiamaling bituminous sandstone at Lujiazhuang (Kuancheng) in Jibei depression

of bituminous sandstone can be traced for 10 km at Lujiazhuang on surface (in Kuancheng, northern Hebei; Fig. 11.37). The discovery of extensive bituminous sandstone would symbolize the actual existance of the oldest Mesoproterozoic fossil-oil-reservoirs (1400 Ma; Wang and Simoneit 1995; cf. Chap. 12).

11.3.2.3 Asphalt/Bituminous Sandstone-Source Rock Correlation

A novel biomarker series of C_{18}–C_{23} 13α(*n*-alkyl)-tricyclic terpanes had been initially detected and identified from the aliphatic fractions of Mesoproterozoic bituminous sandstone, oil-seep and asphalt in Jibei Depression (Fig. 11.38d–f; Wang 1991). So far the biomarker series is only found in the Meso-Neoproterozoic sedimentary organic matters, either in YFDZ, NCC (Wang and Simoneit 1995; Zhang et al. 2007; Wang et al. 2011) and in the Sinian-sourced asphaltic veins at Longmenshan, western Yangtze Craton (Huang and Wang 2008; cf. Chap. 15), which may be act as a specific biomarker series for the organic matter of Precambrian age.

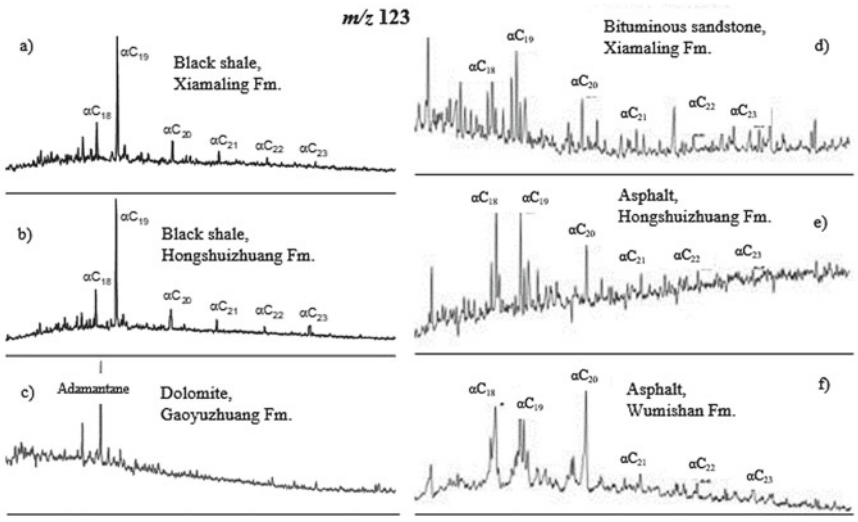

Fig. 11.38 The *m/z* 123 mass chromatographs for oil-source correlation of the Mesoproterozoic bituminous sandstone and asphalts in Jibei Depression. **a–c** Aliphatic fractions of source rocks; **d–f** Aliphatic fractions of oil-seeps and bituminous sandstone. C_{18}–C_{23}. 13α(*n*-alkyl)-tricyclic terpanes

Based on a systematically geochemical investigation of source beds in the Jibei Depression, 13α(*n*-alkyl)-tricyclic terpanes had also been detected from the aliphatic fractions of Hongshuizhuang and Xiamaling black shales (Fig. 11.38a, b), which are comparable to above oil-seeps, bituminous sandstone and asphalt (Fig. 11.39d–f), but never found in the Gaoyuzhuang black micrite dolostone (Fig. 11.38c).

By way of degradation technique of catalytical hydrocracking for kerogens isolated and purified from above source rocks, 13α(*n*-alkyl)-tricyclic terpanes were only detected in the kerogen-degraded products of Hongshuizhuang black shale (Fig. 11.39b), and well correlated with the bituminous sandstone, oil-seeps and asphalt in Jibei Depression (Fig. 11.39d–f), indicating the Hongshuizhuang black shale as the sole or major source bed for the bituminous sandstone, oil-seeps and asphalt in Jibei Depression (Fig. 11.38a).

11.3.2.4 Significance of the Xiamaling Basal Bituminous Sands

Obviously, asphalt or solid bitumen is not fluid and can't directly be filled into the intergranular opening of Xiamaling basal sandstone (Plate 11.1a, c, d), and thus, the Xiamaling basal bituminous sandstone should actually be the original oil sandstone, and then be altered into bituminous sandstone by the late thermo-alteration (cf. Chaps. 10 and 12). Therefore, the bituminous sandstone itself would act as the symbol of fossil-oil-reservoir, particularly at Longtangou (in Lingyuan, western

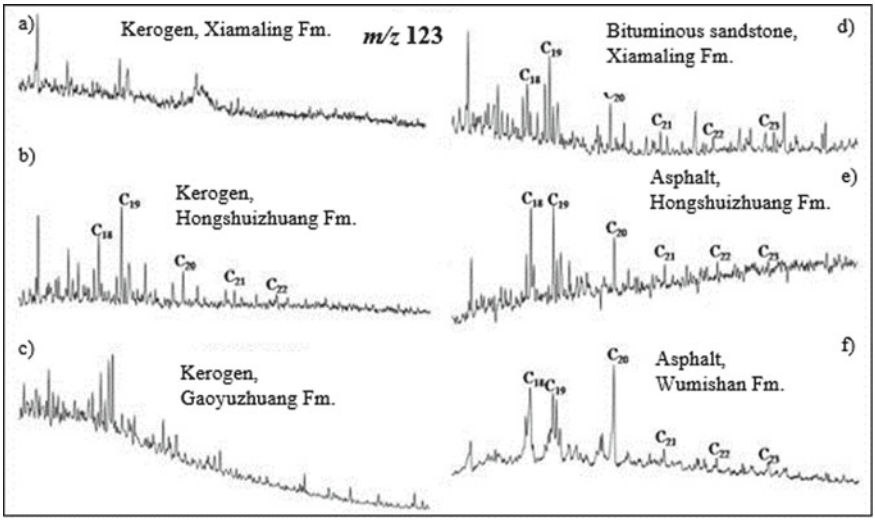

Fig. 11.39 The *m*/*z* 123 mass chromatographs for oil-source correlation of the Mesoproterozoic bituminous sandstone and asphalts in Jibei Depression. **a**–**c**. Degradation products of catalytical hydrocracking for source rock kerogens; **d**–**f**. Aliphatic fractions of oil-seeps and bituminous sandstone; C_{18}–C_{23}. 13α(*n*-alkyl)-tricyclic terpanes

Liaoning), where flesh uncemented bituminous sands are also found by means of artificial trenching operation on the outcrop of Xiamaling basal sandstone, which implies that when liquid oil was filling and entrapping into the Xiamaling basal sand-body, the sand-body had been just commenced to be cemented and its cementation was still unfinished yet during the early diagenesis. Owing to the known bottom limit age of Xiamaling Formation is 1400 Ma, i.e., equivalent to the basal boundary age of Mesoproterozoic, hence, it could also date the oil entrapment age of Xiamaling basal fossil-oil-reservoir back to 1400 Ma.

11.4 Conclusions

(1) As for global Meso-Neoproterozoic indigenous petroleum resources, there are four regions/countries, (Lena-Tounguska Petroleum Province in Russia, Anyue Gasfield in China, Oman Basins and Baghewala Oilfield in India) containing proven geological reserves and/or commercial production; nine regions/countries having confirmed the indigenous oil, oil-seep and/or asphalts, but still no commercial production found yet; five regions/countries being revealed to possess hydrocarbon generating potential in the Infracambrian strata in the word. All the indigenous petroleum was sourced from Meso-Neoproterozoic source beds, in some cases, it could be derived from Early Cambrian source bed, and thus it is also called Infracambrian petroleum.

(2) Mesoproterozoic to Early Cambrian indigenous petroleum occurrence includes oil, gas-condensate, gas and even asphalt (bitumen)/pyroasphalt (pyrobitumen). In view of organic matter thermo-evolution stages, the indigenous petroleum appears as different thermo-maturities from marginal mature (e.g., Baghewala oil), through mature (e.g., Oman oil and wet gas) and high-mature (e.g., Lena-Tounguska oil, gas-condensate and gas) to over-mature (e.g., Anyue cracking dry gas and pyrobitumen) phases.
(3) Almost all the known Infracambrian oil and gas reservoirs could be attributed to late entrapment/emplacement causes. In many cases, the entrapment/emplacement ages of Meso-Neoproterozoic oil and gas reservoirs are not earlier than Early Palaeozoic time, even the oil/gas field could be formed during Mesozoic time, which would facilitate the preservation of Infracambrian oil and/or gas resources.
(4) The Cambrian wide-spread salt beds in Lena-Tounguska Petroleum Province (Russia) and large, irregular salt bodies (salt dome) in Oman are regional super-seal favorable to Infracambrian oil and gas entrapment and preservation.
(5) So far some distinct biomarkers such as conspicuous mid-chain monomethyl-alkanes (so called "X compounds") and 13α(*n*-alkyl)-tricyclic terpanes are found in Precambrian oil and sedimentary organic matter, which may be significant to distinguish the indigenous Meso-Neoproterozoic oil and asphalt for oil-source rock correlation.
(6) As new types of Infracambrian oil reservoir found in Oman, both intra-salt "silicilyte" and carbonate "stringer" reservoirs are self-sourced, self-reservoired and enclosed by large salt bodies. "Silicilyte" is a new petrological term specially for the microcrystalline silicon matrix, or called microcrystalline chert.

References

Aadil N, Sohail GM (2011) Stratigraphic correlation and isopach of Punjab Platform in Middle Indus Basin, Pakistan. GEOIndia, pp 1–6

Albert-Villanueva E, Permanyer A, Tritlla J, Levresse G, Salas R (2016) Solid hydrocarbons in Proterozoic dolostones, Taoudenni Basin, Mauritania. J Petrol Geol

Aley AA, Nash DF (1984) A summary of the geology and oil habitat of the eastern flank hydrocarbon province of south Oman. In: Proceedings of seminar on the source and habitat of petroleum in Arab countries. Kuwait, pp 521–541

Amthor JE, Ramseyer K, Faulkner T, Lucas P (2005) Stratigraphy and sedimentology of a chert reservoir at the Precambrian-Cambrian boundary: the AI shomou silicilyte, South Oman salt basin. GeoArabia 10:89–122

Amthor JE, Smith W, Nederlof NI, Frewin N L, Lake S (1998) Prolific oil production from a source rock—the Athel silicilyte source rock play in south Oman. Am Assoc of Petrol Geol Annu Convention A22

Anderson RR (1989) Gravity and magnetic modeling of central segment of Mid-continent Rift in Iowa—new insights into its stratigraphy, structure, and geological history. Am Asso Petrol Geol Bull 73(8):1043

Aplin AC, Larter SR, Bigge MA, Macleod G, Swarbrick RE, Grunberger D (2000) PVTX history of the North Sea's Judy oilfield. J Geochem Explor 69:641–644

Asim S, Zhu P, Qureshi SN, Naseer MT (2015) A case study of Precambrian to Eocene sediments' hydrocarbon potential assessment in Central Indus Basin of Pakistan. Areb J Geosci 8:10339–10357

Beijing Petroleum Exploration, Development Institute and North China Petroleum Bureau (1992) Reservoir beds and phase forecast of deep oil and gas pool-taking Jizhong depression and South Caspian Basin as examples. Petroleum Industry Press, Beijing, pp 273–357 (in Chinese)

Behrendt JC, Green AG, Cannon WF, Hutchinson DR, Lee MW, Milkereit B, Ahena WF, Spencer C (1988) Crustal structure of the Mid continent rift system: results from GLIMPCE deep seismic reflection profile. Geology 16:81–85

Bhat GM, Craig J, Hafiz M, Hakhoo N, Thurow JW, Thusu B, Cozzi A (2012) Geology and hydrocarbon potential of neoproterozoic-Cambrian Basins in Asia: an introduction. In: Bhat GM et al (eds) Geology and hydrocarbon potential of neoproterozoic-Cambrian Basins in Asia. Geological Society Special Publication 366, The Geological Society, London

Bowring SA, Grotzinger JP, Condon DJ, Ramezani J, Newall M (2007) Geochronologic constraints on the chronostratigraphic framework of the neoproterozoic Huqf supergroup, sultanate of Oman. Am J Sci 307:1097–1145

Bronner G, Roussel J, Trompette R (1980) Genesis and geodynamic evolution of the Taoudenni Cratonic Basin (Upper Precambrian and Paleozoic), Western Africa. Dyn Plat Inter Geodyn Ser 1:73–80

Cai XY (2012) Hydrocarbon generation-expulsion mechanisms and efficiencies of lacustrine source rocks: a case study from the Dongying sag, Bohai Bay Basin. Oil Gas Geol 33(3):329–334 (in Chinese with English abstract)

Chen JY (2004) Dawn of animal would. Jiangsu Science Press, Nanjing (in Chinese)

Chen JY, Zhou GQ, Zhu MY, Ye KY (1996) The Chengjiang Biota: a unique window of the Cambrian explosion. State Science Nature Museum, Taiwan (in Chinese)

Clauer N (1981) Rb-Sr and K-Ar dating of Precambrian clays and glauconies. Precambr Res 15:53–71

Craig J, Thurow J, Thusu B, Whitham A, Abutarruma Y (2009) Global neoproterozoic petroleum systems: the emerging potential in North Africa. In: Craig J et al (eds) Global Neoproterozoic Petroleum systems: the emerging potential in North Africa. Geological Society Special Publication 326, The Geological Society, London, pp 1–25

Crick IH, Boreham CJ, Cook AC (1988) Petroleum geology and geochemistry of Middle Proterozoic McAuthur Basin, Northern Australia II: assessment of source rock potential. AAPG Bull 72:1495–1514

Daniels PA Jr (1982) Upper Precambrian sedimentary rocks: oronto group, Michigan-Wisconsin. In: Wold RJ, Hinze WJ (eds) Geology and tectonics of the lake superior basin, vol. 156. Geological Society of America Memoir, pp 107–133

Dickes AB (1986a) Precambrian as a hydrocarbon exploration target. Geosci Wis 11:5–7

Dickes AB (1986b) Worldwide distribution of Precambrian hydrocarbon deposits. Geosci Wis 11:8–11

Dickes AB (1986c) Comparative Precambrian stratigraphy and structure along the Mid-continent Rift. Am Assoc Geol Bull 70(3):225–238

Du RL, Tian LF, Hu HB, Sun LM, Chen J (2009) Chinese Precambriam Palaeontology research: neoproterozoic Qinbaikouan Longfengshan Biota. Science Press, Beijing (in Chinese)

Du JH, Wang ZC, Zou CN, Xu CC, Shen P, Zhang BM, Jiang H, Huang SP (2016) Discovery of intra-cratonic rift in the Upper Yangtze and its control effect on the formation of Anyue giant gas field. Acta Patrolei Sin 37(1):1–16 (in Chinese with English abstract)

Efimov AS, Cert AA, Mel'nikov PN, Starosel'tcev VS, Vymyatin AA, Akimov VG, Cherepanova II, Brazhnikov MV (2012) About current state and trends of hydrocarbon Resource potential, geological exploration and licensing in East Siberia and Sakha Republic (Yakutia). Geol Neft Gasa, 5:57–74 (in Russian)

Elmore RD, Milavec GJ, Imbus SW, Engel MH (1989) The Precambrian Nonesuch Formation of the North American Mid-continent rift, sedimentology and organic geochemical aspects of lacustrine deposition. Precambr Res 43:181–213

Emerry D, Robinson A (1993) Inorganic geochemistry: application to petroleum geology. Blackwell Scientific Publication, Oxford, pp 41–66

Fedorov Dl (1997) The stratigraphy and hydrocarbon potential of the Riphean-Vendian (Middle-Late Proterozoic) succession on the Russian Platform. J Petr Geol 20(2):205–222

Filipstove YA, Petrishina YV, Bogorodskaya LI, Kontrorovich AA, Krinin VA (1999) Evaluation of maturity and oil- and gas-generation properties of the organic matter in Riphean and Vendian rocks of the Baykit and Katanga petroleum regions. Geol 1 Geofiz 40:1362–1374

Frolov SV, Akhmanov GG, Bakay EA, Lubnina NV, Korobova NI, Karnyushina EE, Kozlova EV (2015) Meso-neoproterozoic petroleum systems of the Eastern Siberian sedimentary basins. Precambr Res 259:95–113

Gang WZ (2009) Hydrocarbon generation conditions and exploration potential of the Taoudenni Basin, Mauritania. Pet Sci 6:29–37 (in Chinese with English abstract)

Gang WZ, Wu Y, Gao G, Ma Q, Pang XQ (2012) Geochemical features and geologic significances of source rocks in Nanpu Sag, Bohai Bay Basin. Pet Geol Exp 34(1):57–61 (in Chinese with English abstract)

Gaters G (2005) Hydrocarbon project in mauritania and Mali, West Africa. Technical experts Report in farmout brochure by Baraka Petroleum. South Perth, Australia

Ghori KAR, Craig J, Thusu B, Lüning S, Geiger M (2009) Global Infracambrian petroleum system: a review. In: Craig J et al (eds) Global Neoproterozoic petroleum systems: The emerging potential in North Africa. Geological Society Special Publication 326, The Geological Society, London, pp 110–136

Grantham PJ (1986) The occurrence of unusual C_{27} and C_{29} sterane predominances in two types of Oman crude oil. Org Geochem 9(1):1–10

Grantham PJ, Lijmbach GWM, Postthuma J, Hughes Clarke MW, Willink RJ (1987) Origin of crude oils in Oman. J Pet Geol 11:61–80

Grosjean E, Love GD, Stalvies C, Fike DA, Summons RE (2009) Origin of petroleum in the Neoproterozoic-Cambrian South Oman salt basin. Org Geochem 40:87–110

Hanor J (1980) Dissolved methane in sedimentary brines; potential effect on the PVT properties of fluid inclusions. Econ Geol 75(4):603–609

Hao F, Zou HY, Fang Y, Hu JW (2006) Kinetics of organic matter maturation and hydrocarbon generation in overpressure environment. Acta Petrolei Sinica 27(5):9–18 (in Chinese with English abstract)

Hasany ST, Aftab M, Siddiqui RA (2012) Refound Exploration Opportunities and Cambrian Sediments of Punjab Platform. Pakistan Petroleum Limited, Pakistan. Karachi

Heward AP (1989) Early Ordovician alluvial fan deposits of the Marmul oil field south Oman. J Geol Soc London 146:557

Hou XG, Bergstrom J, Wang HF, Feng XH, Chen AL (1999) The Chengjiang Fauna: exceptionally well-preserved animals from 530 million years ago. Yunnan Science and Technology Press, Kunming (in Chinese)

Huang DF, Wang LS (2008) Geochemical characteristics of bituminous dike in Kuangshanliang area and its significance. Petrolei Sinica 29(1):23–28 (in Chinese with English abstract)

Hunt J (1991) Generation of gas and oil from coal and other terrestrial organic matter. Org Geochem 17(6):673–680

Immerz P, Oterdoom WH, Yonbery El (2000) The Huqf/Haima hydrocarbon system of Oman and the terminal phase of the Pan-African Orogeny: evaporite deposition in a compressive setting. In: The 4th middle east geoscience conference, GEO2000. GeoArabia, Abstract, pp 387–433

Jackson JM, Powell TG, Summons RE, Sweet IP (1986) Hydrocarbon shows and petroleum source rocks in sediments as old as 1.7×10^9 years. Nature 322:727–727

Jackson JM, Sweet IP, Powell TG (1988) Studies on petroleum geology and geochemistry of the of Middle Proterozoic McArthur Basin, northern Australia I: petroleum potential. Aust Petrol Explor Assoc J 28:283–302

Jean-Pierre G, Herbert E, Amir K (2014) Petroleum system, migration and charge history in the Neo- and Meso-Proterozoic series of the Taoudenni Basin, Adrar: insights from fluid inclusions. In: International petroleum technology conference, IPTC-18011-MS, pp 1–5

Kah CL, Bartley JK, Stagner AF (2009) Reinterpreting a Proterozoic enigma: conophyton-Jacutophyton stromatolites of the Mesoproterozoic Atar Group, Mauritania. Spec Publ Int Assoc Sedimentol 41:277–296

Kao CS, Hsiung YH, Kao P (1934) Preliminary notes on Sinian stratigraphy of North China. Bull Geol Soc China 13(2):243–288

Katz BJ, Everett MA (2016) An overview of pre-Devonian petroleum systems—unique characteristics and elevated risks. Mar Pet Geol 73:492–516

Klemme HD, Ulmishek GF (1991) Effective petroleum source rocks of the world: stratigraphic distribution and controlling factors. AAPG Bull 75(12):1809–1851

Knott DJ (1998) Omam prepares for oil expansion and gas production for LNG export. Oil Gas J 96:29–34

Kuznetsov VG (1997) Riphean hydrocarbon reservoir of the Yurubchen-Tokhom zone, Lena-Tunguska Province, NE Russia. J Pet Geol 20(4):459–474

Lahondére D, Roger J et al (2005) Notice explicative des cartes geologiques á 1/20,000 et 1/500,000 de l' extréme sud de la Mauritanie. DMG, Ministére des mine et de l'Industrie, Nouakchott, 610

Larichev AI, Melenevskii VN, Shvedenkov GY, Sukhoruchko VI (2004) Aquapyrolysis of organic matter from the Riphean carbon-rich argillite of the Yurubchen-Takhom oil and gas accumulation zone. Dokl Earth Sci 398(7):961–963

Lee LS, Chao YT (1924) Geology of the Gorge district of the Yangtze (from Ichang to Tzeckuei) with special reference to the development of the Gorges. Bull Geol Soc Chin 3(3–4):351–391

Liu DH, Xiao XM, Mi JK, Li XQ, Shen JK, Song ZG, Peng PA (2003) Determination of trapping pressure and temperature of petroleum inclusions using PVT simulation software—a case study of Lower Ordovician carbonates from the Lunnan Low Uplift, Tarim Basin. Mar Pet Geol 20(1):29–43

Liu SG, Ma YS, Cai XY, Guo S, Wang GZ, Yong ZQ, Sun W, Yuan HF, Pan CL (2009) Characteristic and accumulation process of the natural gas from Sinian to Lower Palaeozoic in Sichuan Basin, China. J Chengdu Univ Technol (sci Technol Ed) 36(4):345–354 (in Chinese with English abstract)

Liu W, Qiu NS, Xu QC, Liu Y (2018) Precambrian temperature and pressure system of Gaoshiti-Moxi block in the central palaeo-uplift of Sichuan Basin, southwest China. Precambr Res 313:91–108

Lottaroli F, Craig J, Thusu B (2009) Neoproterozoic–early Cambrian (Infracambrian) hydrocarbon prospectivity of North Africa: a synthesis. In: Craig J et al (eds) Global neoproterozoic petroleum systems: The emerging potential in North Africa. Geological Society Special Publication 326, The Geological Society, London, pp 137–156

Mauk JL, Hieshima GB (1992) Organic matter and copper mineralization at White Pine, Michigan, USA. Chem Geol 99:189–211

Melanie AE (2010) Characterizing the Precambrian petroleum systems of Eastern Siberia: evidence from oil geochemistry and basin moleling. SPE 136334:1–11

Menchikoff N (1949) Quelques traits de I'hisoire geologique du Sahara occidentail. Annales Hebert Et Haug 7:303–325

O'Dell M, Lamers E (2003) Subsurface uncertainty management in the Harweel Cluster, south Oman. SPE 84189. Int Soc Petrol Eng

Ojha PS (2012) Precambrian sedimentary basins of India: an appraisal of their petroleum otential. In: Bhat GM, et al (eds) Geology and hydrocarbon potential of neoproterozoic–Cambrian basins in Asia. Geological Society Special Publication, vol. 366. Geological Society, London, pp 19–58

Ozimic S, Passmore VL, Pain L, Lavering IH (1986) Australian petroleum accumulation report 1: amadeus basin, central Australia. Australian Government Publication Service, Canberra
Palacs JG (1997) Source-rock potential of Precambrian rocks in selected Basin of United States. US Geol Surv Bull 02146-J:125–134
Peters KE, Watters CC, Gupta Das U, McCaaffrey MA, Lee CY (1995) Recognition of an Infracambrian source rock based on biomarkers in the Baghewala Oil field, India. AAPG 79:1481–1494
Peters JM, Filbrandt JB, Grotzinger JP, Newall MJ, Shuster MW, Al-Syabi HA (2003) Surface-piercing salt domes of interior North Oman, and their significance foe the Ara carbonate "stringer" hydrocarbon play. Geo Arab 8:231–270
Pollastro RM (1999) Ghaba Salt Basin province and Fuhud Salt Basin province, Oman—geological overview and total petroleum systems. US Geol Surv Bull 2167:1–41
Pratt LM, Summons RE, Hieshima GB (1991) Sterane and triterpane biomarkers in the Precambrian Nonesuch Formation, North American Midcontinent Rift. Geochimca Et Cosmochimica Acta 55:911–916
Priss WV, Forbes BG (1981) Stratigrahpy, correlation and sedimentary history Adelaidean (Latest Proterozoic) basin in Australia. Precambr Res 15:255–304
Pruvost P (1951) L'Infracambrien. Bull de la Soc Belge Geol Palaeontologie Hydrol 60:43–65
Qadri IB (1995) Petroleum geology of Pakistan. Pakistan Petroleum Limited, Karachi
Rahmani A, Goucem A, Boukhallat S, Saadallah N (2009) Infracambrian petroleum play elements of the NE Taoudenni Basin (Algeria). In: Craig J et al (eds) Global neoproterozoic petroleum systems, the emerging potential in North Africa. Geological Society Special Publication 326, Geological Society, London, pp 221–229
Ram J (2012) Neoproterozoic successions in Peninsular India and their hydrocarbon prospectivity. In: Bhat GM et al (eds) Geology and hydrocarbon potential of neoproterozoic-Cambrian Basins in Asia. Geological Society Special Publications 366. Geological Society, London, pp 75–90
Rawlings DJ (1999a) Stratigraphic resolution of a multiphase intracratonic basin system: the McArthur Basin, northern Australia. Aust J Earth Sci 46:1–17
Rawlings DJ (1999b) Stratigraphic resolution of a multiphase intracraton basin system: the McArthur Basin, northern Australia. Aust J Earth Sci 46:703–723
Rooney AD, Selby D, Houzay JP, Renne PR (2010) Re-Os geochemistry of a Mesoproterozoic sedimentary succession, Taoudenni Basin, Mauritania: implications for basin-wide correlations and Re-Os organic-rich sediments systematic. Earth Planet Sci Lett 289:486–496
Sheikh RA, Jamil MA, McCann J, Saqi MI (2003) Distribution of Infracambrian reservoirs on Punjab Platform in central Indus Basin of Pakistan. ATC 2003 conference and oil show. Society of Petroleum Engineers (SPE) and Pakistan Association of Petroleum Geoscientists (PAPG), Islamabad, pp 1–17
Shu DG et al (2016) Ancestors from Cambrian explosion. Northwest University Press, Xian (in Chinese)
Smith AG (2009) Neoproterozoic timescales and stratigraphy. In: Craig J et al (eds) Global neoproterozoic petroleum systems: the emerging potential in North Africa. Geological Society Special Publication, vol. 326, The Geological Society, London, pp 27–54
Sun SF (2006) Meso- to Neoproterozoic Micropaleobotany in Jixian, China. Geology Press, Beijing (in Chinese)
Terken JMJ, Frewin NL, Indrelid SL (2001) Petroleum systems of Oman: charge timing and risks. AAPG Bull 85:1817–1845
Tong XG, Xu SB (2004) Global petroleum exploration and development atlas: Fascicle of former soviet union countries. Petroleum Industry Press, Beijing, pp 138–163 (in Chinese)
Ulmishek GF (2001) Petroleum geology and resources of the Baykit High Province, Eastern Siberia, Russia. US Geological Survey Bulletin 2201-F, U S Geological Survey, Washington
Visser W (1991) Burial and thermal history of Proterozoic source rocks in Oman. Precambrian Researches 54:15–36

Vysotsky IV, Korehagina YuI, Sokolov BA (1993) Genetic aspects of assessment of the petroleum potential of the Moscow syneclise. Geol Nefit i Gaza 12:26–29 (in Russia)
Wade BP, Hand M, Barovich KM (2005) Nd isotopic and geochemical constraints on provenance of sedimentary rocks in the eastern Officer Basin, Australia; implications for the duration of the intracratonic Precambrian Orogeny. J Geol Soc Lond 162:513–530
Wang TG (1980) Primary properties of Sinian Suberathem oil-seep and its petroleum geological significance in Yanshan region. Pet Explor Dev 7(2):34–52 (in Chinses)
Wang TG (1991) A novel tricyclic terpane biomarker series in the Upper Proterozoic bituminous sandstone, eastern Yanshan region. Sci China (series B) 34(4):479–489
Wang TG, Han KY (2011) On Meso-Neoproterozoic primary petroleum resources. Acta Petrolei Sin 32(1):1–7 (in Chinese with English abstract)
Wang TG, Simoneit BRT (1995) Tricyclic terpanes in Precambrian Bituminous sandstone from the eastern Yanshan region, North China. Chem Geol 120:155–170
Wang TG, He FQ, Li MJ, Hou Y, Guo SQ (2004) Alkyl-dibenzothiophenes: molecular tracers for filling pathway in oil reservoirs. Chin Sci Bull 49(22):2399–2404
Wang TG, Zhong NN, Wang CJ, Zhu YX, Liu Y, Song DF (2016) Source bed and oil entrapment-alteration histories of fossil-oil-reservoirs in the Xiamaling Formation basal sandstone, Jibei depression. Pet Sci Bull 1(1):24–36 (in Chinese with English abstract)
Wang CJ, Wang M, Xu J, Li YL, Yu Y, Bai J, Dong T, Zhang XY, Xiong XF, Gai HF (2011) 13α(*n*-alkyl)-tricyclic terpanes: a series of biomarkers for the unique microbial mat ecosystem in the Middle Mesoproterozoic (1.45–1.30 Ga) North China Sea. Mineral Mag 75:2, 114
Wei GQ, Shen P, Yang W, Zhang J, Jiao GH, Xie WR, Xie ZY (2013) Formation conditions and exploration prospects of Sinian large gas fields, Sichuan Basin. Pet Explor Dev 40(2):129–138 (in Chinese with English abstract)
Wells AJ, Forman DJ, Ranferd LC, Cooks PJ (1970) Geology of the Amadeus Basin. Bur Miner Resour Aust Bull
Wilkins N (2007) Proterozoic evangelist tries to convent the unbelievers. Oil and gas gazette, Dec 2006-Jan 2007, 2–3
Womer MB (1986) Hydrocarbon occurrence and diagenetic history within proterozoic sediments, McArthur river area, Northern territory, Australia. Aust Petrol Explor Assoc J 26:363–374
Wong SW, Ford S, Turner B (1998) Massive fracture stimulation in deep, high-pressure Athel formation. Soc Petrol Eng Pap 50614:407–412
Yang CY (2018) Petroleum entrapment and evolution history of Leshan-Longnvsi uplift, SW China. China University of Petroleum-Beijing, Beijing (in Chinese with English abstract)
Yang CY, Wen L, Wang TG, Wang B, Luo B, Li MJ, Tian XW, Ni ZY (2020) Timing of hydrocarbon accumulation for palaeo-oil reservoir in Anyue gasfield in Chuanzhong uplift. Oil Gas Geol 41(3):48–58 (in Chinese with English abstract)
Yang CY, Ni ZY, Wang TG, Chen ZH, Hong HT, Wen L, Luo B, Wang WZ (2018) A new genetic mechanism of natural gas accumulation. Sci Rep 8(1):8, 336
Zhang SC, Zhang BM, Bian LZ, Jin ZJ, Wang DR, Chen JF (2007) The Xiamaling oil shale generated through Rhodophyta over 800 Ma ago. Sci China Ser D Earth Sci 50(4):527–535
Zhu MZ, Chen JY (2002) Hydrocarbon-generating threshold of the source rocks in Palaeogene of Linnan subsag. Petrol Geol Recovery Eff 9(2):35–37 (in Chinese with English abstract)
Zhu CQ, Hu SB, Qiu NS, Rao S, Yuan YS (2016) The thermal history of the Sichuan Basin, SW China: evidence from the deep boreholes. Sci China Earth Sci 59:70–82
Zou CN, Du JH, Xu CC, Wong ZC, Zhang BM, Wei GQ, Wang TS, Yao GS, Deng SW, Liu JJ, Zhou H, Xu AT, Yang Z, Jiang H, Gu ZD (2014) Formation, distribution, resource potential and discovery of the Sinian-Cambrian giant gas field, Sichuan basin, SW China. Petrol Explor Dev 41(3):278–293 (in Chinese with English abstract)